[redacted]



LA - 1003

[redacted]

October 28, 1946

This document contains 155 pages

VOL. I EXPERIMENTAL TECHNIQUES

Part II Ionization Chambers and Counters

Section A

Written By:

Bruno Rossi
Hans Staub

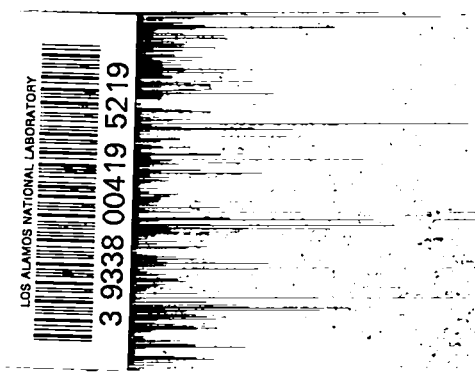


NOTE: IT IS PROPOSED THAT THIS DOCUMENT WILL BE ISSUED IN AN EDITED FORM AS PART OF THE LOS ALAMOS SECTION OF THE MANHATTAN PROJECT TECHNICAL SERIES AT A SUBSEQUENT DATE.

MANHATTAN PROJECT TECHNICAL SERIES

CONTRIBUTION OF

LOS ALAMOS PROJECT

---

The following material may be subject to certain minor revisions in the event that factual errors are discovered previous to final publications of this part of the Technical Series. Any such changes will be submitted for patent clearance and declassification in the usual manner.

UNCLASSIFIED

LOS ALAMOS TECHNICAL SERIES

VOL. I - EXPERIMENTAL TECHNIQUES

PART II

# IONIZATION CHAMBERS AND COUNTERS

By Bruno Rossi and Hans Staub



UNCLASSIFIED

TABLE OF CONTENTS

TABLE OF CONTENTS (Cont'd.)

TABLE OF CONTENTS (Cont'd.)

TABLE OF CONTENTS (Cont'd.)

## FORWARD

The first four chapters of Part II deal with the fundamental features of ionization and the general properties of detectors based upon the ionization process. The last five chapters describe the construction of some typical detectors and their operation. Most of the detectors described were developed at the Los Alamos Laboratory, a few at other projects connected with the development of the atomic bomb. It is not intended to give a complete list of all detectors used at this project.

The material contained in Part II was collected with the collaboration of many members of the Los Alamos staff. In particular, the authors wish to express their appreciation to Dr. F. C. Chromey and Dr. D. B. Nicodemus, who are responsible for compiling a large part of the information presented and who contributed valuable discussion.

# CHAPTER 8

# BEHAVIOR OF FREE ELECTRONS AND IONS IN GASES (1)

## 8.1 GENERAL CONSIDERATIONS

The ionization of a gas by an ionizing radiation, as it is well known, consists in the removal of one electron from each of a number of gas molecules. This changes the neutral molecules into positive ions. In some gases the electrons will remain free for a long time. In other gases, they will, more or less promptly, attach themselves to neutral molecules forming heavy negative ions. It is also possible for an electron or a negative ion to recombine directly with a positive ion, giving rise to a neutral molecule. This phenomenon, however, will be of importance only in the regions of the gas where the ionization is very dense. In an ionized gas not subject to any electric field, the electrons and ions will move at random, with an average energy equal to the average thermal translational energy of the gas molecules. This is given by 3/2 kT, where k is the Boltzmann constant. At the temperature of 15°C, 3/2 kT is approximately equivalent to $3.7 \times 10^{-2}$ eV.

When an electric field is present, the electrons and ions, while still moving at random through the gas, will in addition undergo a general drift in a direction parallel to the electric field. At the same time their agitation energy will be increased above the thermal value 3/2 kT.

The average energy of electrons or ions when an electric field is present is generally measured by its ratio $\epsilon$ to the thermal agitation energy at 15°C. It may be characterized also by giving the root mean square velocity of agitation, u. The

---

(1) The discussion presented in this chapter follows to some extent that given in Healy, R. H. and Reed, J. W., "The Behavior of Slow Electrons in Gases". Amalgamated Wireless Ltd., Sidney, 1941. This volume will be referred to in what follows as H.R.

relation between $\epsilon$ and u is obviously:

$$\epsilon(3/2\ kT) = 1/2\ mu^2 \qquad (1)$$

where m is the mass of the particle under consideration. It may be noted here that for positive or negative ions in an electric field, the average energy of agitation is always very close to the thermal value, while for electrons it is often considerably larger. The actual value of $\epsilon$ in a given gas and with a given electric field is determined by an equilibrium condition between the energy supplied by the electric field to the charged particles per unit time and that lost by these particles through collisions with the gas molecules.

The phenomenon of the attachment of electrons to neutral gas molecules mentioned above can be described by the attachment coefficient $\alpha$, giving the probability of attachment per unit time. The coefficient $\alpha$ depends on the nature of the gas and on the energy distribution of the electrons. For a given gas and a given energy distribution, it is proportional to the number of collisions per second; i.e., it is proportional to the pressure.

The probability for an electron (or a negative ion) to recombine with a positive ion in a given time interval is clearly proportional to the density of positive ions. Thus the number of recombination processes per unit volume and unit time is given by the expression

$$\beta\ n^+\ n^-$$

where $n^+$ and $n^-$ are the densities of positive ions and of electrons (or negative ions) respectively. The quantity $\beta$ will be called the recombination constant. It depends on the nature of the particles which recombine as well as on their agitation energy.

## 8.2 THE DIFFUSION EQUATION FOR IONS AND ELECTRONS IN A GAS.

The motion of the electrons and ions through the gas, as determined by the action of the electric field and by the collisions with the gas molecules can be described by a diffusion equation. In the absence of an electric field, this equation has the following form:

$$\vec{j} = -D \text{ grad } n \qquad (2)$$

where n is the density of particles in question, D is the so-called diffusion coefficient, $\vec{j}$ is the current vector or, more accurately, the density vector for the material current, the magnitude of which gives the net number of particles per second crossing a surface of unit area perpendicular to its direction. The product of $\vec{j}$ times the electric charge of each particle (+e or -e) gives the density of electric current. Whether an electric field is present or not, the collisions with gas molecules are so frequent, or in other words, the diffusion coefficient is so small, that the "transport velocity", defined as $\vec{j}/n$, is always very small compared with the velocity of agitation u.

We want now to write the expression for $\vec{j}$ in the case where an electric field is present. For the sake of simplicity, we shall assume that the field is uniform. Then for any type of charged particle the average energy of agitation and the diffusion coefficient (which is a function of the energy of agitation) are also constant in space.

The equation required can be obtained by considering the momentum balance in a volume element within the ionized gas. The total momentum of the charged particles in the volume element under consideration is modified (a) by the action of the electric field on the charged particles, (b) by the collisions of the charged particles with gas molecules, and (c) by exchange of charged particles with neighboring elements. The rate of change of the momentum per unit volume due to the electric field is $ne\vec{E}$, where $\vec{E}$ is the electric field strength; that caused by loss through collisions will be denoted by $-\vec{M}$. In order to calculate the rate of exchange of momentum with the neighboring elements, let us consider a surface element dS in the ionized gas and a unit vector $\vec{a}$ perpendicular to dS. If we consider $\vec{j}$ as negligible compared with nu, and if we assume for a moment that all of the charged particles under consideration have the same velocity of agitation u, the number of particles per second crossing dS and moving at angles between $\theta$ and $\theta + d\theta$ with respect to $\vec{a}$ is given by

$$1/2\ mu \cos\theta \sin\theta \quad d\theta$$

The total momentum carried by these particles is, for reason of symmetry, in the direction of $\vec{a}$ and has a value

$$(1/2\ mu \cos\theta \sin\theta \quad d\theta)\ mu \cos\theta$$

Integration over $\theta$ from 0 to $\pi/2$ gives the following expression for the increase of momentum per unit time on that side of dS toward which the vector $\vec{a}$ is pointing

$$1/3\ nmu^2\ a\ dS$$

Hence the rate of increase of momentum in a volume A bounded by a closed surface S has the expression

$$\int_S 1/3\ nmu^2\ \vec{a}\ dS = -\int_A 1/3\ mu^2\ \text{grad}\ n\ dA$$

from which it follows that the rate of change of momentum per unit volume is

$$-1/3\ mu^2\ \text{grad}\ n$$

This expression is valid also if the charged particles do not all have the same velocity of agitation, provided one considers u as the root mean square velocity. The principle of conservation of momentum is then expressed by the following equation

$$ne\vec{E} - 1/3\ mu^2\ \text{grad}\ n - \vec{M} = \frac{d(m\vec{j})}{dt}$$

The quantity to the right-hand side of the above equation represents the rate of change of the net momentum of the charged particles contained in the unit volume. Its value depends on the value of the diffusion coefficient D, while the left-hand side of the equation contains terms (like $ne\vec{E}$) which do not depend on D. In most practical cases, D is so small that $d(m\vec{j})/dt$ is negligible compared with the terms on the left-hand side of the equation (just as the transport velocity $\vec{j}/n$ is negligible compared with the agitation velocity u). Therefore the equation above may be written as follows

$$me\vec{E} - 1/3\ mu^2\ \text{grad}\ n = \vec{M} \qquad (3)$$

In order to determine $\vec{M}$ we note that $\vec{M}$, by its nature, must be a definite function of $\vec{j}$, independent of whether the current which $\vec{j}$ represents is produced by a gradient of the density or by an electric field. The form of this function can therefore be determined from Equations 2 and 3 under the assumption $\vec{E} = 0$. One obtains:

$$\vec{M} = 1/3\ \frac{mu^2}{D}\ \vec{j} \qquad (4)$$

With this expression for $\vec{M}$, Equation 3 becomes

$$\vec{j} = -D\ \text{grad}\ n + \frac{3D}{mu^2}\ ne\vec{E} \qquad (5)$$

The drift produced by the electric field is best described by the drift velocity $\vec{w}$, which is defined as the velocity of the center of gravity of the charged particles in the uniform electric field.(1)

---

(1) The drift velocity $\vec{w}$ may also be defined as the average vector velocity of all the charged particles under consideration, as opposed to the transport velocity $\vec{j}/n$, which represents the average velocity of the particles contained in a volume element at a given point of the gas.

---

According to this definition, $\vec{w}$ is given by the equation

$$\vec{w} = \left(\int_A \vec{j}\ dA\right)/\left(\int_A n\ dA\right) \qquad (6)$$

where the integrations are extended over a volume which contains all of the particles under consideration. Since n is zero at the surface which limits this volume, $\int_f$ grad n dA is zero. It then follows:

$$\vec{w} = \frac{3\ D}{mu^2}\ e\vec{E} \qquad (7)$$

or remembering Equation 1,

$$\vec{w} = \frac{D}{\varepsilon kT}\ e\vec{E} \qquad (7')$$

Equation 5 can now be rewritten as follows:

$$\vec{j} = -D \text{ grad } n + \vec{w}n \tag{8}$$

Let us consider a region of the gas where no ions or electrons are formed and none disappear by attachment or recombination. In this region the number of particles of each type is conserved and the following Equation holds

$$\frac{\partial n}{\partial t} = -\text{div } \vec{j} \tag{9}$$

which, together with Equation 8 gives

$$\frac{\partial n}{\partial t} = D \text{ div grad } n - \text{div } (\vec{w}n) \tag{10}$$

We want to apply this equation to the problem of determining the motion of a number of particles produced in a very small volume at the time $t = 0$. Mathematically, this means solving Equation 10 with the condition that the solution should become a $\delta$-function for $t = 0$. If we write Equation 10 in cartesian coordinates with the z axis in the direction of w and introduce the transformation

$$z' = z - wt$$

we obtain the ordinary diffusion equation without convection. The solution of this equation for the boundary condition indicated is well known (see, for instance, Slater and Frank, "Introduction to Theoretical Physics", McGraw Hill, 1933). By transforming back to the original variables one finally obtains the following expression for n:

$$n(x, y, z, t) = \frac{N}{(\sqrt{2\pi}\,\ell(t))^3} e^{-\frac{x^2 + y^2 + (z - wt)^2}{2\ell^2(t)}} \tag{11}$$

where N is the total number of particles and

$$\ell^2(t) = 2Dt \tag{12}$$

Physically, the solution represented by Equation 11 indicates that the particles, originally contained in an infinitesimal volume at the origin of the

coordinate system, drift with an average velocity $\vec{w}$ in the direction of the positive z axis and at the same time, spread into a cloud which becomes increasingly diffused as time goes on. The length $\ell$ represents the root mean square distance of the particles from any plane through the center of gravity of the cloud at the time t. Equation 12 shows that $\ell$ increases as the square root of the time.

## 8.3 MEAN FREE PATH.- ENERGY LOSS PER COLLISION. MIXTURE OF GASES.

One often finds the drift velocity expressed in terms of the mean free path between collisions of the charged particles with gas molecules. This mean free path is inversely proportional to the pressure. Its value at the pressure p will be indicated with $\lambda/p$ where $\lambda$ is the mean free path at unit pressure. The relation between $\vec{w}$ and $\lambda/p$ can be determined easily if one makes the two following crude simplifying assumptions: (a) all of the particles under consideration have the same agitation velocity u; (b) the direction of the motion of the particle after the collision is completely independent of the direction of its motion before the collision. Under these assumptions, each particle undergoes on the average $(up/\lambda)$ collisions per second, in which it loses on the average a momentum equal to $(up/\lambda)\, m\vec{w}$. On the other hand, each particle gains every second a momentum equal to $e\vec{E}$ through the action of the electric field. Hence, once equilibrium is established, the following equation holds:

$$\frac{u\, p\, m\, \vec{w}}{\lambda} = e\vec{E} \tag{13}$$

or

$$\vec{w} = \frac{e}{m}\,\frac{\lambda}{u}\,\frac{\vec{E}}{p} \tag{14}$$

Similarly, one may express the mean agitation energy $\epsilon$ in terms of $\lambda$ and of the average fractional energy loss per collision, which we shall indicate with h. The principle of conservation of energy gives the following equation:

$$\epsilon\,(3/2\,k\Theta)\,(up/\lambda)\,h = e\vec{E}\vec{w} \tag{15}$$

We know, of course, that neither of the two conditions (a) and (b) mentioned above corresponds to reality. However, we can always consider $\lambda$ and h as two quantities which are defined in terms of experimental quantities by Equations 13 and 15, and are representative of the momentum loss and of the energy loss through collisions. If we take this view, Equation 13 states the obvious fact that the momentum loss per second through collisions is proportional to the pressure, to the drift velocity and, for a given pressure and drift velocity, it depends on the nature of the gas and on the energy distribution of the particles under consideration. Similarly Equation 15 indicates merely that the energy loss per second through collisions is proportional to the pressure and that this loss depends on the nature of the gas and the energy distribution of the particles.

In practice, $\lambda$ and h can be determined as a function of $\epsilon$ for a given gas by measuring $\vec{w}$ and $\epsilon$ as a function of E/p. Equations 13 and 1 will then provide the functional relation between $\lambda$ and $\epsilon$, while Equations 15 and 1 will provide that between $h/\lambda$ and $\epsilon$.

The quantities $\lambda$ and h are particularly useful in connection with the problem of determining the behavior of electrons and ions in a mixture of gases from data relative to their behavior in the pure components. For this purpose we will make the hypothesis that the energy distribution of the charged particles whether in a mixture of gases or in any pure gas, is completely determined by their average energy $\epsilon$. It would be difficult to justify this hypothesis except by the remark that it seems to lead to results in agreement with the experimental data.

Now, let $p_o$ be the total gas pressure and let $p_1$, $p_2$, $p_3$, etc., be the partial pressures of the various components. Similarly, let $\lambda_o$ and $h_o$ be the values of $\lambda$ and h for the mixture, let $\lambda_1$, $\lambda_2$, $\lambda_3$, etc., and $h_1$, $h_2$, $h_3$, etc., be the values of the same quantities for the various components. If we write that the average momentum loss and the average energy loss of electrons or ions in the mixture are equal respectively to the sum of the average momentum losses and to the sum of the average energy losses in the separate components, we obtain from Equations 13

and 15 the following equations (after dividing each equation by a factor, which is the same for all terms since it only depends on $\vec{w}$, m, u).

$$p_o/\lambda_o = p_1/\lambda_1 + p_2/\lambda_2 + p_3/\lambda_3 + \cdots\cdots$$

$$p_o h_o/\lambda_o = p_1 h_1/\lambda_1 + p_2 h_2/\lambda_2 + p_3 h_3/\lambda_3 + \cdots\cdots \quad (16)$$

After $\lambda_o$ and $h_o$ have been calculated by means of Equation 16, Equations 13 and 15 can be used to compute $\epsilon$ and $\vec{w}$ as functions of E/p for the mixture.

The diffusion coefficient too may be expressed in terms of $\lambda$. By comparing Equations 14 and 17 one obtains the well-known relation

$$D = \frac{\lambda u}{3p} \quad (17)$$

So far we have assumed that the electric field is uniform. If the field is not uniform but does not vary appreciably over a distance of the order of one mean free path, we may still define an average agitation energy $\epsilon$; this quantity, however, as well as all the quantities which depend on $\epsilon$, like D, $\lambda$, h, will vary from point to point. The fundamental Equation 8 will still hold, provided the current produced by the gradient of "temperature" is negligible compared with that produced by the electric field or by the gradient of density.

Another question concerns the time interval between the moment when the ions are produced and the moment when they reach the equilibrium condition between loss and gain of momentum which leads to Equation 8. This time is of the order of the time between collisions $\lambda/pu$ which, at atmospheric pressure is generally between $10^{-11}$ and $10^{-12}$ seconds.

For the convenience of the reader, we list in Table 8.3-1 the symbols for the most important quantities defined above, along with the units in which they are measured.

Table 8.3-1

List of Symbols

| Symbol | Quantity | Unit |
|---|---|---|
| u | Root mean square velocity of agitation | cm/sec |
| $\epsilon$ | Average agitation energy | $(3/2)kT = 3.7 \times 10^{-2}$ eV(at 15°C) |
| w | Drift velocity | cm/sec |
| D | Diffusion coefficient | $cm^2/sec$ |
| p | Pressure | mm Hg |
| $\lambda$ | Mean free path at 1 mm Hg | cm • (mm Hg) |
| h | Fractional energy loss per collision | dimensionless |
| $\alpha$ | Attachment coefficient | $sec^{-1}$ |
| $\beta$ | Recombination constant | $cm^3/sec$ |

## 8.4 EXPERIMENTAL DATA RELATIVE TO FREE ELECTRONS

Equation 14 indicates that the drift velocity is a function of the ratio E/p. Experimental determinations of the drift velocity of electrons confirm this relation. The dependence of $\bar{w}$ on E/p is given for a number of different gases in Figures 1 to 6. Most of the data used in the construction of these graphs were taken from the book by Healey and Reed, "The Behavior of Slow Electrons in Gases", where various methods for the measurement of $\bar{w}$, $\epsilon$ and $\alpha$ are described. Some were obtained at Los Alamos by the methods described in Section 10.8.

We wish to direct attention to the data obtained with argon-$CO_2$ mixtures and shown in Figure 6. One sees that, for a given value of E/p, the drift velocity in a mixture containing a large proportion of argon and a small proportion of $CO_2$ is considerably greater than in either pure argon or pure $CO_2$ (see Figures 3 and 4). This fact, which was established through experiments carried out at Los Alamos, is of considerable practical importance for the construction of "fast" chambers. The physical reason for it can be understood through the following analysis.

Inelastic collisions between electrons and gas molecules occur only when the electrons have an energy larger than the energy of the first excitation level of the molecule. Argon is a monoatomic gas, and the first excitation level of the argon atom is 11.5 eV. Hence in pure argon, even with moderate fields, the electrons will reach a very high agitation energy, namely of the order of 10 eV or $\epsilon \approx 300$. This is confirmed by direct measurements, as shown in Figure 9. In $CO_2$, however, inelastic collisions occur very frequently for small electron energies, because of the large number of low excitation levels of the $CO_2$ molecule. It follows that the addition of a small amount of $CO_2$ to argon will reduce the average energy of the electrons considerably (from about 10 eV to about 1 eV, with 10 per cent $CO_2$ and E/p = 1). In a mixture containing only a small amount of $CO_2$, the drift velocity is limited mainly by the collisions with the argon molecules. The mean free path of electrons in argon increases rapidly with decreasing energy in the energy region between 10 and 1 eV, a phenomenon known as the Ramsauer effect.

Figure 1

Drift Velocity of Electrons as a Function of E/p in $H_2$ and $N_2$
(Townsend and Bailey; H.R. pp. 92, 93)

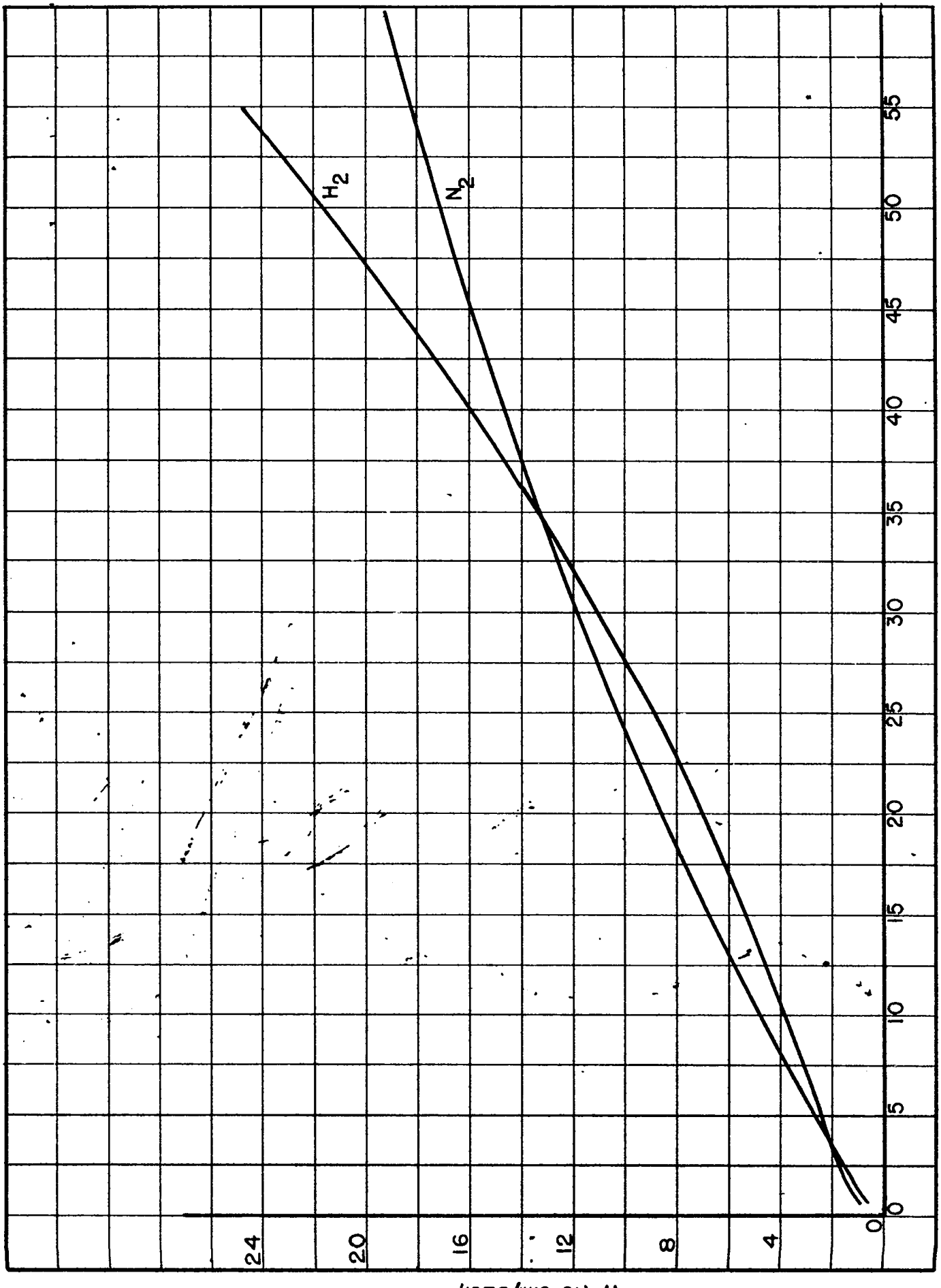

Figure 2

Drift Velocity of Electrons as a Function of E/p in He and in Ne Containing 1 per cent of He.
(Townsend and Bailey; H.R., pp. 89, 90)

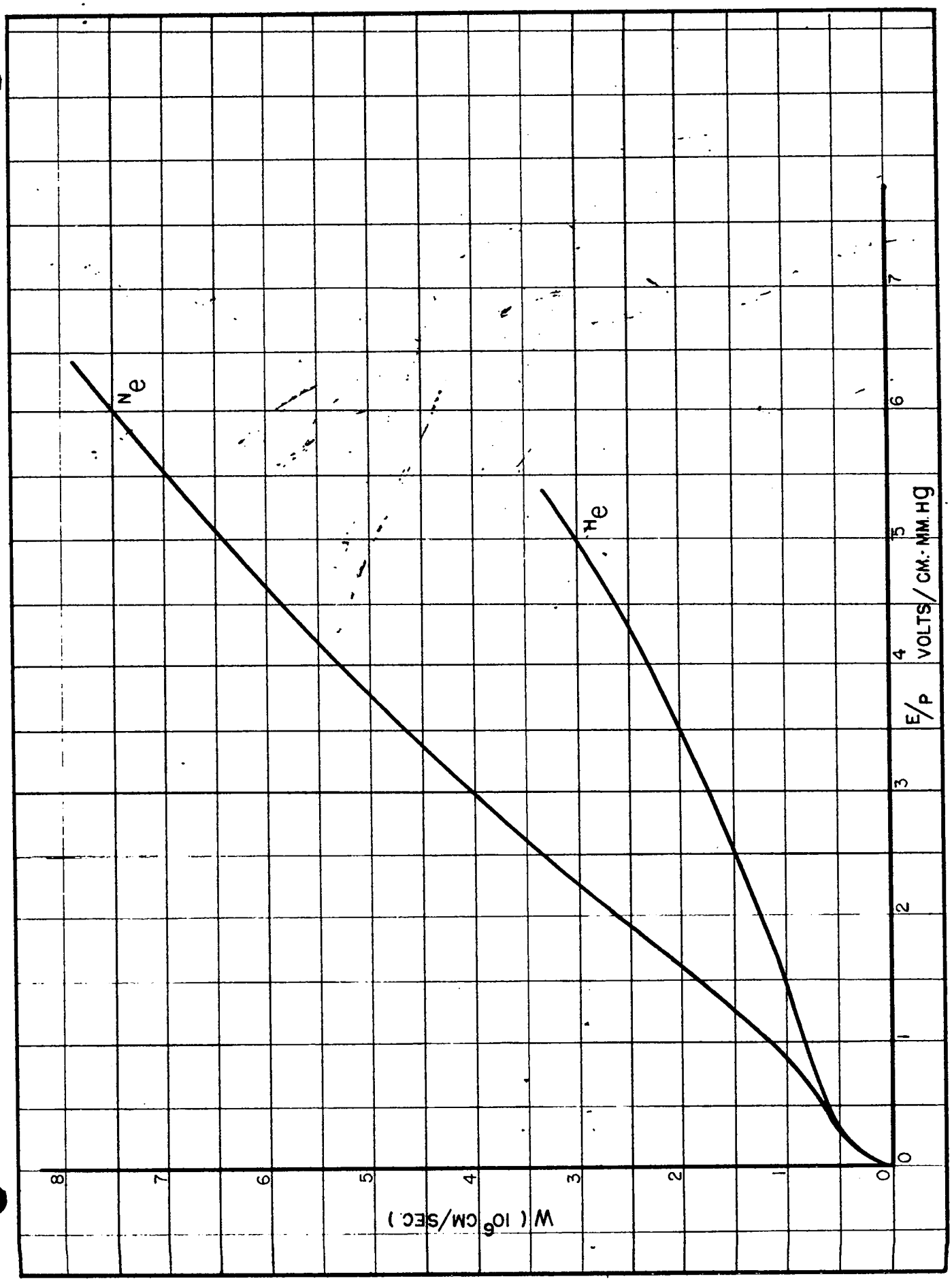

Figure 3

Drift Velocity of Electrons as a Function of E/p in Argon.

△ Townsend and Bailey; H.R., p. 91.
○ Los Alamos, p = 84 mm Hg
+ Los Alamos, p = 1274 mm Hg

The Los Alamos data at p = 86 mm Hg were obtained from observation of $\alpha$-particle pulses, as described in Section 10.8. Their accuracy was estimated to be about 20 per cent. The data at p = 1274 mm Hg were obtained by means of the pulsed x-ray source, as described in Section 10.8. Their accuracy was estimated to be about 5 per cent. The disagreement between the various sets of measurements is very striking and not easily explained, especially if compared with the good agreement obtained for $CO_2$ with different methods (see Figure 4). It is possible that it may be due, in part at least, to different degrees of purity of the gases used, since the drift velocity in argon is strongly affected by impurities.

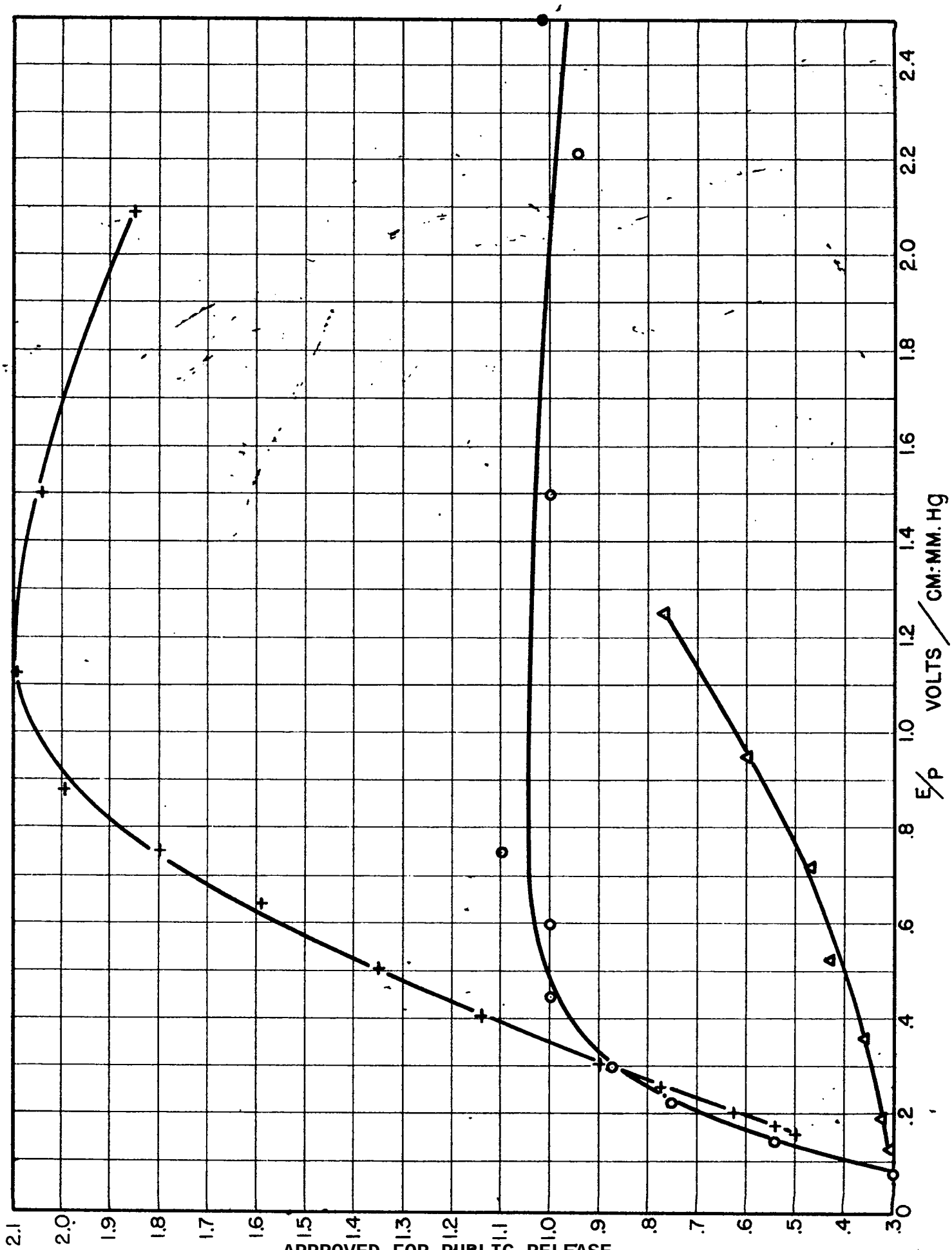

Figure 4

Drift Velocity of Electrons as a Function of E/p in $CO_2$

□ Rudd (see H.R., p.98)
x Skinker (see H.R., p. 99)
△ Los Alamos, p = 660 mm Hg
○ Los Alamos, p = 305 mm Hg
◇ Los Alamos, p = 160 mm Hg

The Los Alamos data were obtained from observation of $\alpha$-particle pulses as described in Section 10.8.

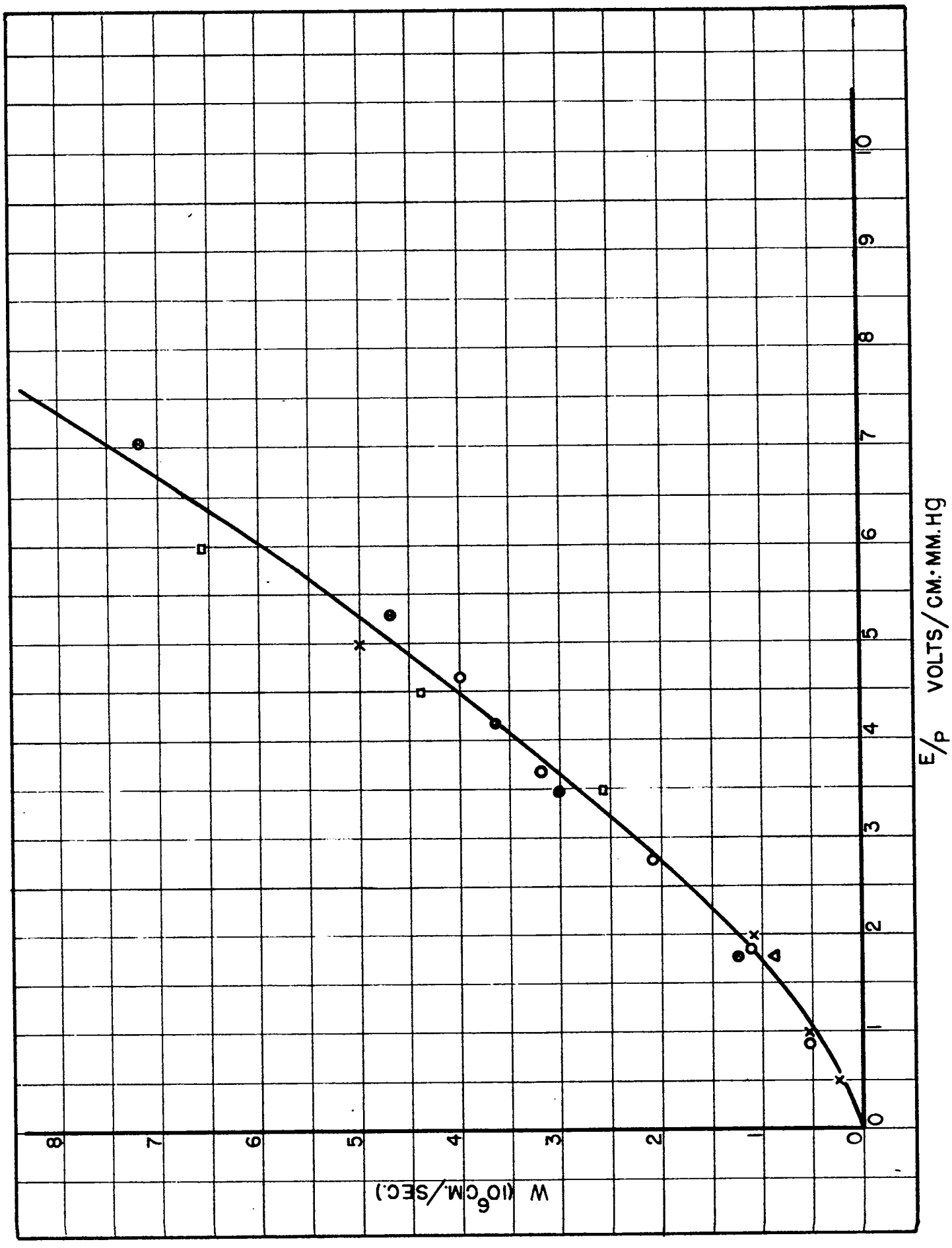

Figure 5

Drift Velocity of Electrons as a Function of E/p in $BF_3$

△ $BF_3$ from $C_6H_5N_2BF_4$, p = 379 mm Hg
○ $BF_3$ from tank p = 388 mm Hg
× $BF_3$ from $C_6H_5N_2BF_4$, p = 339 mm Hg
□ $BF_3$ from tank, p = 294 mm Hg
The data were obtained from observation of $\alpha$-particle pulses as described in Section 10.8.

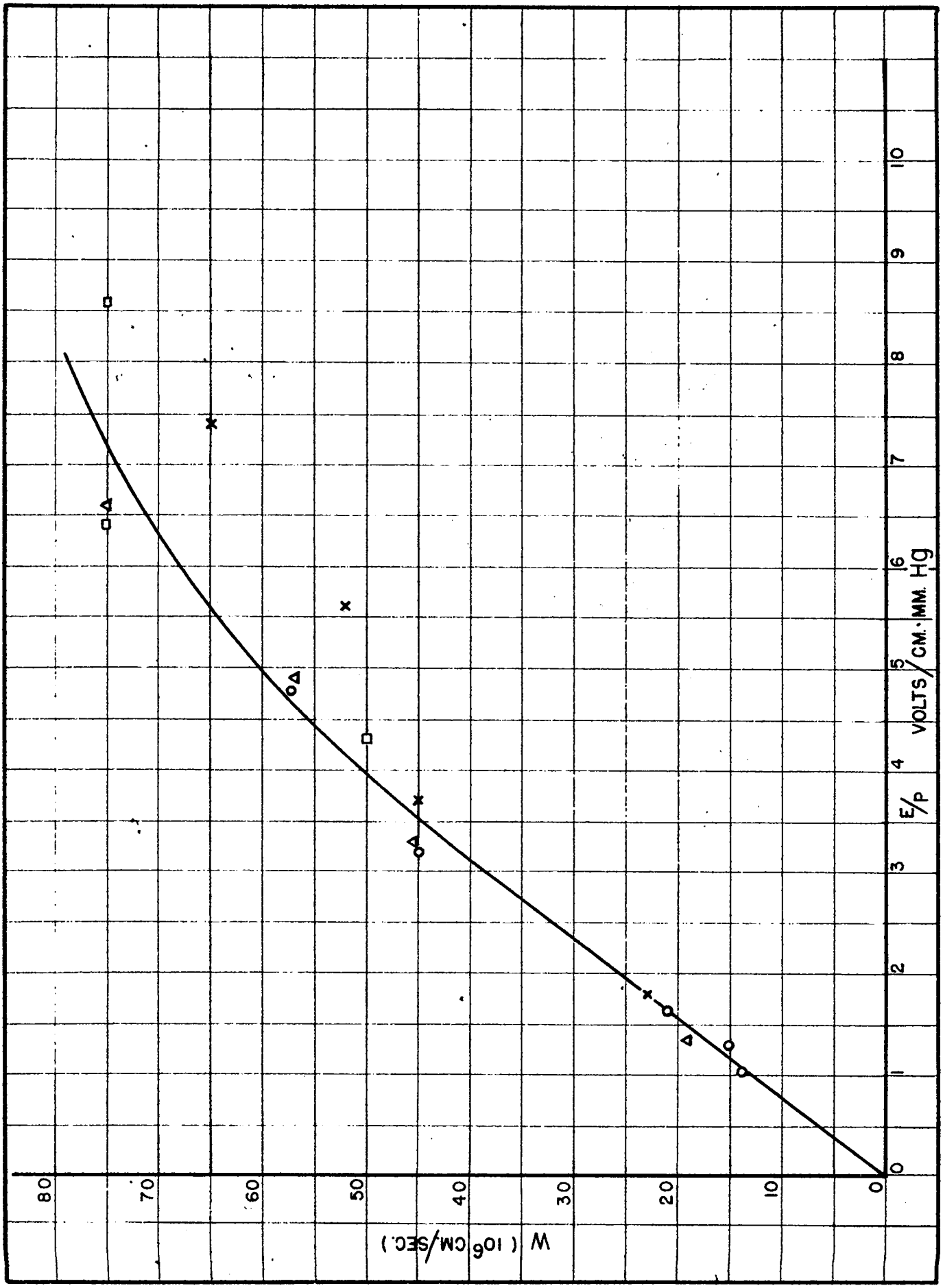

Figure 6

Drift Velocity of Electrons as a Function of E/p in mixtures of Argon and $CO_2$. (The data were obtained from observation of $\alpha$ -particle pulses as described in Section 10.8).

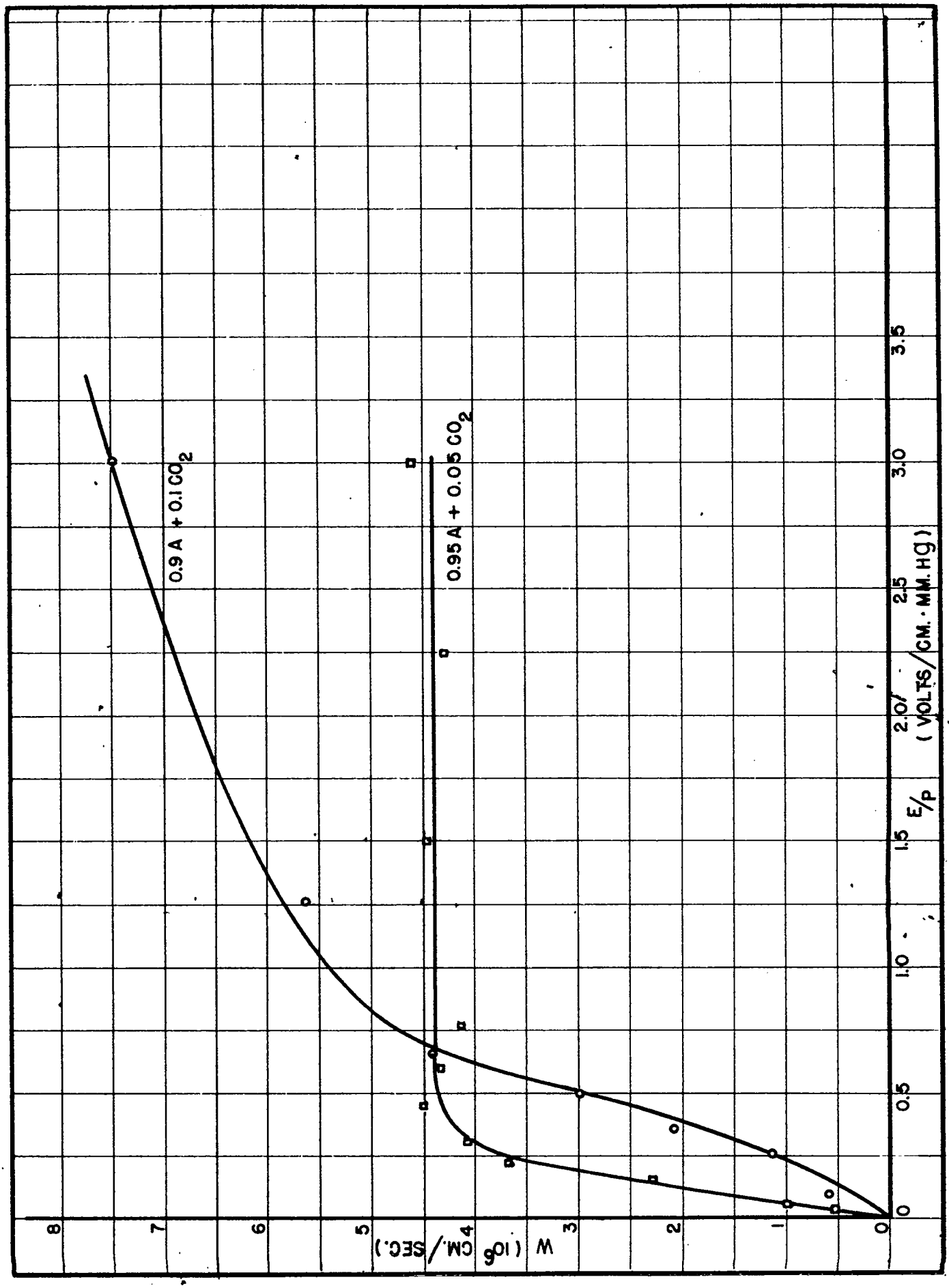

Since the drift velocity is directly proportional to the mean free path and inversely proportional to the square root of the agitation energy (see Equation 14) the decrease of the latter quantity caused by the addition of $CO_2$ to argon will, in two ways, result in an increase of the drift velocity. We wish to remark here that the experimental values of drift velocities are by no means as accurate as one would desire. This applies also to the values obtained recently at the Los Alamos Laboratories. Here the pressure under which the work was conducted made it impossible to carry out measurements of high precision when high precision was not needed for the immediate objective to be achieved. It is felt, however, that the methods developed at Los Alamos (see Section 10.8), when properly applied, would be capable of yielding accurate results.

The average agitation energy $\epsilon$, according to Equation 15, is also a function of E/p. Figures 7 to 10 give the dependence of $\epsilon$ on E/p for free electrons and for a number of different gases. The experimental data was taken from the book by Healey and Reed, quoted above.

The attachment coefficient $\alpha$ is practically zero for $H_2$, He, A, N, $CO_2$ if these gases are sufficiently pure. Some experimental data on the attachment of electrons in two of the most common impurities, namely $O_2$ and $H_2O$, are summarized in Figure 11. The ordinates in this figure give the ratio $\alpha/pw$ which represents the probability for electrons to attach themselves to a gas molecule while traveling one centimeter in the direction of the field in the gas at 1 mm Hg of pressure.

No reliable data on the recombination of electrons with positive ions are available. According to Kenty, as quoted by Loeb (Fundamental Processes of Electric Discharge in Gases, Wiley, 1939, p. 158) the approximate value of the recombination constant for electrons in argon is

$$\beta = 2 \times 10^{-10} \text{ cm}^3/\text{sec}$$

The values of $\beta$ for other gases do not seem to differ materially from that

Figure 7

Mean Electron Energy as a Function of E/p for $H_2$ and $N_2$
(Townsend and Bailey; H.P., pp. 92, 93)

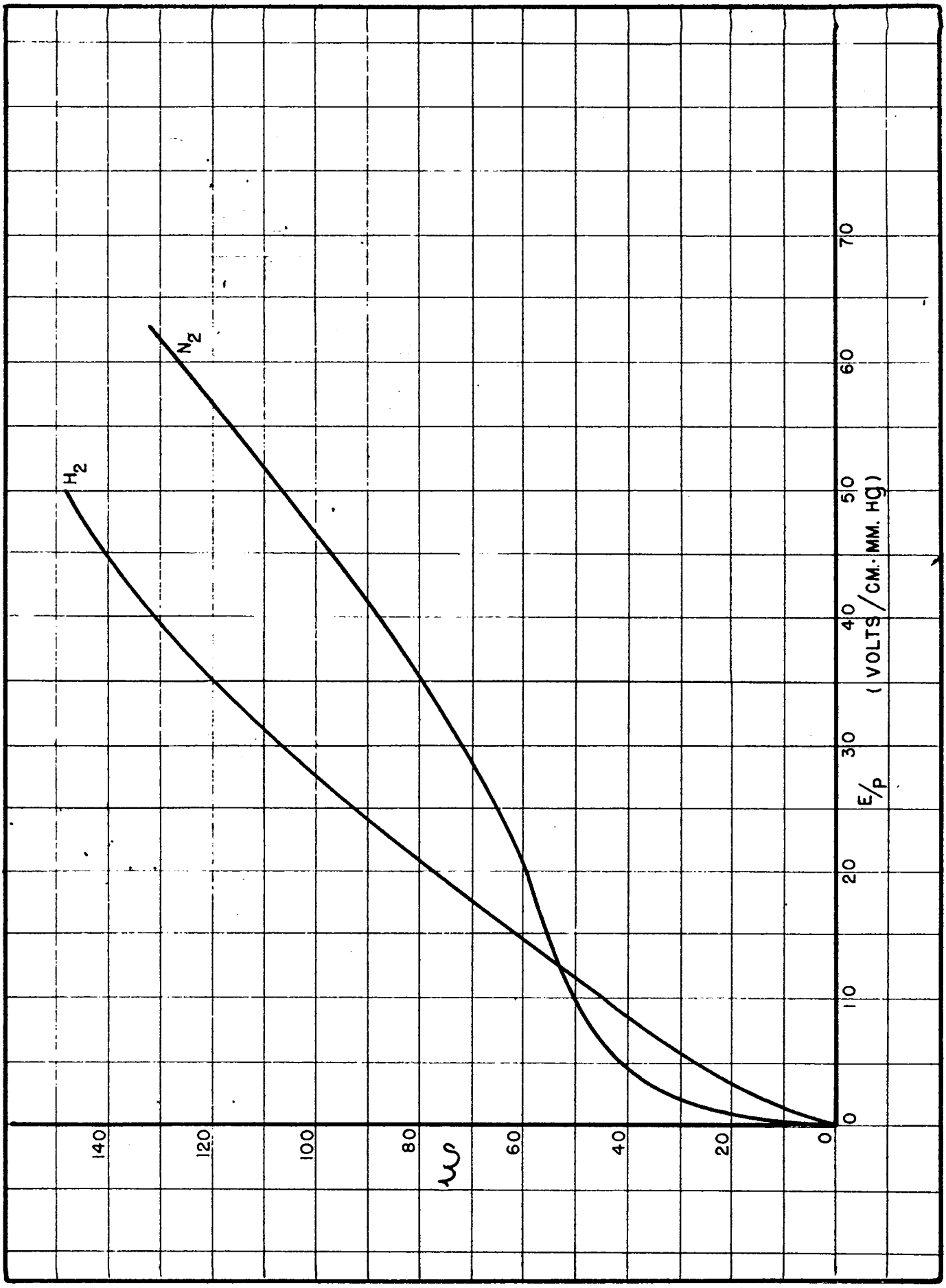

Figure 8

Mean Electron Energy as a Function of E/p for He and Ne.

(Townsend and Bailey; H.R., pp. 89,90)

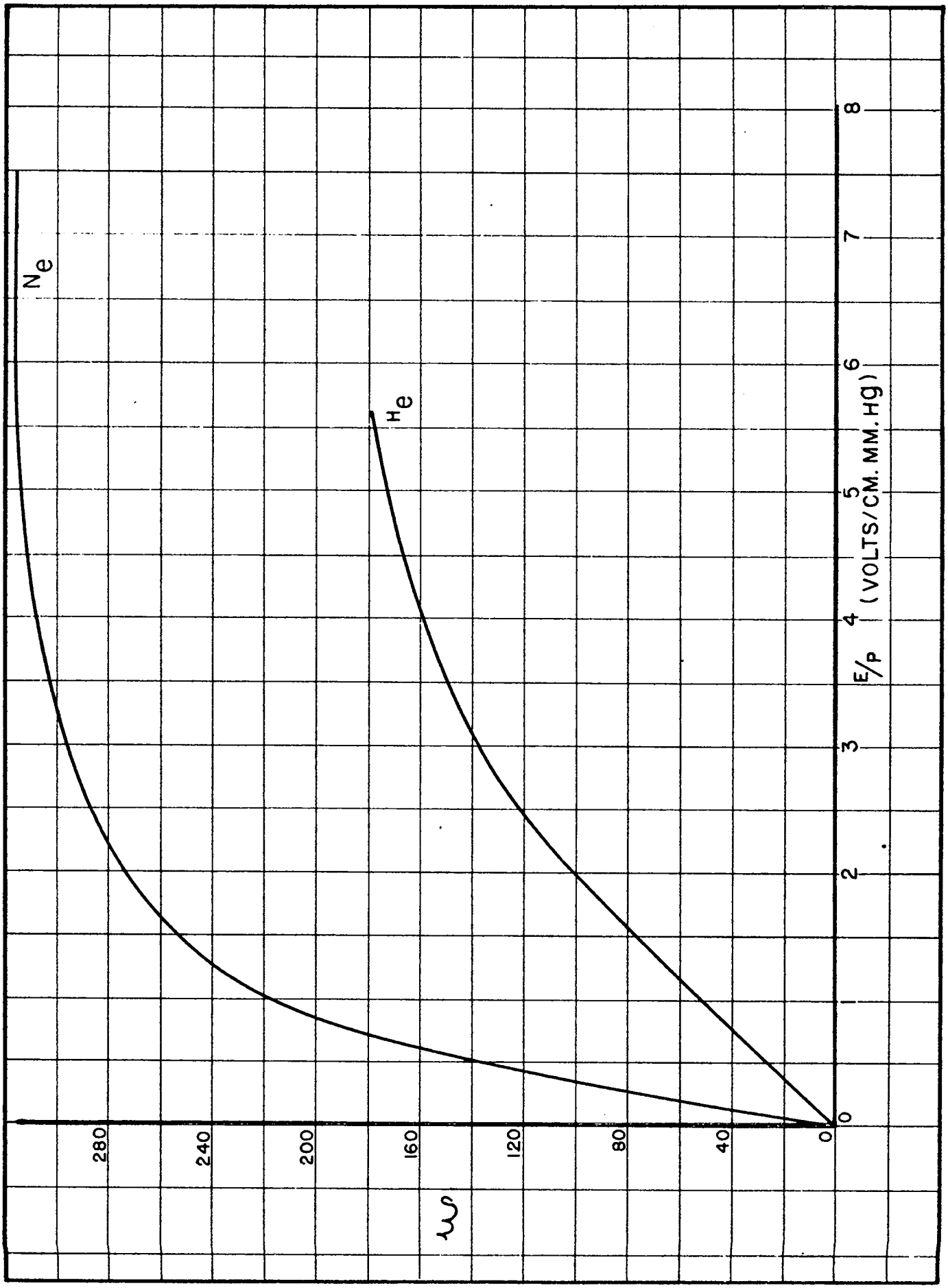

Figure 9

Mean Electron Energy as a Function of E/p for Argon.

(Townsend and Bailey; H.R., p. 91)

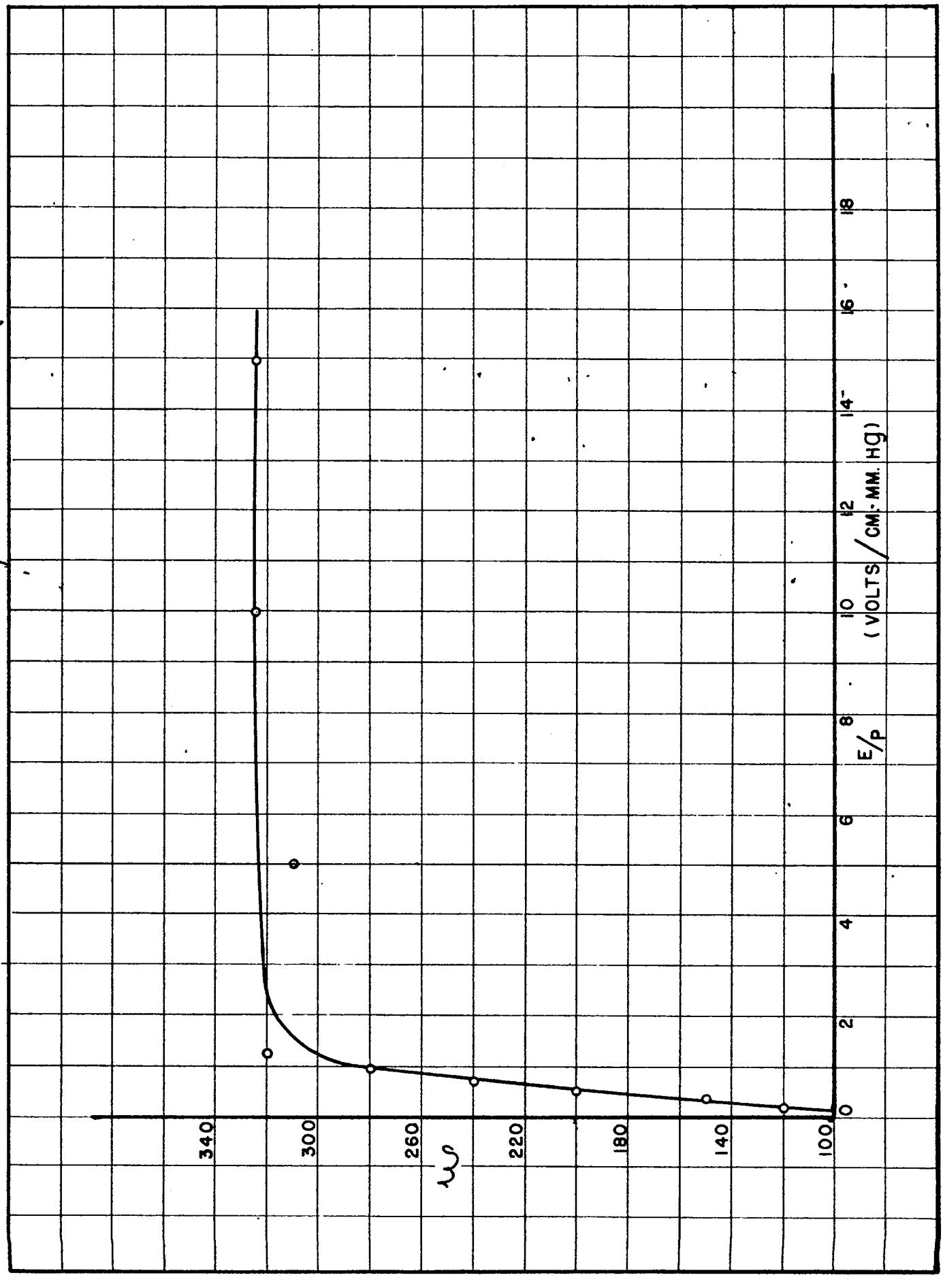

Figure 10

Mean Electron Energy as a Function of E/p for $CO_2$

(Rudd, Skinker; H.R., pp. 98, 99)

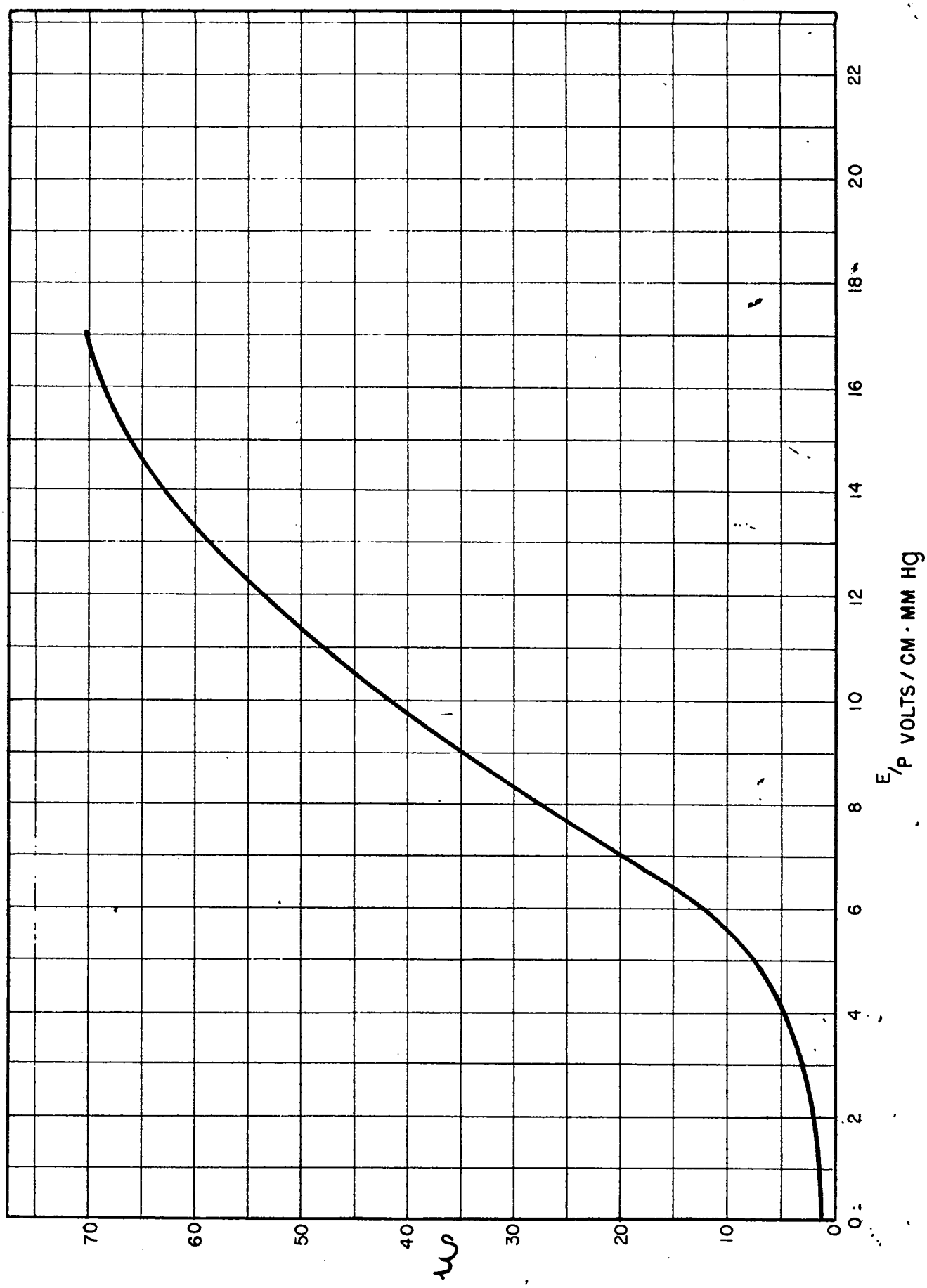

Figure 11

Probability for Electron Attachment per cm Path at 1 mm Hg as a Function of E/p in $O_2$ and $H_2O$ (Healey and Kirkpatrick; Bailey and Duncanson; H.R., pp. 94, 99)

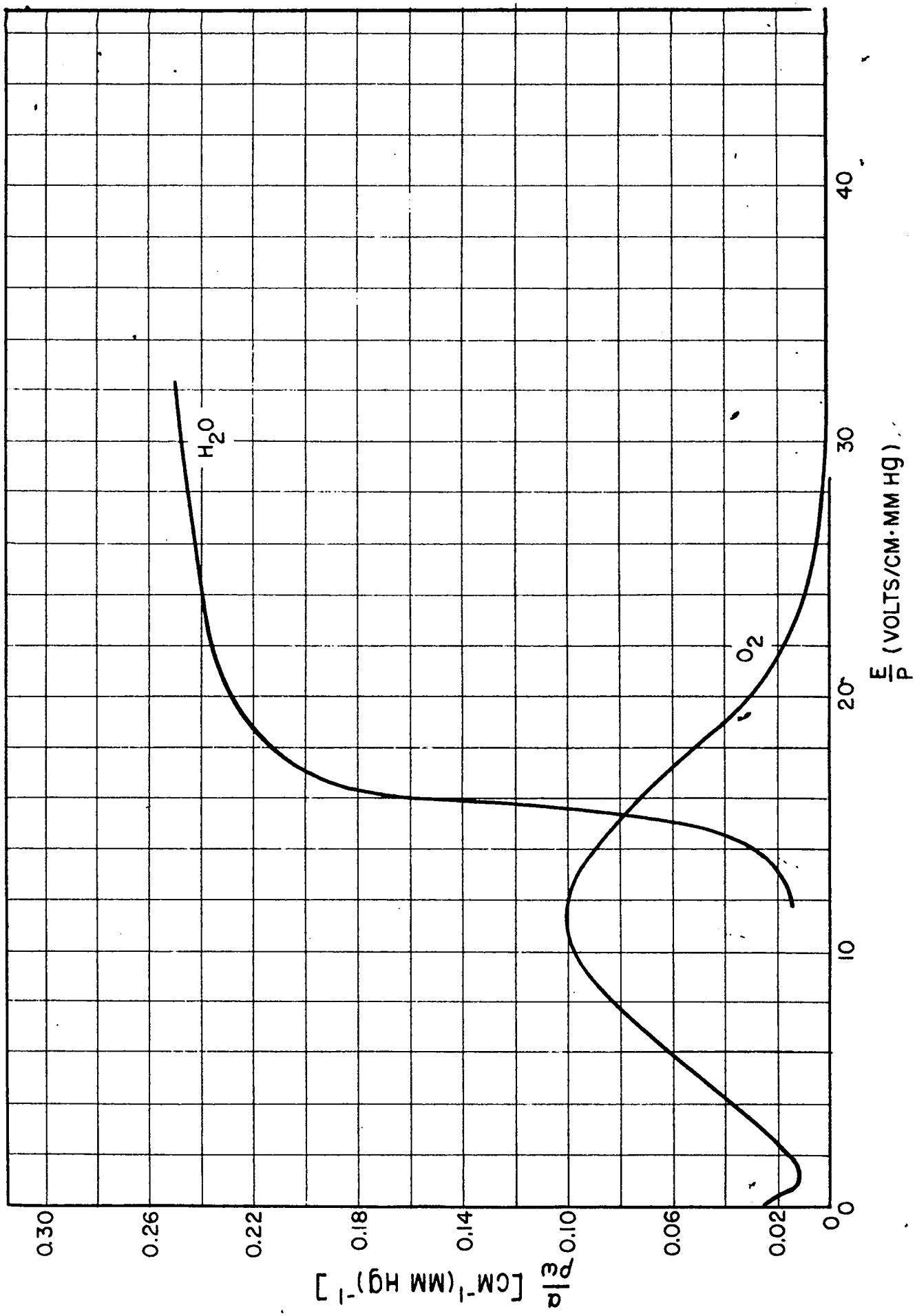

relative to argon. It must be pointed out here that the ions are seldom uniformly distributed in the volume of the gas. This is especially true when the ionization is produced by heavily ionizing particles like $\alpha$-particles. In this case, of course, the actual density of positive ions at the place where electrons are present determines the recombination rate, and this density may be considerably higher than the average volume density, at least as long as electrons and positive ions have not diffused sufficiently far from the place where they have both been produced. The recombination of positive ions with electrons (or negative ions), which takes place before diffusion spreads these particles apart, is often referred to as "preferential recombination" or "columnar recombination".

The root mean square velocity of agitation u, the diffusion coefficient D, the mean free path $\lambda$, and the fractional energy loss per collision $h$ can all be obtained from the experimental values of w and $\epsilon$, as explained in Section 3. A significant quantity is $\sqrt{2D/w}$, which gives a measure for the lateral diffusion which electrons undergo while travelling a distance of one centimeter in the gas (see Equations 11 and 12). This quantity is related to the average agitation energy $\epsilon$ by the simple equation

$$\sqrt{2D/w} = \sqrt{\frac{2kT\epsilon}{eE}} = \sqrt{\frac{5 \times 10^{-2}}{E}}\sqrt{\epsilon} \qquad (18)$$

where E is measured in volts per centimeter and $\sqrt{2D/w}$ in $cm^{\frac{1}{2}}$. The values of w, $\epsilon$, u, $\lambda/p$, $\sqrt{2D/w}$ for various gases at 1 atmosphere (760 mm Hg) pressure, and with E = 760 volts/cm (E/p = 1), are listed in Table 8.4-1.

Table 8.4-1

Drift velocity (w), average agitation energy ($\epsilon$), root mean square agitation velocity (u), mean free path ($\lambda/p$) and lateral diffusion per cm path ($\sqrt{2D/w}$) for electrons in various gases at 1 atmosphere pressure, with E = 760 volts/cm (E/p = 1). Values derived from the tables given by H.R.

| Gas | $w(10^6 cm/sec)$ | $\epsilon$ | $u(10^6 cm/sec)$ | $\lambda/p(10^{-4} cm)$ | $\sqrt{2D/w}\ (10^{-2} cm^{\frac{1}{2}})$ |
|---|---|---|---|---|---|
| $H_2$ | 1.2 | 9.3 | 35 | 0.3 | 2.5 |
| He | 0.8 | 53 | 84 | 0.5 | 6 |
| Ne | 1.2 | 214 | 168 | 1.5 | 12 |
| A | 0.6 | 287 | 195 | 0.9 | 14 |
| $N_2$ | 0.9 | 21.5 | 53 | 0.3 | 3.7 |
| $CO_2$ | 0.55 | 1.5 | 14 | 0.06 | 1.0 |

## 8.5 EXPERIMENTAL DATA RELATIVE TO POSITIVE AND NEGATIVE IONS.

A large number of experiments have shown that the drift velocities of positive and negative ions for a given gas and for a given pressure are quite accurately proportional to the electric field strength.

$$|\vec{w}| = \mu |\vec{E}| \qquad (19)$$

The proportionality factor $\mu$ is called the mobility, and is measured in cm/sec per volt/cm (or $cm^2$/volt sec). For a given gas and a given electric field, the mobility is inversely proportional to the pressure.

The values of $\mu$ for positive ions in a number of gases are listed in Table 8.5-1. These values were taken from the article of Loeb in "International Critical Tables" (1929, Vol. VI, p. 111). The mobilities of negative ions, when negative ions exist, are nearly equal, but generally slightly larger, than those of the corresponding positive ions.

Table 8.5-1

Mobilities and diffusion coefficients of positive ions in various gases at one atmosphere pressure ( p = 760 mm Hg)

| Gas | $H_2$ | He | A | $N_2$ | $O_2$ | $CO_2$ | Air | Ethane |
|---|---|---|---|---|---|---|---|---|
| $\mu$ (cm/sec per volt/cm) | 5-6 | 5.1 | 1.3 | 1.3 | 1.3 | 0.8 | 1.3-1.4 | 1.07 (neg.ions) |
| D ($10^{-2}$ $cm^2$/sec) | 12 | -- | -- | 3 | 2.5-3.0 | 2.5 | 2.8 | |

The diffusion coefficient D, according to Equation 7' is related to the mobility $\mu$ by the following equation

$$D = \frac{\varepsilon}{e} kT \mu \qquad (20)$$

If one recalls that $kT/e = 2.5 \times 10^{-2}$ volts and if one remembers that for positive or negative ions, $\epsilon$ is always close to one, one can write

$$D = 2.5 \times 10^{-2} \mu \text{ cm}^2/\text{sec} \qquad (21)$$

In Table 8.5-1 some experimental values of D at one atmosphere pressure are listed along with the corresponding values of $\mu$ (from International Critical Tables Volume VI, p. 115). On account of the moderate accuracy in the measurements of both D and $\mu$, Equation 21 may be considered as fairly well verified.

The data on the recombination of positive and negative ions are very inaccurate. For most gases the values of the recombination constant $\beta$ seem to be between 1 and $2 \times 10^{-6}$ $\text{cm}^3/\text{sec}$, which is about $10^4$ times larger than the recombination constant between positive ions and electrons.

# CHAPTER 9

# OPERATION OF IONIZATION CHAMBERS WITH CONSTANT IONIZATION

## 9.1 GENERAL DESIGN OF AN IONIZATION CHAMBER

The essential parts of an ionization chamber are two electrodes kept at different potentials and a gas which fills the space between the two electrodes. The electrode to which the measuring instrument is attached is called the collecting electrode. The collecting electrode is ordinarily (but not necessarily) at a potential close to ground potential. The other electrode, which is ordinarily kept at a constant voltage, $V_0$, of several hundred to several thousand volts, is called the high voltage electrode. The collecting electrode is usually supported through insulators by another electrode which is held at a constant voltage, approximately equal to that of the collecting electrode itself, and is called the guard electrode. This, in turn, is connected through insulators to the high voltage electrode. The purpose of the guard electrode is to prevent leakage currents from reaching the collecting electrode. Also, the guard electrode is usually so shaped as to prevent irregularities of the electric field near the edges of the collecting electrode. The general design of an ionization chamber is schematically represented in Figure 1.

Let us consider the volume limited by the surface of the collecting electrode, the tube of force passing through the periphery of the collecting electrode and that portion of the high voltage electrode which is intercepted by this tube of force. This volume will be called the sensitive volume of the chamber. Every ion of sign opposite to

Figure 1

Schematic diagram of an ionization chamber.

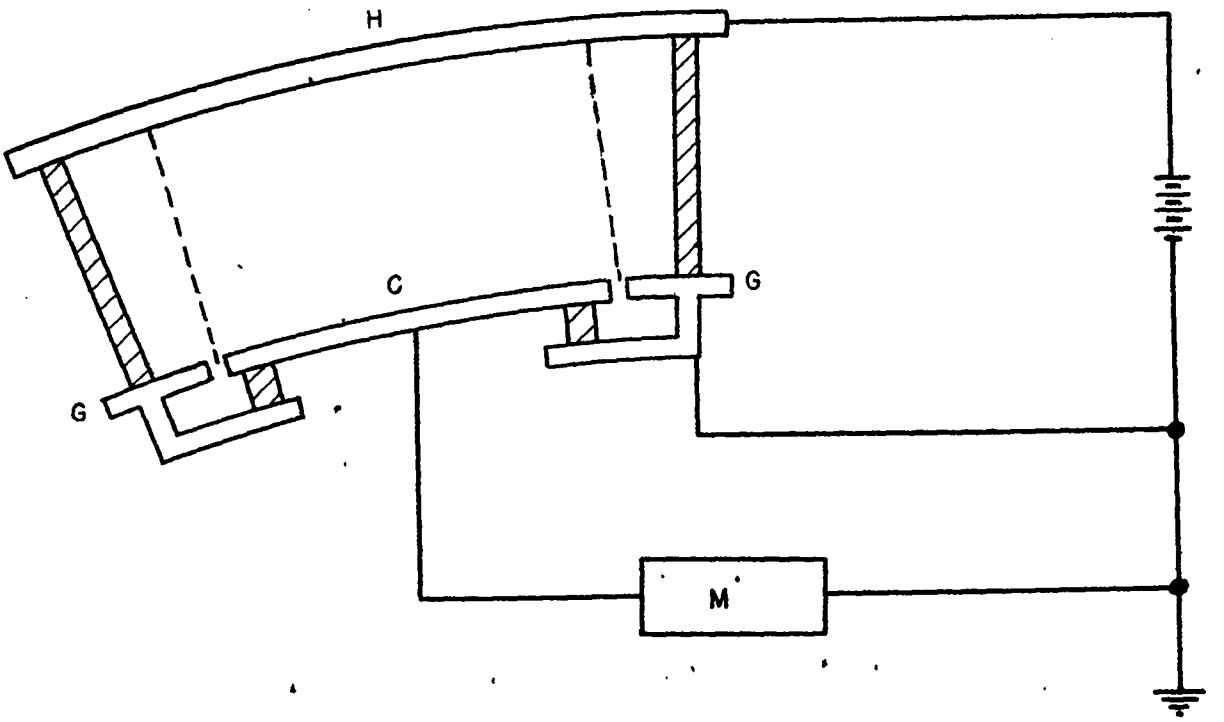

that of the collecting electrode formed within the sensitive volume will reach the collecting electrode, provided diffusion and recombination can be neglected.

## 9.2 CONSTANT IONIZATION; DIFFUSION AND RECOMBINATION NEGLECTED

Let us assume now that the ionization chamber is irradiated with a source of ionization of constant intensity, and let $n_0(x,y,z)$ be the number of ion pairs produced per unit volume and per unit time at the point $(x,y,z)$. Let $n^+(x,y,z)$ and $n^-(x,y,z)$ be the densities of positive and negative carriers, respectively; let $\vec{w}^+(x,y,z)$ and $\vec{w}^-(x,y,z)$ be their drift velocities. For the sake of simplicity we will assume that the negative carriers are all of one kind, i.e., either free electrons (no attachment) or negative ions (complete attachment). If we neglect diffusion the current vectors for the positive and negative particles are given by

$$\vec{j}^+ = n^+\vec{w}^+, \quad \vec{j}^- = n^-\vec{w}^- \tag{1}$$

If we moreover assume that no recombination takes place, the following equations hold:

$$\text{div } \vec{j}^+ = \text{div } \vec{j}^- = n_0 \tag{2}$$

The density of electric current has the expression

$$e\vec{j} = e(\vec{j}^+ - \vec{j}^-) = e(n^+\vec{w}^+ - n^-\vec{w}^-) \tag{3}$$

and from Equation 2 it follows

$$\text{div } \vec{j} = 0 \tag{4}$$

If we neglect diffusion, $\vec{j}$ is parallel to the lines of force, and it follows from Equation 4 that the total current through any surface intercepted by the lateral boundary of the sensitive volume has the same value I. This may be called the ionization current in the chamber. We may expect I to equal the product of e times the number

of ion pairs formed in the chamber per second:

$$I = e\int_A n_o \, dA \qquad (5)$$

where A is the sensitive volume of the chamber. Actually, Equation 5 can be easily shown to be a consequence of Equations 1, 2 and 3. Suppose, for instance, that the collecting electrode is negative. We have:

$$\int_A n_o \, dA = \int_A \text{div} \, (n^+ \vec{w}^+) \, dA = \int_S n^+ \vec{w}_n^+ \, dS$$

where S is the surface which limits the sensitive volume and $\vec{w}_n^+$ indicates the component of $\vec{w}^+$ in a direction perpendicular to this surface and pointing towards the outside of the sensitive volume. Now $\vec{w}_n^+$ is zero along the lateral surface, while $n^+$ is zero on the surface of the high voltage electrode which is assumed to be positive. This can be easily seen if one realizes that the positive ions, as soon as they are formed, drift away from the positive electrode and are not replaced by positive ions coming from behind this surface. For the same reason, $n^-$ is zero at the surface of the collecting electrode. Hence, if we indicate with $S^-$ the surface of the collecting electrode, we have:

$$e\int_A n_o \, d\,A = e\int_{S^-} n^+ \vec{w}_n^+ \, d\,S = e\int_{S^-} \vec{j}_n \, d\,S$$

which proves Equation 5.

Thus the problem of determining the ionization current when diffusion and recombination are neglected is a trivial one.

We will discuss next the problem of determining, under the same assumptions, the space charge distribution, which is defined by

$$\rho = e\,(n^+ - n^-) \qquad (6)$$

For the determination of $\rho$ we must consider, in addition to Equations 1, 2 and 6, the equations for the electric field strength

$$\operatorname{div} \vec{E} = 4\pi\rho \tag{7}$$

$$\operatorname{curl} \vec{E} = 0 \tag{8}$$

and the equations which relate $\vec{w}^+$ and $\vec{w}^-$ to $\vec{E}$.

The mathematical problem is, in general, rather involved. However, it becomes easy to handle in the case of some simple geometries or when the density of ionization is sufficiently small so as not to affect appreciably the field stength (and therefore the drift velocities).

Consider, for instance, a parallel plate chamber. We assume that its collecting electrode is surrounded by an appropriate guard electrode so that the electric field is practically uniform up to the boundary of the sensitive volume. We take as a frame of reference a cartesian coordinate system with its origin on the positive electrode and its x axis in the direction of the electric field. Let us suppose that the chamber is uniformly irradiated over the active volume and outside of it for a sufficient distance from its boundary so that any additional electric field produced by the space charge is also parallel to the x axis and independent of the y,z coordinates.

The problem then becomes one dimensional and Equation 2 can be integrated immediately. If Equation 1 and the boundary conditions at the two electrodes are taken into account, one obtains:

$$\begin{aligned} n^+ w_x^+ &= n^+ w^+ = n_0 x \\ -n^- w_x^- &= n^- w^- = n_0 (d - x) \end{aligned} \tag{9}$$

where d is the separation of the electrodes and $w^+$, $w^-$ are the absolute values of the drift velocities. Equation 7 now becomes:

$$\frac{dE}{dx} = 4\pi e\, n_0 \left[ x/w^+ - (d-x)/w^- \right] \tag{10}$$

If $w^+$ and $w^-$ are known functions of E, Equation 10 can be solved, at least in principle.

The problem can be simplified if we remember that $w^+$ is proportional to E and so is $w^-$ if the negative carriers are ions. In this case, by introducing the mobilities $\mu^+$ and $\mu^-$, Equation 10 becomes:

$$\frac{dE}{dx} = 4\pi e \frac{n_0}{E} \left( \frac{x}{\mu^+} - \frac{d-x}{\mu^-} \right) \tag{11}$$

which gives:

$$E^2 + \text{const.} = 4\pi e n_0 \left( \frac{x^2}{\mu^+} + \frac{(d-x)^2}{\mu^-} \right) \tag{12}$$

where the constant is determined by the condition

$$\int_0^d E \, dx = V_0 \tag{13}$$

On the other hand, if the negative carriers are electrons, then $w^-$ is of the order of 1000 times $w^+$ and no large error is made by neglecting the second term in the parentheses of Equation 10, so that one obtains:

$$E^2 + \text{const.} = \frac{4\pi e n_0}{\mu^+} x^2 \tag{14}$$

Let us now simplify the problem further by assuming that the electric field produced by the space charge is small compared with the externally applied field; i.e., let us put

$$E = V_0/d + E_\rho$$

with

$$E_\rho \ll V_0/d$$

Equation 13 gives for $E_\rho$ the condition $\int E_\rho \, dx = 0$. Then $w^+$ and $w^-$ in Equation 10 can be considered as constant. In the case of negative ions, and under the assumption that the mobilities of positive and negative ions are the same, ($w^+ = w^- = w$), one obtains:

$$
\begin{aligned}
E_\rho &= \frac{4\pi e\, n_0}{w} \quad (x^2 - xd + d^2/6) \\
n^+ &= \frac{n_0}{w}\, x \\
n^- &= \frac{n_0}{w}\, (d-x) \\
\rho &= e\, \frac{n_0}{w}\, (2x - d)
\end{aligned}
\tag{15}
$$

In the case of free electrons and again under the assumption

$$E_\rho \ll V_0/d$$

the solution is:

$$
\begin{aligned}
E_\rho &= \frac{2\pi e\, n_0}{w^+} \quad (x^2 - d^2/3) \\
n^+ &= \frac{n_0}{w^+}\, x \\
n^- &= \frac{n_0}{w^-}\, (d-x) \approx 0 \\
\rho &= e\, \frac{n_0}{w^+}\, x
\end{aligned}
\tag{16}
$$

## 9.3 CONSTANT IONIZATION: DIFFUSION AND RECOMBINATION NOT NEGLECTED

If the diffusion is taken into account, then the expressions for the current vectors $\vec{j}^+$ and $\vec{j}^-$ are (see Equation 8.8):

$$
\begin{aligned}
\vec{j}^+ &= n^+ \vec{w}^+ - D^+ \operatorname{grad} n^+ \\
\vec{j}^- &= n^- \vec{w}^- - D^- \operatorname{grad} n^-
\end{aligned}
\tag{17}
$$

while, if recombination is not neglected, Equations 2 are replaced by the following equations:

$$\operatorname{div} \vec{j}^+ = \operatorname{div} \vec{j}^- = n_0 - \beta n^+ n^- \tag{18}$$

The density of electric current is still given by the equation:

$$\vec{ej} = e\,(\vec{j}^+ - \vec{j}^-) \tag{19}$$

However, $\vec{j}$ is no longer parallel to the lines of force; hence the total electric current will no longer be the same across every surface intercepted by the lateral boundary of the sensitive volume, and the current I through the measuring instrument will no longer equal the total charge $e\int_A n_0 \, d\,A$ produced within the sensitive volume in the unit time. The current I can be calculated easily if one assumes that the effects of recombination and diffusion are small so that they may be treated as corrections. If, for instance, the collecting electrode is negative, I has the expression

$$I = e\int_{S^-}(j_n^+ - j_n^-)\,i\,S = e\int_A n_0 \, d\,A - e\int_A n^+ n^- dA - e\int_{S^-} j_n^- \, dS - e\int_{S^+} j_n^+ \, d\,S - e\int_{S_\ell} j_n^+ \, d\,S$$

where $S_\ell$ is the lateral boundary of the sensitive volume; $S^+$ is the boundary at the positive electrode.

For $j^+$ and $j^-$ we substitute the expressions given by Equations 17 in which, according to our assumption, $n^+$ and $n^-$ are calculated by disregarding the effects of recombination and diffusion (see Section 2). Since $n^+$ is zero at $S^+$, $n^-$ is zero at $S^-$ and $w_n$ is zero at $S_\ell$, we obtain:

$$\begin{aligned} I = {} & e\int_A n_0 \, d\,A - e\int_A \beta n^+ n^- d\,A \\ & + e\int_{S^-} D^- (\text{grad } n^-)_n \, d\,S + e\int_{S^+} D^+ (\text{grad } n^+)_n \, dS \\ & + e\int_{S_\ell} D^+ (\text{grad } n^+)_n \, d\,S \end{aligned} \qquad (20)$$

The physical interpretation of Equation 20 is quite simple. The number of positive charges entering the collecting(negative)electrode is equal to the number of positive ions formed in the active volume (first term), minus the number of positive ions which recombine (second term), minus the number of positive ions which diffuse back to the positive electrode (fourth term, always negative), minus (or plus) the number of positive ions which diffuse

out of (or into) the sensitive volume through its lateral boundary (fifth term). In order to obtain the current in the measuring instrument from the number of positive charges entering the collecting electrode, one must subtract the number of negative charges which diffuse back to this electrode (third term, always negative). The term $e\int_A n_0 \, d\,A$, which represents the saturation current, is independent of the voltage applied, except insofar as the lateral boundary of the sensitive volume is modified by the field produced by the space charge. The other terms decrease with increasing voltage. In the above calculation, the hypothesis has been made that the reflection coefficient of the electrodes for electrons and ions is negligible, so that every charged particle which impinges upon a given electrode is captured.

Such a hypothesis did not enter in the calculation of the current carried out in Section 2. In fact, when diffusion is negligible, ions of a given sign always end up on the electrode of the opposite sign, even if some of them are reflected when they first impinge upon it. When, however, the diffusion is appreciable, a certain number of ions diffuse back to the electrode of the same sign. If some of these ions are reflected, the electric field will most likely prevent them from reaching this electrode again. On account of the small velocity of electrons and ions in gases, the hypothesis that the reflection coefficient is negligible is probably verified quite accurately in all cases of practical importance.

Let us consider now, as an example, a parallel plate chamber, uniformly irradiated over its active volume and beyond it for a sufficient distance from the edge of the collecting electrode. Then the last term in Equation 20 is zero.

If we use the values of $n^+$, $n^-$ given by Equations 15 or 16 and indicate with S the surface of the collecting electrode, the expression for I becomes:

$$I/S = e\, n_o d - e\beta \frac{n_o^2}{w^+ w^-} \frac{d^3}{6} \qquad (21)$$

$$- e\, D^- \frac{n_o}{w^-} - e\, D^+ \frac{n_o}{w^+}$$

The fractional values of the last two terms which represent the lack of saturation caused by diffusion have expressions of the type

$$D/d\, w = \epsilon (2.5 \times 10^{-2} / V_o), \text{ (See Equation 20).}$$

Now $\epsilon$ is practically one for ions, while it may be of the order of several hundred for electrons. Hence, in the case that the negative carriers are electrons, the effect of diffusion may become appreciable for values of $V_o$ of a few hundred volts. If, however, the negative carriers are ions, the effect of diffusion becomes appreciable only at much lower values of $V_o$. The fractional value of the term which represents the recombination is:

$$\beta \frac{n_o}{6} \frac{d^2}{w^+ w^-}$$

When the negative carriers are ions, we may take $\beta = 2 \times 10^{-6}$ and $w^+ = w^- = 1.3$ E. For d = 1 cm the recombination correction thus becomes $2 \times 10^{-7} \frac{n_o}{V_o^2}$. With an intensity of ionization of one roentgen per second ($n_o \approx 2 \times 10^9$) and $V_o = 100$ volts, the correction is about four per cent. The correction is enormously smaller when the negative carriers are free electrons.

LOS ALAMOS TECHNICAL SERIES

VOLUME I

EXPERIMENTAL TECHNIQUES

PART II

CHAPTER 10

# OPERATION OF IONIZATION CHAMBERS WITH VARIABLE IONIZATION

by

BRUNO ROSSI AND HANS STAUB

# CHAPTER 10

## OPERATION OF IONIZATION CHAMBERS WITH VARIABLE IONIZATION

### 10.1 GENERAL CONSIDERATIONS

The results obtained in the preceding section are valid not only when the source of ionization is constant in time, but also when its intensity varies with time, provided the variations are sufficiently slow. By sufficiently slow we mean that no appreciable change of intensity takes place in a time of the order of the transit time of the positive ions through the chamber. This time is usually of the order of milliseconds. We will now consider the case of a rapidly varying ionization, which includes, as a limit, the case of a large number of ion pairs being produced simultaneously in the chamber by an ionizing particles like, for instance, an $\alpha$-particle.

In order to calculate the current in the external circuit as a function of time we have now to consider separately the charges induced on the collecting electrode by the motion of the various types of charged particles present in the gas. For the sake of simplicity and also because this is practically the most important case, we will assume that no attachment takes place, so that the negative carriers are free electrons. Also, recombination and diffusion will be neglected. Furthermore we will assume, for the time being, that the main part of the ionization is produced sufficiently far from the guard electrode so that the charge induced on the guard electrode by the motion of the ions and electrons can be disregarded. The "edge effects", i.e., the phenomena observed when the charged particles move in the neighborhood of the boundary of the active volume, will be discussed separately in Section 7.

Under the above assumptions, the effects of the motion of charged particles between the electrodes of an ionization chamber can be calculated most easily and most generally by applying the principle of conservation of energy.

Let us consider first an ionization chamber connected to a voltage supply through a current meter as indicated in Figure 1, and let us assume that the resistance of the external circuit is negligible so that the collecting electrode will be permanently at zero voltage, while the high voltage electrode will be at the constant voltage $V_0$. If ions and electrons are present in the gas of the chamber, the electric field in the chamber may be regarded as the superposition of two fields, one produced by the voltage difference between the electrodes and described by the field strength $\vec{E}$ and the potential V, the other produced by the space charge $\rho = e(n^+ - n^-)$ and described by the field strength $\vec{E}_\rho$ and the potential $V_\rho$. The corresponding quantities for the actual field will be $\vec{E} + \vec{E}_\rho$, $V + V_\rho$.

The voltage V satisfies the equation

$$\nabla^2 V = 0 \tag{1}$$

and the boundary conditions

$$\begin{aligned} V &= 0 \text{ at the collecting electrode} \\ V &= V_0 \text{ at the high voltage electrode} \end{aligned} \tag{2}$$

The voltage $V_\rho$ satisfies the equation

$$\nabla^2 V_\rho = -4\pi\rho = -4\pi e(n^+ - n^-) \tag{3}$$

and the boundary conditions

$$V_\rho = 0 \text{ at both electrodes} \tag{4}$$

If we compute now the electrostatic energy of the field we obtain

$$\frac{1}{8\pi}\int_A (\vec{E} + \vec{E}_\rho)^2 dA = \frac{1}{8\pi}\int_A E^2 dA + \frac{1}{8\pi}\int_A E_\rho^2 dA + \frac{1}{4\pi}\int_A \vec{E}\cdot\vec{E}_\rho\, dA$$

where A is the sensitive volume of the chamber.

The third integral on the right-hand side can be transformed as follows

Figure 1

Connection diagram of an ionization chamber.

Figure 2

Connection diagram of an ionization chamber.

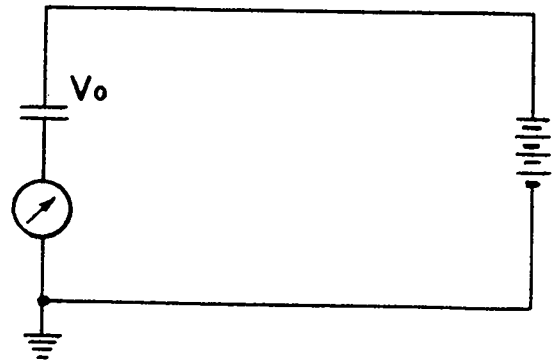


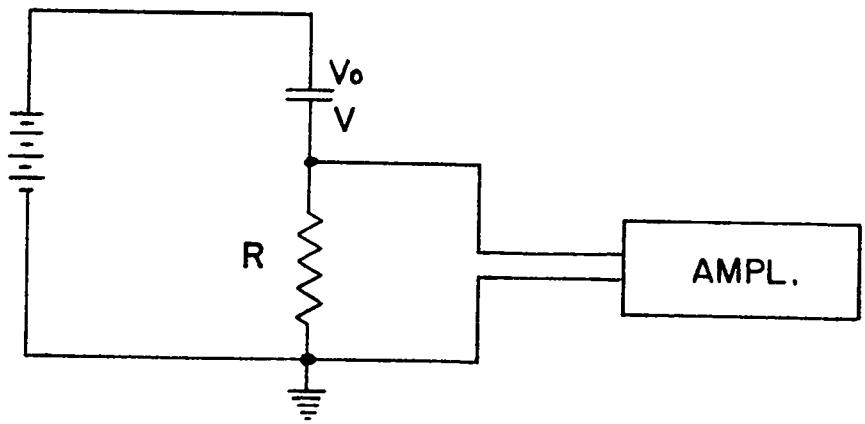

$$\int_A \vec{E} \cdot \vec{E}_\rho \, dA = -\int_A \vec{E} \cdot \text{grad } V_\rho \, dA$$
$$= -\int_A \text{div } (V_\rho \vec{E}) \, dA + \int_A V_\rho \, \text{div } \vec{E} \, dA$$
$$= \int_A V_\rho \, \text{div } \vec{E} \, dA - \int_S V_\rho E_n \, dS$$

where S is the combined surface of the two electrodes and $E_n$ is the component of $\vec{E}$ perpendicular to this surface. ($\vec{E}_\rho$, $V_\rho$ are assumed to be zero at the lateral boundary of the active volume.) Now $\text{div } \vec{E} = -\nabla^2 V = 0$ while $V_\rho = 0$ at the surface S. Hence, $\int \vec{E} \cdot \vec{E}_\rho \, dA = 0$ and, if we denote with W and $W_\rho$ the electrostatic energies of the fields represented by $\vec{E}$ and $\vec{E}_\rho$, respectively, we obtain for the total electrostatic energy the expression:

$$\frac{1}{8\pi} \int_A (\vec{E} + \vec{E}_\rho)^2 \, dA = W + W_\rho \qquad (5)$$

Electrons and ions in the ionized gas move along the lines of force with a comparatively small velocity, which is constant except insofar as the electric field strength varies from point to point. Hence, variations of the kinetic energy of electrons and ions are wholly negligible and practically all of the work performed by the electric field on the charged particles during their motion is used up to overcome the "frictional forces" represented by the collisions with the gas molecules. The principle of conservation of energy can then be expressed by writing that this work plus the variation of the electrostatic energy equals the work performed by the voltage supply. Since W is constant in time, we thus obtain the equation

$$e \int_A (\vec{E} + \vec{E}_\rho) \cdot (n^+ \vec{w}^+ - n^- \vec{w}^-) \, dA + \frac{d W_\rho}{d t} = V_o I \qquad (6)$$

where I is the current in the external circuit and $n^+$, $n^-$, $\vec{w}^+$, $\vec{w}^-$ are, as before, the densities and the drift velocities of positive ions and electrons respectively.

Since $V_\rho = 0$ at the surface S which bounds the volume A, the two following equations hold

$$\int_A \text{div} \left[ V_\rho \left( n^+ \vec{w}^+ - n^- \vec{w}^- \right) \right] dA = 0$$

$$\int_A \text{div} \left[ V_\rho \frac{\partial \vec{E}_\rho}{\partial t} \right] dA = 0$$

from which it follows

$$\int_A \vec{E}_\rho \cdot \left( n^+ \vec{w}^+ - n^- \vec{w}^- \right) dA = \int_A V_\rho \text{ div } \left( n^+ \vec{w}^+ - n^- \vec{w}^- \right) dA$$

$$\int_A \vec{E}_\rho \cdot \frac{\partial \vec{E}_\rho}{\partial t} dA = \int_A V_\rho \text{ div } \frac{\partial \vec{E}}{\partial t} dA$$

$$= 4\pi \int_A V_\rho \frac{\partial \rho}{\partial t} dA$$

On the other hand,

$$\frac{1}{4\pi} \int_A \vec{E}_\rho \frac{\partial \vec{E}}{\partial t} dA = \frac{\partial W}{\partial t}$$

$$\frac{\partial \rho}{\partial t} = - \text{div } e \left( n^+ \vec{w}^+ - n^- \vec{w}^- \right)$$

so that one obtains from the two equations above:

$$e \int_A \vec{E}_\rho \cdot \left( n^+ \vec{w}^+ - n^- \vec{w}^- \right) dA + \frac{\partial W}{\partial t} = 0 \qquad (7)$$

By subtracting Equation 7 from Equation 6 we finally find the following relation giving the external current I in terms of the motion of the electrons and ions in the chamber

$$I = \frac{e}{V_0} \int_A \vec{E} \cdot \left( n^+ \vec{w}^+ - n^- \vec{w}^- \right) dA \qquad (8)$$

This equation may be written as follows

$$I = I^+ + I^-$$

If we introduce the notations:

$$I^+ = \frac{e}{V_o} \int_A n^+ \vec{E} \cdot \vec{w}^+ dA$$
$$I^- = -\frac{e}{V_o} \int_A n^- \vec{E} \cdot \vec{w}^- dA \qquad (9)$$

or

$$I^+ = \frac{e}{V_o} \sum \vec{E}_i^+ \cdot \vec{w}_i^+$$
$$I^- = -\frac{e}{V_o} \sum \vec{E}_i^- \cdot \vec{w}_i^- \qquad (9')$$

where $\vec{w}_i^+$, $\vec{w}_i^-$ represent the drift velocities of the $i^{th}$ ion or electron at the moment under consideration, while $\vec{E}_i^+$, $\vec{E}_i^-$ are the electric field strengths at the place where these particles find themselves. The summations are extended to all ions and electrons present in the chamber. $I^+$ and $I^-$ represent the currents induced by the motion of the positive ions and of the electrons, respectively. They will be denoted briefly as "positive ion current" and "electron current". It may b pointed out that, in computing these currents, the values of the field to be taken into consideration are those which exist in the chamber when no space charge is present. Also, it may be pointed out that the vectors $\vec{E}/V_o$ depend only on the geometrical configuration of the chamber and are independent of the value $V_o$ of the applied voltage.

We will also introduce the notations

$$Q^+ (t) = \int_o^t I^+ (t) \, dt$$
$$Q^- (t) = \int_o^t I^- (t) \, dt \qquad (10)$$

The quantities $Q^+$ and $Q^-$ may be regarded as the charges induced on the collecting electrode in the time interval between 0 and t by the motion of the positive ions and electrons, respectively.

Ordinarily, for the measurement of variable ionization currents, the collecting electrode is connected to ground through a leak resistor R, and the voltage V

developed across this resistor by the ionization current is fed to the input of an electronic amplifier (see Figure 2). Application of the energy principle to this case, under the assumption that $V \ll V_o$ yields the following equation for V

$$V + RC \frac{dV}{dt} = R \; I \; (t) \tag{11}$$

where I is given by Equation 8 and C is the total capacity of the collecting electrode and of the amplifier input. If the product RC is very small, the second term on the left-hand side can be neglected and Equation 11 reduces to

$$V(t) = R \; I \; (t) \tag{12}$$

If RC is very large , the first term can be neglected and Equation 11 yields

$$V(t) - V(0) = Q \; (t)/C \tag{13}$$

where $Q = Q^+ + Q^-$ and $Q^+$ , $Q^-$ are given by Equation 10. In the general case, Equation 11 has the solution

$$V(t) - V(0) = e^{-\frac{t}{RC}} \frac{1}{C} \int_o^t e^{\frac{t}{RC}} \; I \; (t) \; dt \tag{14}$$

## 10.2 IONIZATION PULSE

Suppose that $N_o$ ion pairs are simultaneously produced in the chamber at the time t = 0, for instance by an $\alpha$-particle. If one neglects the effect of the space charge on the drift velocities, $\vec{w}^+$ and $\vec{w}^-$ are known functions of the position and it is possible, at least in principle, to determine the motion of each positive ion and each electron. Once this is done, $I^+$ (t) and $I^-$ (t) can be calculated as functions of time by means of Equation 9'. By integrating with respect to time one obtains the following expressions for $Q^+$ (t) and $Q^-$ (t)

$$Q^+ (t) = \frac{e}{V_o} \sum_{1}^{N_o} \left[ V_i (0) - V_i^+ (t) \right]$$
$$Q^- (t) = -\frac{e}{V_o} \sum_{1}^{N_o} \left[ V_i (0) - V_i^- (t) \right] \qquad (15)$$

In the above equations $V_i (0)$ represents the potential at the point where the $i^{th}$ ion pair is formed, $V_i^+ (t)$ represents the potential at the point where the $i^{th}$ positive ion finds itself at the time t, and $V_i^- (t)$ has a similar meaning for the $i^{th}$ electron. The electrons have large drift velocities hence $Q^-$ varies very rapidly with time, until all the electrons have reached the positive electrode. From this time on $Q^-$ has the constant value

$$Q_o^- = -\frac{e}{V_o} \sum_{1}^{N_o} \left[ V_i (0) - V^+ \right] \qquad (16)$$

where $V^+$ is the voltage of the positive electrode. The positive ions have much smaller drift velocities. Hence $Q^+ (t)$ reaches its final value after a much longer time. This value is given by

$$Q_o^+ = \frac{e}{V_o} \sum_{1}^{N_o} \left[ V_i (0) - V^- \right] \qquad (17)$$

where $V^-$ is the voltage of the negative electrode.

The sum of $Q_o^-$ and $Q_o^+$ is of course equal to $N_o e$, as it can be shown by adding Equations 16 and 17 and remembering that $V^+ - V^- = V_o$.

Suppose now that the leak resistor R is chosen so as to make the time constant RC large compared with the time of collection of the positive ions. Then, according to Equation 13, the voltage V of the collecting electrode (assumed to be zero at $t = 0$) is proportional to $Q(t) = Q^-(t) + Q^+(t)$. Therefore it increases very rapidly at first, until all electrons have been collected, then very slowly until the positive ions have also been collected. When both electrons and positive ions have been swept from the chamber the voltage of the collecting electrode becomes

$$V_p = \frac{Q_o^- + Q_o^+}{C} = \frac{N_o e}{C} \qquad (18)$$

Subsecuently, it decays exponentially with the time constant RC.

A chamber operated under the conditions specified above will be called an ion pulse chamber. The advantage of an ion pulse chamber is the fact that the pulse height $V_p$ is proportional to the total number $N_o$ of ions produced in the chamber, irrespective of the position where they are produced. The main disadvantage is that the time for collection of the positive ions is usually of the order of milliseconds, so that the decay constant RC must be at least of the order of 0.01 seconds and the amplifier must have its low frequency cut off at a correspondingly small frequency (see Section 3). This makes the arrangement unsuitable for fast counting and very sensitive to microphonic disturbances and to A.C. pick-up.

For these reasons, the value of the resistance R is often chosen so that RC is large compared with the time for collection of the electrons, but small compared with the time for collection of the positive ions. A chamber operated under these conditions responds only to the fast part of the pulse; i.e., to that part of the pulse due to the motion of the electrons; therefore it will be called an electron pulse chamber. Since the time for collection of electrons is ordinarily of the order of one microsecond, the time constant RC does not need to be larger than 10 or 20 microseconds. Hence the chamber will be able to record pulses following one another at very short time intervals, and the arrangement will be insensitive to microphonics or to A.C. disturbances.

The disadvantage of an electron pulse chamber is that the pulse height will depend not only on the total number $N_o$ of ion pairs produced in the chamber, but also on the position where they are produced. To a very good approximation, (i.e., neglecting terms of the order of $w^+/w^-$), the pulse height can be computed by considering the effect of the motion of the electrons and neglecting the effect of the motion of the positive ions altogether. Since RC is assumed to be large compared with the time for collection of the electrons, the value of the pulse height will then be given by

$$V_p = Q_o^-/C \qquad (19)$$

It is appropriate to mention here a simple device by which the pulses of an electron pulse chamber may be made independent in size of the position where the ionization is produced. This device consists of a grid placed between the two electrodes and held at an appropriate intermediate voltage. Suppose that the collecting electrode is positive and that the ionization is produced between the grid and the negative electrode. The grid shields the collecting electrode from the effects of the motion of charged particles as long as they are between the grid and the high voltage electrode. The positive ions never penetrate the region between the grid and the collecting electrode. The electrons however will penetrate this region, except for the few which may be captured by the grid wires. While travelling between the grid and the collecting electrode, each electron will induce on this electrode a charge equal to its own. Therefore the total charge induced on the collecting electrode by the motion of the electrons will be proportional to the number of ion pairs produced in the chamber, while no charge will be induced by the motion of the positive ions. A practical application of this principle will be described in Section 13.1.

## 10.3 INFLUENCE ON THE PULSE SHAPE OF THE TRANSIENT RESPONSE OF THE AMPLIFIER. MEASURE OF PULSE HEIGHTS IN eV.

We have considered so far the voltage pulse produced by the ionization current at the input of the amplifier. In order to determine the voltage pulse as it is observed at the output of the amplifier, the transient response of the amplifier must be taken into account. In order to define the transient response of the amplifier, let us suppose that a charge, Q, is brought onto the collecting electrode at the time t = 0. This can be done by applying, at t = 0, a square voltage wave to the high voltage electrode of the chamber. The voltage, V, of the collector rises abruptly to a value equal to Q/C and then decays exponentially with a time constant RC, as indicated by curve (a) in Figure 3. Let curve (b) in the same figure represent the voltage $V_e$ (t) at the output of the amplifier as a function of

Figure 3

Transient response of an amplifier.

Curve (a): input voltage; curve (b): output voltage.

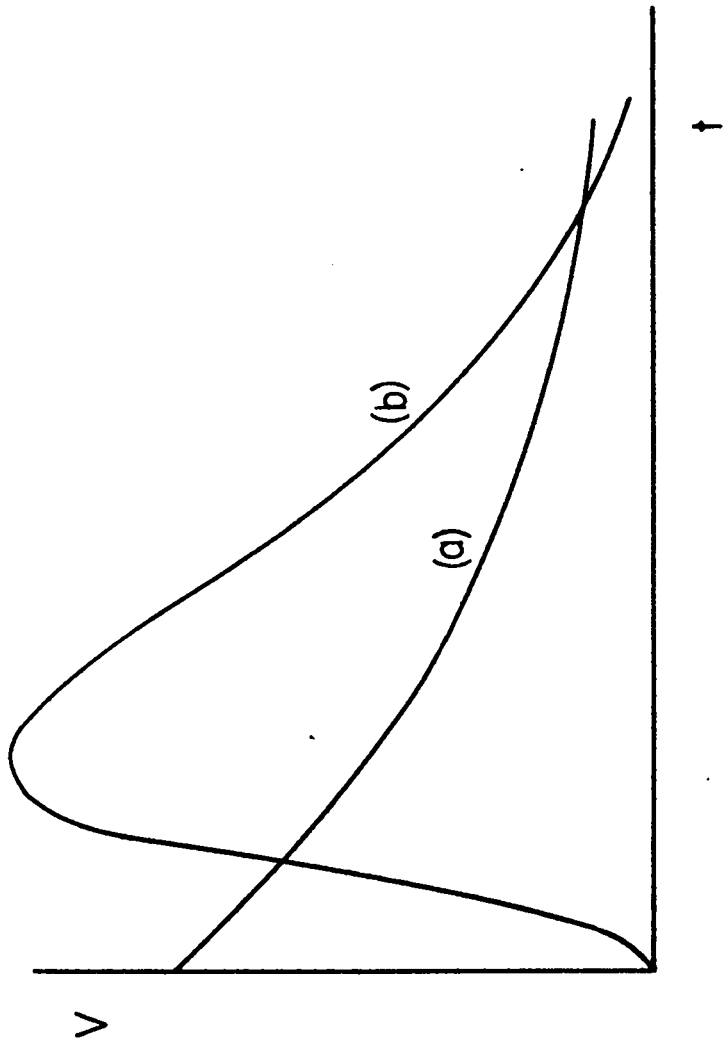

time. The function $\psi(t) = V_e(t)/Q$, which if the amplifier is linear is independent of Q, is defined as the transient response of the amplifier (see also Volume 1, Part I, Chapter 3).

The output voltage is given in terms of the ionization current I and of the transient response $\psi$ by the equation:

$$V_e(t) = \int_0^\infty I\ (t - t_1)\, \psi\ (t_1)\ dt_1 \qquad (20)$$

which can be considered as a generalization of Equation 14. It may be pointed out that the function $\psi(t)$ depends on the characteristics of the input circuit (capacity C, resistance R) as well as on those of the amplifier proper. It reduces to the exponential function, exp (-RC), if the amplifier has infinite bandwidth.

The area under the curve $\psi(t)$ divided by its maximum ordinate may be defined as the "resolving time" of the amplifier. For an exponential response of the type represented by curve (a), the resolving time is equal to RC.

Another quantity to which one often refers in connection with the transient response of an amplifier is the "rise time". It is difficult to give a rigorous definition for the rise time which applies to an arbitrary transient response. We may take it as equal to the time during which the voltage pulse rises from 10 per cent to 90 per cent of its maximum value.

It is convenient to define the transient response of an ionization chamber by the equation

$$I\ (t) = N_o e\ f(t) \qquad (21)$$

where I(t) represents the current at the time t under the assumption that $N_o$ ion pairs are produced at the time t = 0. It should be pointed out that f(t) depends not only on the properties of the ion chamber, but also on the space distribution of the ionization.

The function f(t) may be split into the sum of two functions $f^+(t)$ and $f^-(t)$ relative to the positive ion and to the electron current, which are defined as

follows:

$$I^+(t) = N_o e f^+(t)$$
$$I^-(t) = N_o e f^-(t) \qquad (21')$$

Comparison with Equations9 gives for $f^+(t)$ and $f^-(t)$ the following expressions:

$$f^+(t) = \frac{1}{N_o V_o} \int_A n^+(t)\vec{E} \cdot \vec{w}^+ \cdot dA = \frac{1}{N_o V_o} \sum_i^{N_o} \vec{E}_i^+ \cdot \vec{w}_i^+$$
$$f^-(t) = -\frac{1}{N_o V_o} \int_A n^-(t)\vec{E} \cdot \vec{w}^- \cdot dA = -\frac{1}{N_o V_o} \sum_i^{N_o} \vec{E}_i^- \cdot \vec{w}_i^- \qquad (22)$$

One sees that $f^+(t)$ and $f^-(t)$ may be considered as the averages, over all the positive ions and all the electrons, respectively, of the quantities $\vec{w}^+ \cdot (\vec{E}/V_o)$ and $-\vec{w}^- \cdot (\vec{E}/V_o)$ at the time t after the ionization pulse. In the computation of these averages a particle which has been collected is considered as still existing but having velocity zero.

Finally one may define the transient response $\chi(t)$ of the detecting equipment consisting of a given ionization chamber and a given amplifier by means of the equation

$$V_e(t) = N_o e \chi(t) \qquad (23)$$

where $V_e(t)$ represents the output voltage as a function of time in the case that $N_o$ ion pairs are produced in the chamber at $t = 0$. From Equations 20, 21, 23, and considering that $f(t) = 0$ for $t < 0$, one obtains the following relation

$$\chi(t) = \int_0^\infty f(t - t_1)\, \psi(t_1)\, dt_1 = \int_0^t f(t - t_1)\, \psi(t_1)\, dt_1 \qquad (24)$$

The conditions stated in the preceding section for the operation of a chamber as an ion pulse or an electron pulse chamber may be appropriately generalized to include the influence of the amplifier on the observed pulse shape by considering the resolving time of the amplifier in place of the time constant RC. We will

therefore refer to a chamber as an ion pulse chamber if the resolving time of the amplifier is long compared with the time of collection of the positive ions and as an electron pulse chamber if the resolving time is short compared with the time of collection of positive ions but long compared with the time of collection of electrons. As a convenient measure for the size of ionization pulses, we will use the quantity $P = \frac{Q}{e} W_o$ where Q is the charge induced on the collecting electrode ($Q = Q_o^+ + Q_o^- = N_o e$ for an ion pulse chamber; $Q = Q_o^-$ for an electron pulse chamber) and $W_o$ is the energy for the formation of an ion pair in eV (see Section A.2). P is thus expressed in eV and, in the case of an ion pulse chamber, it simply represents the energy $N_o W_o$ dissipated in the chamber by the ionizing particle which produces the pulse. In the case of an electron pulse chamber, P represents a fraction of this energy, given by the expression

$$P = N_o W_o \frac{Q_o^-}{Q_o^+ + Q_o^-}$$

For an absolute calibration of a given chamber operated in conjunction with a given amplifier and a given recording device, the most direct procedure consists in observing the pulses from a source of $\alpha$-particles of uniform and known energy, usually a polonium source, placed in the chamber in such a way that the whole range of the $\alpha$-particle is within the sensitive volume. If the chamber is operated as an ion pulse chamber, the output pulses all have the same size and this size corresponds to ionization pulses of magnitude P equal to the energy of the $\alpha$-particles. If the chamber is operated as an electron pulse chamber, the output pulses, in general, will have different sizes. The relation between the response of the measuring instrument and the value P of the corresponding ionization pulse is obtained by first computing theoretically the distribution in size of the ionization pulses and then fitting the computed curve to the experimental pulse height distribution (see, for instance Section 13.1).

A more convenient but less direct method of calibration consists in feeding known voltage pulses, $V_p$, to the high voltage electrode of the ionization chamber

and observing the corresponding output pulses. If we denote by $C_1$ the partial capacity of the collecting electrode with respect to the high voltage electrode and by C its total capacity, the corresponding voltage pulse at the input of the amplifier is $V_P = V_1 C_1/C$.

According to our definition, the P value of this pulse is given by $(V_1C_1/e)W_o$. In other words, the signal obtained by applying a voltage pulse $V_1$ to the high voltage electrode of the ionization chamber is equal to the signal produced by an ionizing particle which liberates a charge $Q = V_1C_1$ in the chamber, under the assumption that the chamber is operated for ion pulses.

It will be noted that the method outlined requires knowledge of $W_o$ and of the partial capacity $C_1$ of the collecting electrode with respect to the high voltage electrode, which usually can be computed quite accurately. It does not require knowledge of the stray capacity, which, in general, could only be determined by direct measurement.

## 10.4 CONTINUOUSLY VARIABLE IONIZATION

Let us suppose now that the ionization chamber is irradiated with a continuous source of ionization of variable intensity, so that a total of $N(t)dt$ ion pairs are produced within its sensitive volume in the time interval between t and $t + dt$. If, for the same chamber and for the same spacial distribution of the ionization the currents $I^+(t)$ and $I^-(t)$ have been determined in the case of an instantaneous ionization pulse, they can also be calculated for the case under consideration because a continuous ionization can always be subdivided, ideally, into an infinite number of infinitely short ionization pulses. By making use of the functions $f^+(t)$ and $f^-(t)$ defined by Equations 21, we obtain for $I^+(t)$ and $I^-(t)$ the following expressions:

$$I^+(t) = e \int_0^\infty N(t - t_1)\, f^+(t_1)\, dt_1$$
$$I^-(t) = e \int_0^\infty N(t - t_1)\, f^-(t_1)\, dt_1 \qquad (25)$$

In particular, if N is constant, $I^+$ and $I^-$ become

$$I_o^+ = e\,N \int_0^\infty f^+(t_1)\,dt_1$$
$$I_o^- = e\,N \int_0^\infty f^-(t_1)\,dt_1 \qquad (25')$$

Equations 25' acquire a simple physical meaning if one considers that, according to Equations 22

$$\int_0^\infty f^+(t)\,dt = \frac{1}{N_o V_o} \sum_1^{N_o} \int \vec{E}_i \cdot \vec{w}_i\,dt$$
$$= \frac{1}{N_o V_o} \sum_1^{N_o} \left[V_i(0) - V^-\right]$$
$$= \frac{1}{V_o} \left[V_i(0) - V^-\right]_{av}$$

and similarly

$$\int_0^\infty f^-(t)\,dt = \frac{1}{V_o} \left[V^+ - V_i(0)\right]_{av}$$

where $\left[V_i(0) - V^-\right]_{av}$ and $\left[V^+ - V_i(0)\right]_{av}$ represent the average values of the difference of potential between the place of production of the ions and the negative or positive electrode respectively (see Section 2). Hence Equations 25' yield

$$I_o^+ = e\,N/V_o \left[V_i(0) - V^-\right]_{av}$$
$$I_o^- = e\,N/V_o \left[V^+ - V_i(0)\right]_{av} \qquad (25'')$$

It follows from Equations 25'' that the total ionization current is

$$I_o = I_o^+ + I_o^- = e\,N$$

in agreement with Equation 9.5. The output voltage $V_e(t)$ is given by the equation

$$V_e(t) = e \int_0^\infty N(t - t_3)\,\chi(t_3)\,dt_3 \qquad (26)$$

which may be considered as a direct consequence of Equation 23, or can be derived from Equations 20, 24, and 25, by taking into account that $\psi(t) = 0$ for $t < 0$.

If the source of ionization is suddenly turned on to a constant value at the

time $t = 0$, ($N(t) = 0$ for $t < 0$; $N(t) = N$ = constant for $t > 0$) $I^+$ and $I^-$ are zero for $t \leq 0$ and have the following expressions for $t > 0$

$$I^+(t) = e N \int_0^t f^+(t_1)\, dt_1$$
$$I^-(t) = e N \int_0^t f^-(t_1)\, dt_1 \qquad (27)$$

while, if a constant source of ionization is suddenly turned off at $t = 0$ ($N(t) = N$ = constant for $t < 0$; $N(t) = 0$ for $t > 0$), we have, remembering Equations 25':

$$\left.\begin{aligned} I^+(t) &= I_o^+ \\ I^-(t) &= I_o^- \end{aligned}\right\} \text{for } t < 0$$

$$\left.\begin{aligned} I^+(t) &= I_o^+ \left[1 - \frac{eN}{I_o^+} \int_0^t f^+(t_1)\, dt_1\right] \\ I^-(t) &= I_o^- \left[1 - \frac{eN}{I_o^-} \int_0^t f^-(t_1)\, dt_1\right] \end{aligned}\right\} \text{for } t > 0 \qquad (28)$$

The expressions for the charges $q^+(t)$ and $q^-(t)$ for the case of an instantaneous ionization pulse can be written in terms of $f^+(t)$ and $f^-(t)$ as follows:

$$q^+(t) = N_o e \int_0^t f^+(t_1)\, dt_1$$
$$q^-(t) = N_o e \int_0^t f^-(t_1)\, dt_1 \qquad (29)$$

Comparison with Equations 27 and 28 shows that the positive ion current and the electron current present in a chamber after a constant source of ionization is suddenly turned on or cut off exhibit the same time dependence as the charges induced on the collecting electrode by the motion of the positive ions and of the electrons, respectively, after an infinitely short ionization pulse.

In the general case, one sees that the variations of the ionization current will be proportional to the variations of the source intensity only if these variations are either very slow compared with the time for collection of the positive ions, or very fast compared with the time for collection of the positive ions but

very slow compared with the time for collection of the electrons. In the first instance, as already pointed out, the total ionisation current $I^+ + I^-$ will follow the variations of the intensity of the ionizing radiation. In the second instance the electron current $I^-$ will follow the changes of the ionizing radiation while the positive ion current $I^+$ will remain practically constant. The exact value of the ionization current $I(t) = I^+(t) + I^-(t)$ produced by a given variable source of ionization may be computed by means of Equation 25, if the function $f(t) = f^+(t) + f^-(t)$ is known. This, in turn, can be determined, as we have just seen, by observing the variations of I immediately after a constant source of ionization has been turned on or off.

## 10.5 PARALLEL PLATE CHAMBER

In a parallel plate chamber the electric field is constant, hence the drift velocities of both positive ions and electrons are independent of position. It follows that $I^+(t)$ and $I^-(t)$ are proportional to the numbers of positive ions and of electrons, respectively, present in the chamber at the time t.

The potential difference between two points of the chamber is proportional to the difference of their distances from the negative electrode. Therefore, the expressions for $Q^+(t)$ and $Q^-(t)$ in the case of an instantaneous ionization pulse (see Equation 15) become:

$$Q^+(t) = \frac{e}{h} \sum_{i}^{N_0} \left[ x_i(0) - x_i^+(t) \right]$$
$$Q^-(t) = -\frac{e}{h} \sum_{i}^{N_0} \left[ x_i(0) - x_i^-(t) \right] \qquad (30)$$

where h is the separation of the electrodes, $x_i(0)$ is the distance from the negative electrode to the point where the $i^{th}$ ion pair is formed, $x_i^+(t)$, $x_i^-(t)$ are the distances from the negative electrode to the $i^{th}$ positive ion and to the $i^{th}$ electron, respectively, at the time t after the ionization pulse. From Equation 30 it follows that the charges $Q_0^-$ and $Q_0^+$ induced by the motion of the electrons and of the positive ions after complete collection are given by $N_0$ e/h times the distance of

the center of gravity of the ionization from the positive and from the negative electrode, respectively. Also it follows from Equation 25'' that if the chamber is irradiated by a constant source of ionization so that N ion pairs are produced per unit time, the electron and positive ion currents, $I_o^-$ and $I_o^+$, are given by the product of eN/h times the distance of the center of gravity of the ionization from the positive and from the negative electrode, respectively. If, for instance, the volume of the chamber is uniformly irradiated, the center of gravity of the ionization is halfway between the positive and negative electrodes. The currents $I_o^+$ and $I_o^-$ are then identical and given by

$$I_o^+ = I_o^- = 1/2\ e\ N$$

In the case just considered of a spacially uniform ionization, the functions $f^-(t)$ and $f^+(t)$ have the expressions:

$$\begin{aligned} f^+(t) &= \frac{h - w^+ t}{h^2}\, w^+ && \text{for } t < h/w^+ \\ f^+(t) &= 0 && \text{for } t > h/w^+ \\ f^-(t) &= \frac{h - w^- t}{h^2}\, w^- && \text{for } t < h/w^- \\ f^-(t) &= 0 && \text{for } t > h/w^- \end{aligned} \qquad (31)$$

The expressions for the positive ion and electron currents subsequent to a sudden turning on of a constant source of ionization (see Equation 27) become

$$\begin{aligned} I^+(t) &= e\,\frac{N w^+}{h}\left(t - 1/2\,\frac{w^+}{h}\, t^2\right) && \text{for } t < h/w^+ \\ I^+(t) &= 1/2\ e\ N = I_o^+ && \text{for } t > h/w^+ \\ I^-(t) &= e\,\frac{N w^-}{h}\left(t - 1/2\,\frac{w^-}{h}\, t^2\right) && \text{for } t < h/w^- \\ I^-(t) &= 1/2\ e\ N && \text{for } t > h/w^- \end{aligned} \qquad (32)$$

Similarly, in the case of a sudden turning off of the source (see Equations 22):

$$
\begin{aligned}
I^{+}(t) &= e\ N \left[1/2 - \frac{w^{+}}{h} t + 1/2 \left(\frac{w^{+}}{h} t\right)^{2}\right] && \text{for } t < h/w^{+} \\
I^{+}(t) &= 0 && \text{for } t > h/w^{-} \\
I^{-}(t) &= e\ N \left[1/2 - \frac{w^{-}}{h} t + 1/2 \left(\frac{w^{-}}{h} t\right)^{2}\right] && \text{for } t < h/w^{-} \\
I^{-}(t) &= 0 && \text{for } t > h/w^{-}
\end{aligned}
\tag{33}
$$

## 10.6 CYLINDRICAL CHAMBER

Consider first the case of $N_o$ ion pairs formed instantaneously at a distance $r_o$ from the axis of the chamber, for instance by an $\alpha$-particle travelling parallel to the axis. Suppose that the outer electrode is negative and the inner electrode positive. After all electrons and ions have been collected, the charges $Q_o^{+}$ and $Q_o^{-}$ induced by the motion of the positive ions and the electrons, respectively, are given by the expressions (see Equations 16 and 17):

$$
\begin{aligned}
Q_o^{+} &= e\ N_o \log (b/r)/\log\ (b/a) \\
Q_o^{-} &= e\ N_o \log (r/a)/\log\ (b/a)
\end{aligned}
\tag{34}
$$

where a is the radius of the inner and b that of the outer cylinder.

In Figure 4, $Q_o^{+}$ and $Q_o^{-}$ are plotted as a function of r/a for the case b = 100 a. One sees that when $b \gg a$, as it is assumed here, $Q_o^{-}$ is much larger than $Q_o^{+}$, except when the ions are formed very close to the central electrode.

We want also to calculate the positive ion and electron currents for the case of a cylindrical chamber uniformly irradiated by a constant source of ionization producing N ion pairs per unit time. Equations 25'' give for the case under consideration:

$$
\begin{aligned}
I_o^{+}/eN &= 1/\left[2\log\ (b/a)\right] - a^2/(b^2 - a^2) \\
I_o^{-}/eN &= b^2/(b^2 - a^2) - 1/\left[2\log\ (b/a)\right]
\end{aligned}
\tag{35}
$$

Figure 4

Charges $Q_o^+$ and $Q_o^-$ induced on the collecting electrode of a cylindrical chamber by the motion of positive ions and electrons, respectively, when $N_o$ ion pairs are formed at a distance r from the axis. Inner electrode positive; b = 100 a (b = radius of the outer electrode; a = radius of the inner electrode).

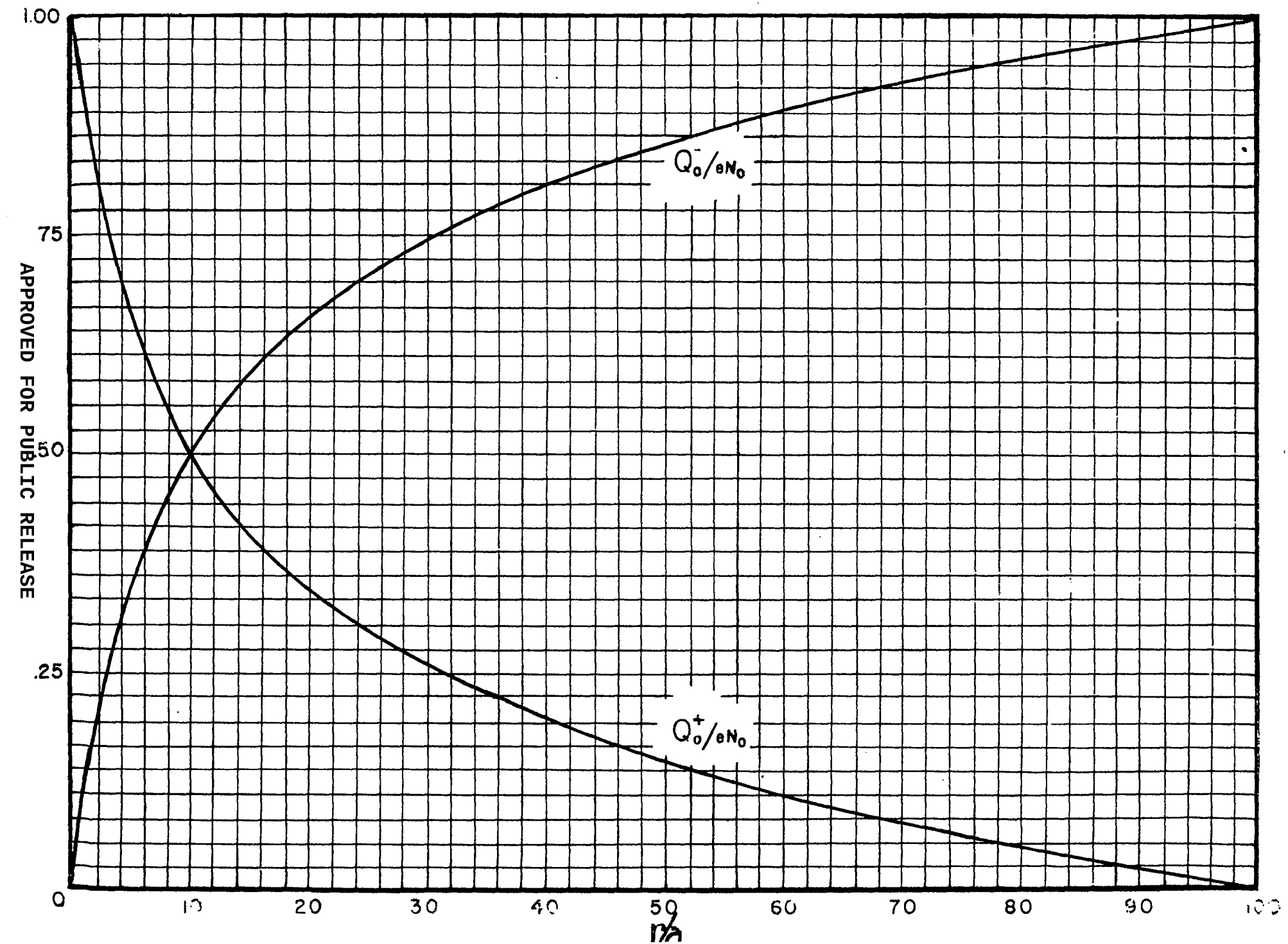

APPROVED FOR PUBLIC RELEASE

or, if $b \gg a$

$$I_o^+/eN = 1/\left[2\log\ (b/a)\right]$$
$$I_o^-/eN = 1 - 1/\left[2\log\ (b/a)\right] \qquad (35')$$

One sees that, if $b \gg a$, the electron current is much larger than the positive ion current. The situation, of course, would be reversed if the inner electrode were negative instead of positive.

## 10.7 EDGE EFFECTS

We have assumed, so far, that the electrons and ions are sufficiently far from the boundary of the active volume so that no appreciable charge is induced on the guard electrode. When the charged particles are near the boundary of the active volume, whether inside or outside of it, they will induce a charge both on the collecting electrode and on the guard electrode, and the computation of the pulse can no longer be carried out in the simple manner outlined in Section I.

The theory of the "edge effects" has been developed for the simple case of a parallel plate chamber, with the collecting electrode and the guard electrode in the shape of two infinite half planes joining along a straight line (see Figure 5). (The case of a parallel plate chamber, in which the linear dimensions of the electrodes arelarge compared with their separation, can be approximated sufficiently well by the ideal case described above).

Let us consider a point charge in the space between the plates, and let us use as our frame of reference a cartesian system of coordinates with the origin on the plane containing the collecting electrode and the guard electrode, the y axis perpendicular to this plane and passing through the point charge, the z axis parallel and the x axis perpendicular to the boundary between the collecting electrode and the guard electrode. Our problem consists in determining the surface density of charge $\omega(x, z)$ induced in the $(x, z)$ plane and then integrating this function separately over the half plane forming the collecting electrode and over the half

Figure 5

Diagram for the calculations of the edge effects.

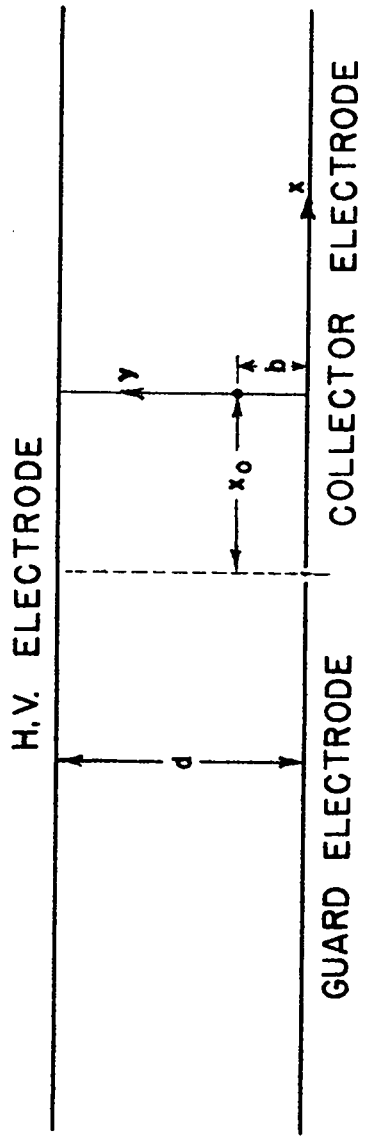

plane forming the guard electrode. The mathematical procedure is simplified by the observation that the ratio between the charges induced on the two electrodes is obviously the same for all charges lying on a line parallel to their boundary. Therefore we may subsitute the point charge with a line charge of uniform density, parallel to the z axis, calculate the surface density of the induced charge for this case, and then integrate along the x axis alone in order to determine the total charge induced on the two electrodes. The charge per unit length, of course, should be so chosen as to give the correct total charge on the (x, z ) plane. As it will be shown below, this is done by taking it equal to the charge e of the particle.

The problem of determining the electric field of a line charge between two conducting planes parallel to it has been solved (see, for instance Smyth, "Static and Dynamic Electricity", McGraw Hill, 1939, pp. 83-84). From the expression for the electric field, one finds the following expression for the surface density of charge:

$$\omega(x) = -\frac{e}{2d}\,\frac{\sin(\pi b/d)}{\cosh(\pi x/d) - \cos(\pi b/d)} \tag{36}$$

In this equation, d is the separation of the plates and b is the y-coordinate of the charge. The - sign indicates that the inducing charge and the induced charge have opposite signs. The indefinite integral of $\omega(x)$ is not difficult to calculate and has the following expression

$$\int \omega(x)\, dx = -\frac{e}{\pi}\tan^{-1}\left(\frac{e^{\pi x/d} - \cos(\pi b/d)}{\sin(\pi b/d)}\right) \tag{37}$$

Let $x_0$ be the distance of the charge from the boundary of the sensitive volume (positive if the charge is inside this volume). The total charge induced on the (x, z) plane is given by

$$Q = \int_{-\infty}^{+\infty} \omega(x)\, dx = -e\,(1 - b/d) \tag{38}$$

while the charge induced on the collecting electrode is given by

Figure 6

Fractional charge $Q_c/e$ induced on the collecting electrode of a parallel plate chamber by a point charge e as a function of its distance $x_o$ from the boundary of the active volume and of its distance b from the collecting electrode; d is the depth of the chamber (see Figure 5) and $z = x_o/d$.

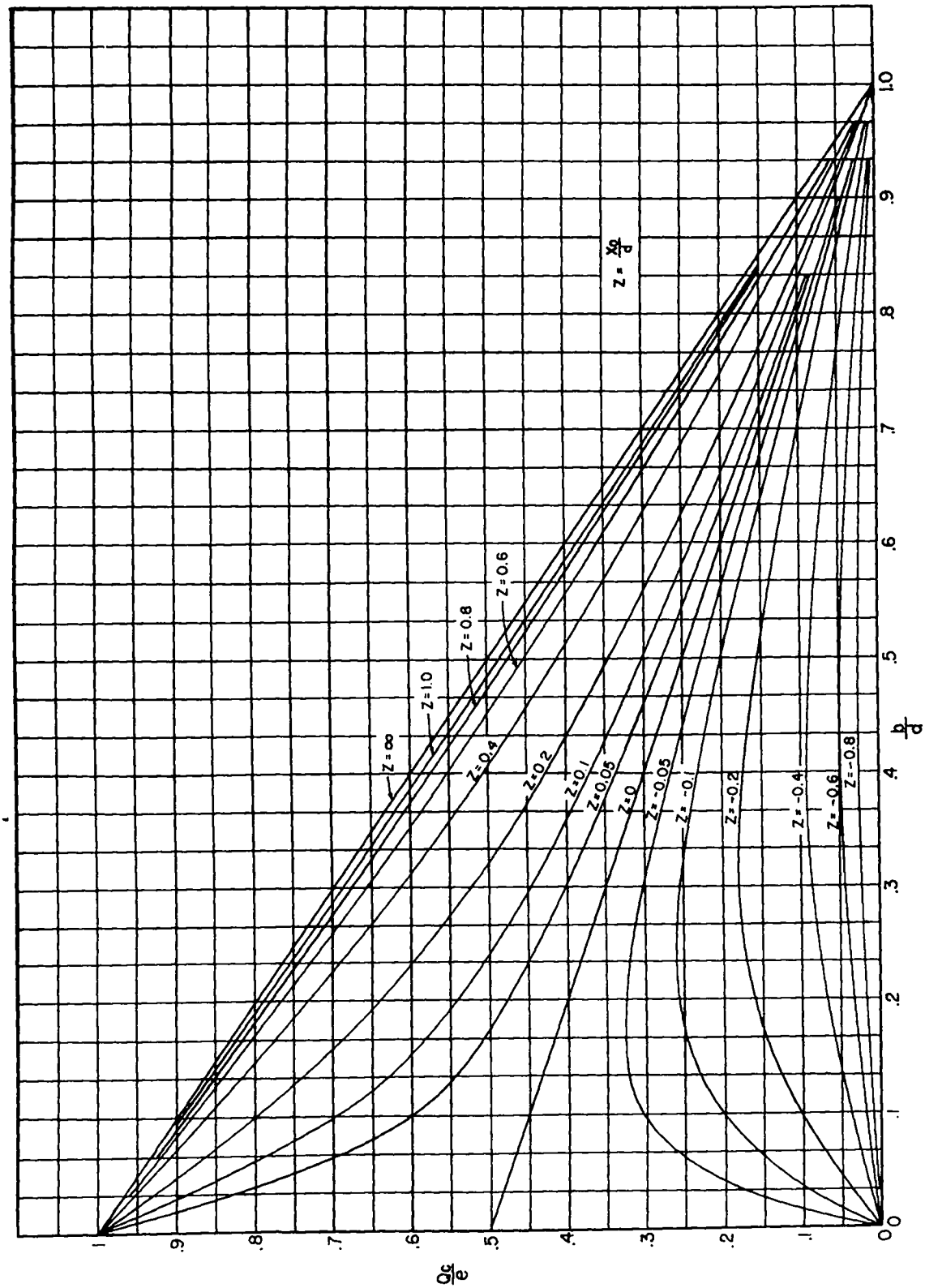

$$Q_c = \int_{-x_c}^{x_c} \omega(x)\, dx = -e\left[1/2 - \frac{1}{\pi}\tan^{-1}\left(\frac{e^{-\pi x_0/d} - \cos(\pi\, b/d)}{\sin(\pi\, b/d)}\right)\right] \quad (39)$$

One sees that Q becomes equal to -e when b = 0, which shows that we have chosen the correct normalization factor. The charge $Q_c$ is a function of the ratios b/d and $x_0/d$. A graphical representation of this function is given in Figure 6.

The shape of the pulse produced by an ionizing particle traversing the chamber near the boundary of the sensitive volume can be calculated immediately if one knows the drift velocities of the electrons and positive ions. The total induced charge is obtained as a function of time, by adding up the contributions of the individual electrons and positive ions as represented by Equation 39, which depend on t through the parameter b.

Figure 7 shows various examples of pulse shapes obtained when an ion pair is formed inside or outside of the sensitive volume at a small distance from its boundary.

In order to make a graphical representation possible, the drift velocity of the positive ions has been taken as 10 times smaller, instead of about 1000 times smaller, than that of the free electrons. For comparison, the pulse produced by an ion pair formed inside the active volume at a large distance from the boundary is also represented in Figure 7. It will be noted that the total charge induced on the collecting electrode after both the electron and the positive ion have been collected is always e when the ion pair has been formed inside the sensitive volume and is always zero, when the ion pair has been formed outside of it. The shape of the pulse, however, varies greatly with the position of the original ion pair and with the polarity of the chamber.

## 10.8 TESTING OF "FAST" IONIZATION CHAMBERS

For many purposes, some of which will be mentioned below, it is often desirable to determine experimentally the function f(t) for a given chamber and for a given distribution of the ionization. As we have seen, this can be done either by studying the shape of voltage pulses produced by single ionizing particles, or by

Figure 7

Pulse shapes obtained when ions are produced near the boundary of the sensitive volume of a parallel plate chamber (see Figure 5)

Curve (A): ion pair produced inside the active volume, at a distance of 0.05 d from the boundary ($x_o = +0.05d$), H. V. electrode positive.

Curve (B); ion pair produced outside of the active volume, at a distance of 0.05d from the boundary ($x_o = -0.05d$), H.V. electrode positive.

Curve (C); $x_o = +0.05d$, H.V. electrode negative.

Curve (D); $x_o = -0.05d$, H.V. electrode negative.

In all cases the ion pair is supposed to be produced half way between the plates ($b = d/2$). The drift velocity of the electrons is taken as equal to 10 times that of the positive ions, in order to make a graphical representation of the pulse shape possible.

Curve (E) represents the pulse produced when an ion pair is formed half way between the plates, at a large distance from the edge of the collecting electrode (H.V. electrode positive).

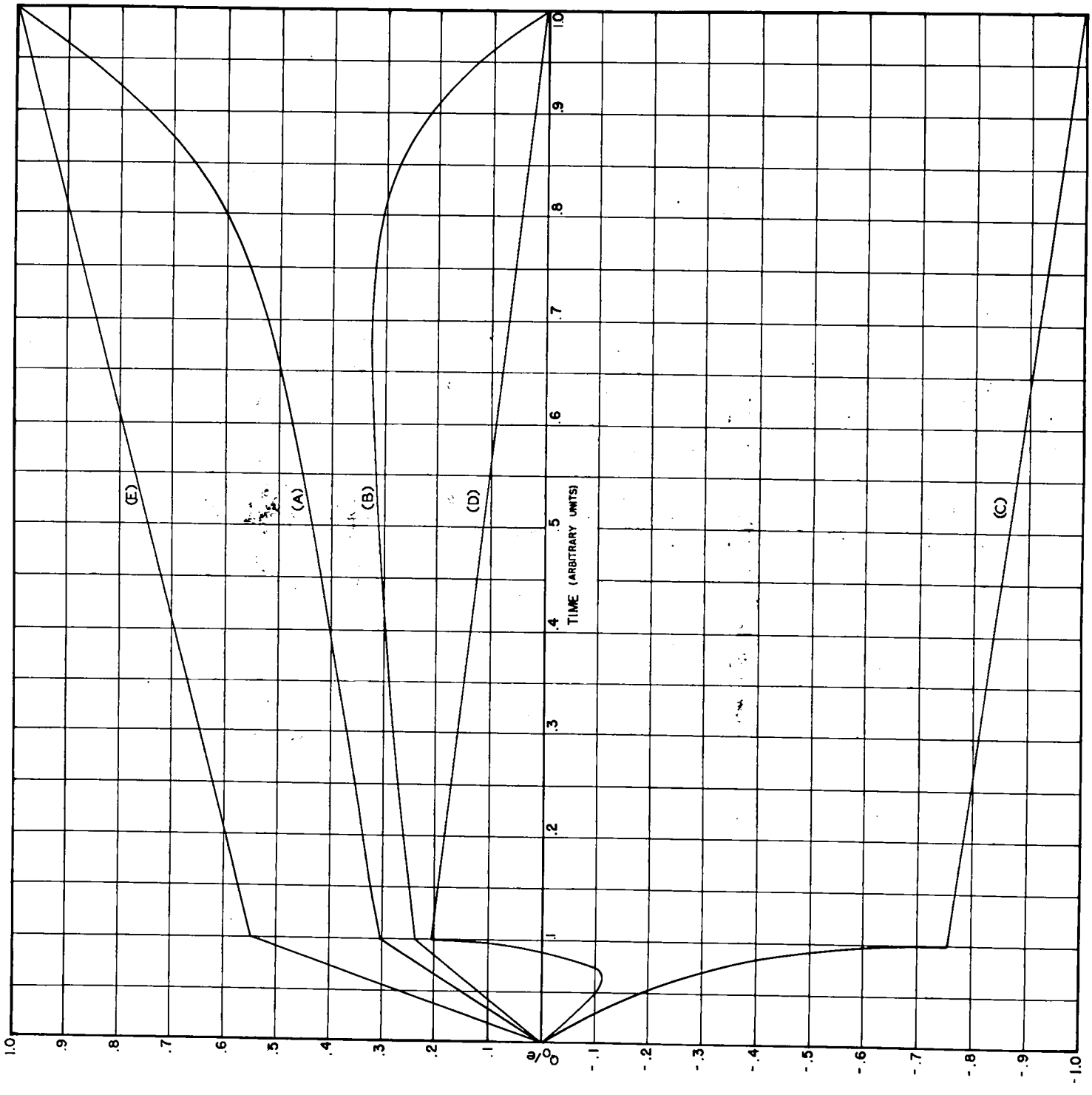

investigating the time dependence of the electron current upon a sudden turning on or off of a source of continuous ionization.

Experiments of the first type can be carried out with the arrangement schematically represented in Figure 8. CH is the ionization chamber, which contains a suitable source of $\alpha$-particles. The pulse V at the collecting electrode is amplified electronically and then applied to one of the vertical deflecting plates of a cathode ray oscilloscope through a delay line, which delays the pulse by one to two microseconds without changing its shape appreciably. The pulse at the output of the amplifier is also used to trigger the sweep circuit. This circuit provides a positive square pulse which is applied to the intensifier electrode of the cathode ray tube, normally biased below cut-off, and turns the beam on for the duration of the pulse. It also provides a saw-tooth pulse, which is applied in push-pull to the horizontal deflecting plates thus producing a linear sweep of appropriate speed. For each $\alpha$-particle entering the chamber, a trace representing the output voltage $V_e$ as a function of time appears on the oscilloscope screen. The delay line between the amplifier and the vertical deflecting plate makes it possible to study the beginning of the pulse which otherwise could not be observed because of the small unavoidable delay in starting the sweep circuit. $V_e(t)$ is related to the function $\chi(t)$ which describes the transient response of the detecting equipment by Equation 23. If the rise time of the amplifier is sufficiently small and its resolving time is sufficiently long, so that the transient response of the amplifier may be approximated with a step function ($\psi(t) = 0$ for $t < 0$; $\psi(t) =$ constant for $t > 0$,) this equation together with Equation 24 yields

$$V_e(t) = \text{constant} \int_0^t f(t_1)\, dt_1$$

The arrangement described was used for determining the shape of the pulses produced by polonium $\alpha$-particles in the parallel plate chamber represented in Figure 9. The $\alpha$-particles were projected across the sensitive volume of the chamber in a direction parallel to the plates. Hence, for an ideal transient response of the amplifier, as specified above, and if edge effects can be

Figure 8

Experimental arrangement for testing "fast" ionization chambers with $\alpha$-particles.

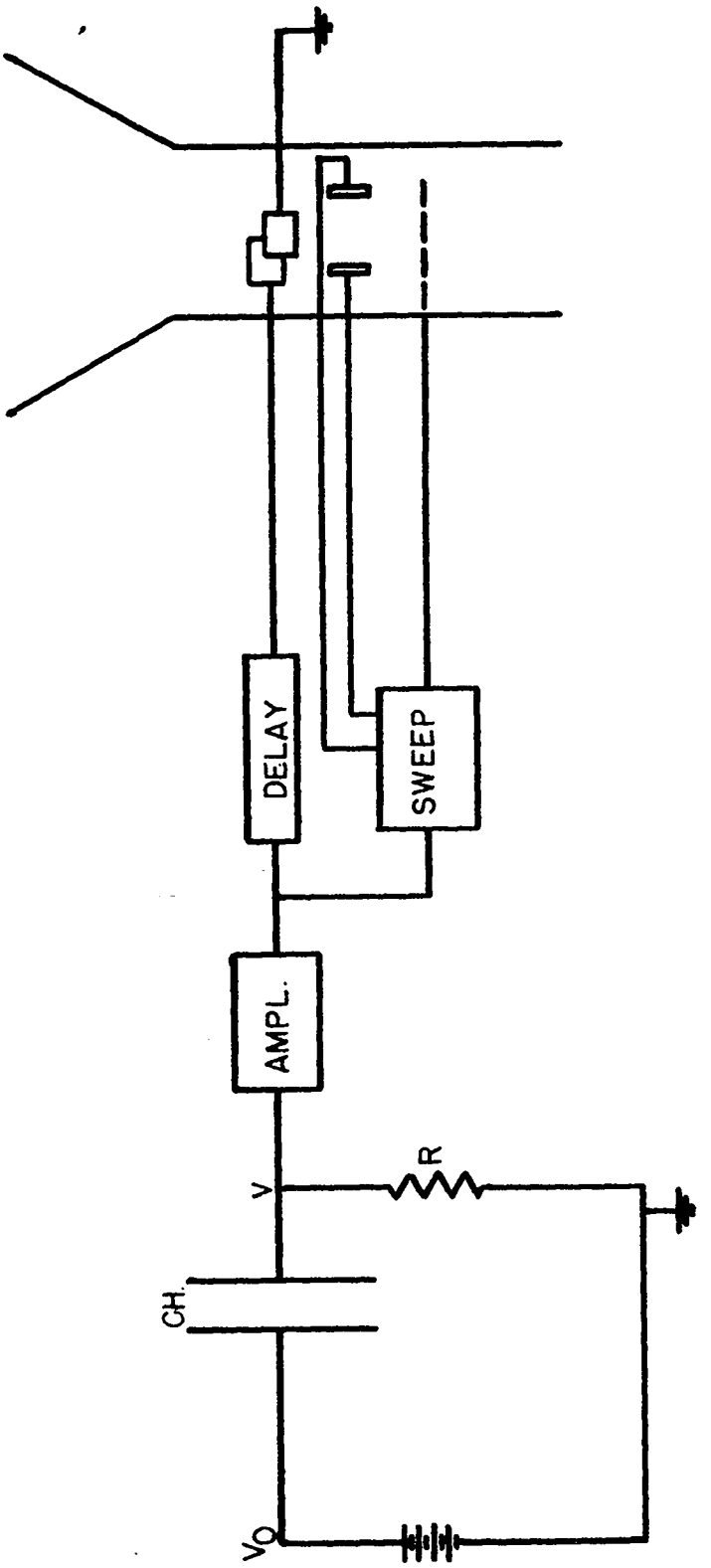

disregarded, the output voltage will rise linearly with time until all electrons are collected and then remain practically constant. The time for the collection of the electrons, of course, is equal to the distance of the track from the positive electrode divided by the drift velocity of the electrons.

The results obtained were used for the determination of the drift velocity in various gases and gas mixtures. The values thus found are included in the graphs given in Figures 8.3, 8.4, 8.5, 8.6. The accuracy claimed for these values is not very high because of some distortion of the pulse shape produced by the electronic circuit and by the edge effects.

Through a study of $\alpha$-particle pulses it is possible, at least in principle, to determine whether or not any electron attachment takes place. This can be done by measuring the ratio between the "fast" part of the pulse (due to the motion of free electrons) and the "slow" part of the pulse (due to the motion of ions). In a parallel plate chamber with the beam of $\alpha$-particles parallel to the plates, this ratio should be equal to the ratio between the distance of the tracks from the positive and the negative electrode, respectively, if there is no electron attachment. Any electron attachment leading to the formation of slow moving negative ions will decrease the fast and increase the slow part of the pulse.

Figure 9

Inner construction of chamber used for determining the shape of α-particle pulses.

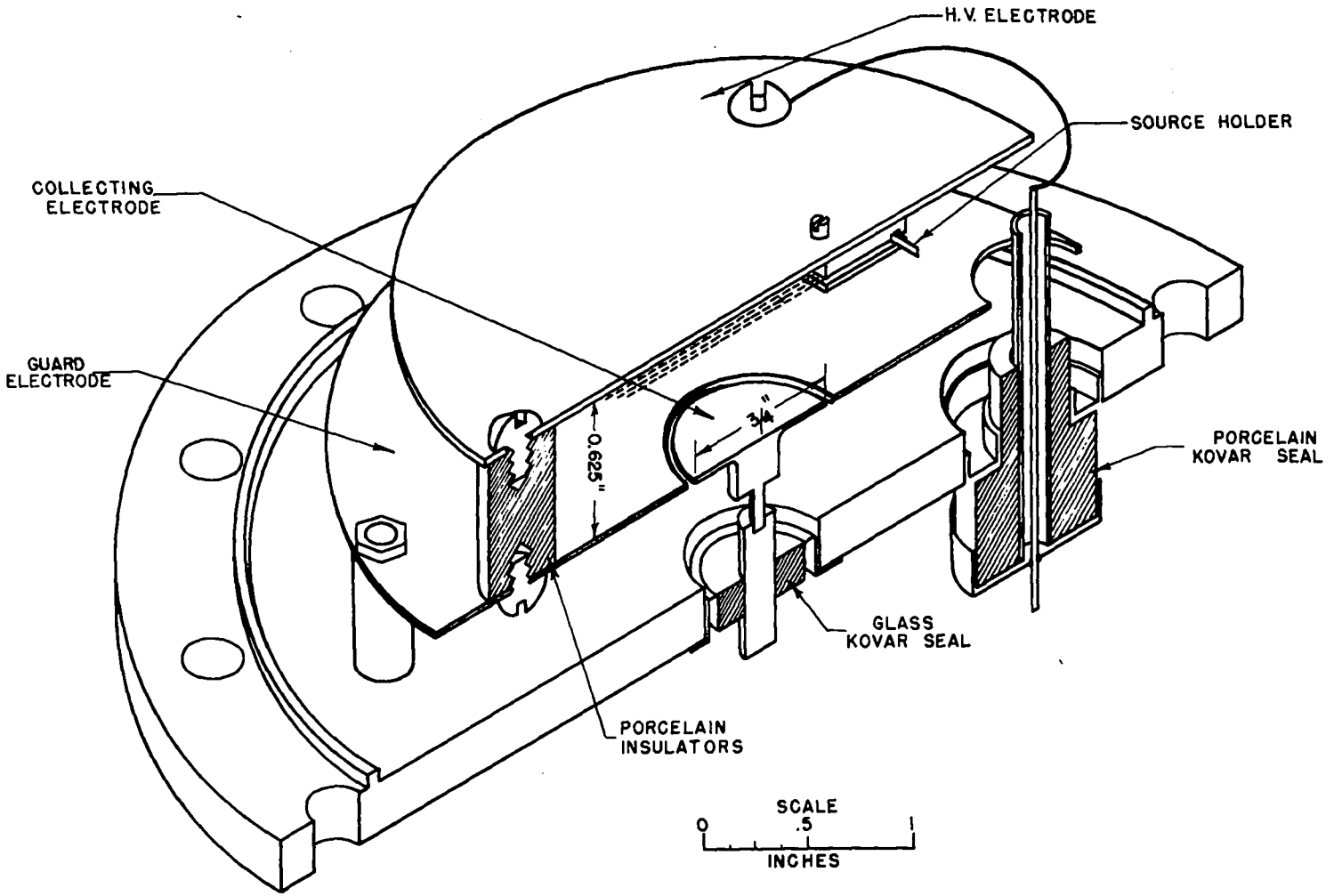


APPROVED FOR PUBLIC RELEASE

No measurements of the electron attachment were carried out by the method outlined above, mainly because no amplifier was available which could amplify without distortion both the slow and the fast part of the pulse. Some information on electron attachment, however, was obtained by studying the dependence of the electron pulse on the voltage difference across the chamber. Any change of pulse height with voltage (except at very low voltages at which diffusion or recombination may play some role) is a proof of electron attachment. On the other hand, the fact that the pulse height is independent of the voltage over a wide range may be taken as an indication that the electron attachment is negligible. As an example, the two curves in Figure 10 give electron pulse heights versus electric field strength as obtained with the chamber represented in Figure 9 filled with argon and with boron trifluoride, respectively. It is evident that a large amount of capture takes place in boron trifluoride while the capture in argon (which has been properly purified) seems to be negigible. The behavior of the curve for boron trifluoride depends critically on the origin of the gas, which seems to indicate that the capture is due, at least partly, to impurities rather than to the boron trifluoride itself.

The experimental arrangement for the second type of measurement mentioned at the beginning of the present section is schematically represented in Figure 11. X represents an x-ray tube in which the beam intensity can be controlled by means of a grid placed in front of the cathode. CH is the ionization chamber to be investigated. Since the x-ray tube is operated at a comparatively low voltage (around 40 kilovolts) a window covered with a thin metal foil must be provided in the wall of the chamber in order to admit the soft x-ray beam. The voltage drop across the leak resistor R, after suitable amplification, is applied to the vertical deflecting plates of a cathode ray oscilloscope. The sweep circuit provides a square positive pulse and a saw tooth pulse, which are used to turn on the beam of the oscilloscope and to produce a horizontal linear sweep, respectively. The sweep circuit also provides a square negative pulse, the beginning of which can be delayed by an adjustable amount with respect to the beginning of the sweep. The sweep circuit

Figure 10

Pulse height as a function of E/p in argon (840 mm Hg pressure) and $BF_3$ (388 mm Hg pressure). Measurements taken with the chamber represented in Figure 9.

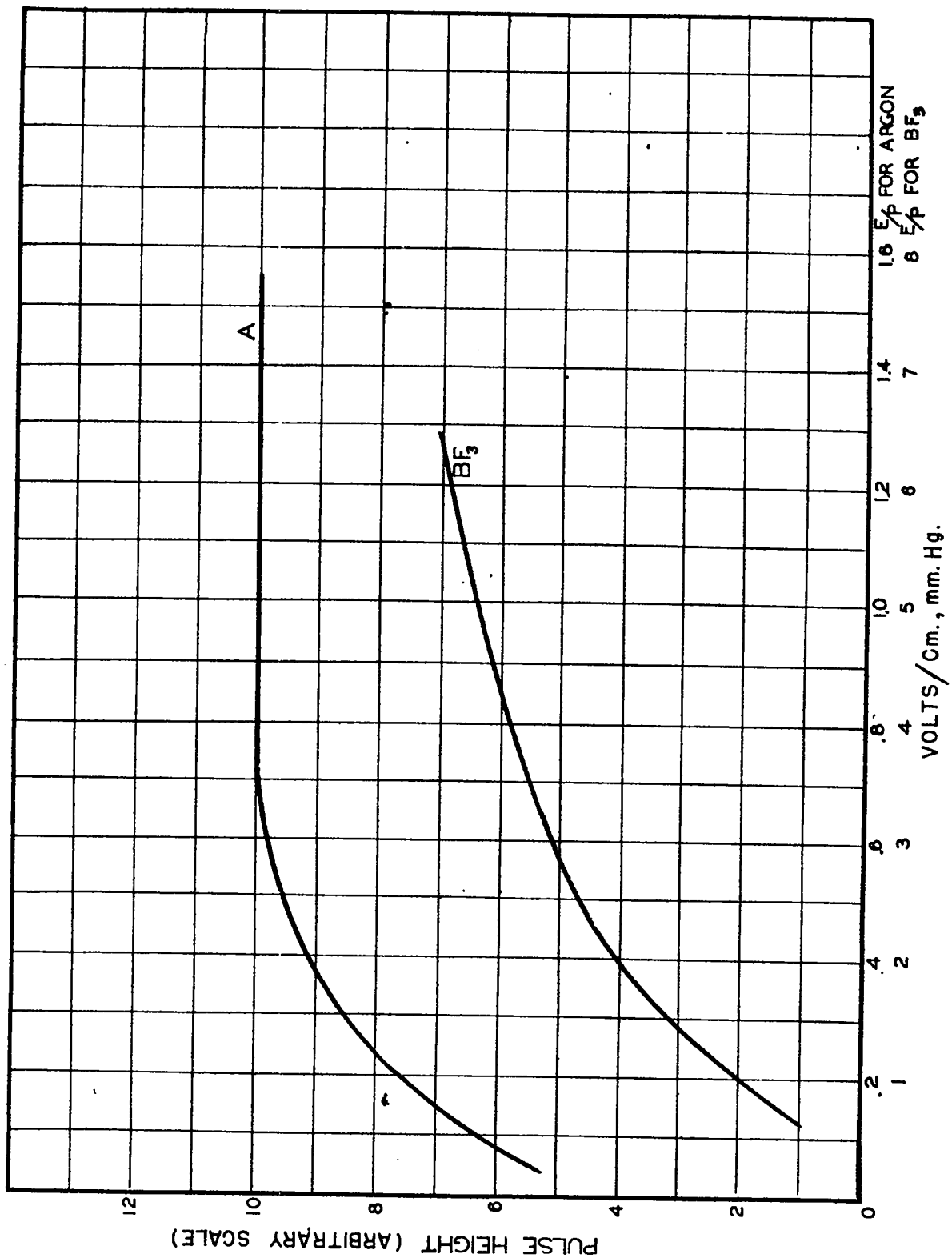

Figure 11

Experimental arrangement for testing "fast" chambers with a modulated x-ray source.

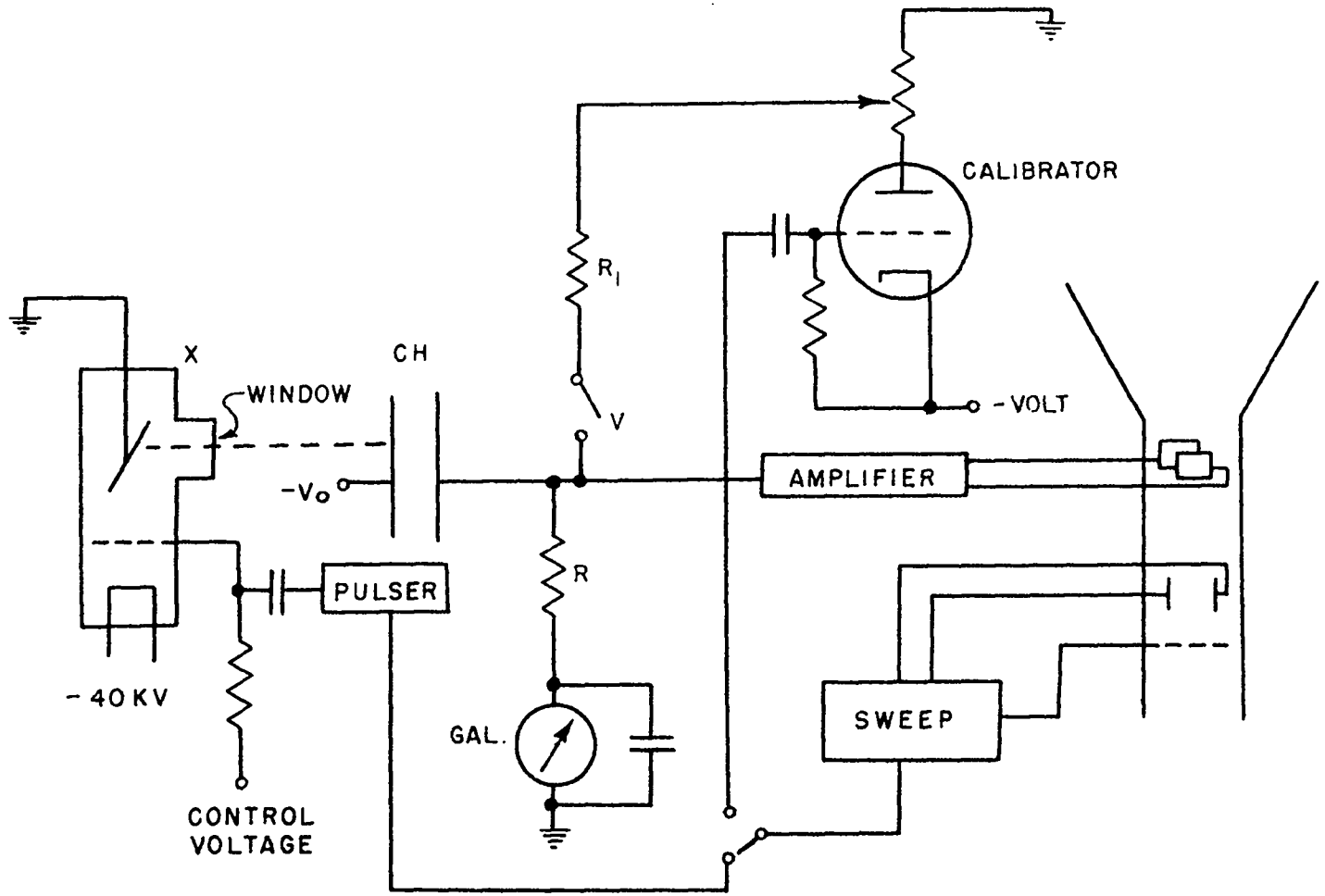


APPROVED FOR PUBLIC RELEASE

can either be made to operate automatically at a rate of the order of one hundred sweeps per second or it may be triggered manually so as to give single sweeps. The delayed signal from the sweep circuit may be used to trigger the circuit marked pulser, the purpose of which is to turn on or off the x-ray beam by suddenly raising or lowering the voltage of the control grid. When the pulser is connected and the sweep circuit is operated, there will appear on the oscilloscope screen a trace which gives the output voltage $V_e$ as a function of time subsequent to the sudden turning on or off of the ionizing beam. $V_e(t)$ is given by Equation 2f, which, in the case, for instance, of a constant source of ionization turned on at the time $t = 0$, yields:

$$V_e(t) = e N \int_0^t \chi(t_1)\, dt_1$$

If the resolving time of the amplifier is sufficiently small, the function $\chi(t)$ can be approximated by a $\delta$-function and, according to Equation 24, $\chi(t) = f(t)$. The equation written above then becomes

$$V_e(t) = \text{constant} \int_0^t f(t_1)\, dt_1$$

This method for testing chambers is superior in many ways to that described previously which makes use of $\alpha$-particle pulses. Successive pulses obtained by turning on or cutting off the x-ray beam are exactly identical, while $\alpha$-particle pulses always differ somewhat from one another because a beam of $\alpha$-particles is never perfectly collimated and is often not perfectly monoenergetic. Also it is possible to calibrate the x-ray equipment so as to determine very accurately the fraction of the ionization current carried by the electrons. The following procedure is used. With the x-ray tube running at a constant intensity, the ionization current $I_c = I_c^+ + I_c^-$ is measured by means of a galvanometer in series with the leak resistor R. Then the sweep circuit is operated manually, thus cutting off the x-ray beam, and the size of the "fast" pulse appearing on the oscilloscope screen is recorded. The height of this pulse is proportional to the intensity of the electron

current $I_o^-$. Then the x-ray tube is turned off and a current equal to the ionization current previously measured is sent through the leak resistor R by connecting its upper end through another resistor $R_1$ ($R_1 \gg R$) to an appropriately chosen point along the plate resistor of the tube marked "calibrator". The output of the sweep circuit giving a delayed square negative pulse is disconnected from the x-ray pulser and connected to the grid of the calibrator tube. When the sweep circuit is now operated, the delayed negative pulse will turn off the calibrator tube thereby interrupting the current through the leak resistor. The height of the pulse appearing on the oscilloscope screen is proportional to the intensity of the current originally present in R, which is equal to the total ionization current $I_o^+ + I_o^-$. Hence, the ratio between the sizes of the pulses obtained by turning off the x-ray beam and by cutting off the calibrator current, respectively, will be equal to the ratio $I_o^-/(I_o^+ + I_o^-)$ of the electron current to the total ionization current. Experience has shown that the fractional value of the electron current can be determined to within one or two per cent by this method.

The testing equipment described above was used to investigate the response of a parallel plate chamber, uniformly irradiated over its sensitive volume. The construction of this chamber is represented in Figure 12.

A photographic record of the oscilloscope deflection obtained by turning on the x-ray beam is reproduced in Figure 13. The chamber was filled with purified argon at 1.8 atmospheres pressure, and the high voltage electrode was kept at -1000 volts.

In Figure 14, the observed pulse shape, curve (3), is compared with the theoretical pulse shape computed for a drift velocity of $1.35 \times 10^6$ centimeters per second, which gives the closest fit with the experimental data.

According to Equation 32, when the x-ray beam is suddenly turned on, the electron current increases as a quadratic function of the time until all electrons have been collected. This function is represented by curve (1) in Figure 14. Curve (2) represents the output pulse corresponding to the current pulse represented by curve (1) and computed by taking into account the transient response of the amplifier, the

Figure 12.

Chamber used for the tests with the pulsed x-ray source. X-rays are admitted into the sensitive volume through the 0.005" brass window in the outer case and the 0.001" dural window in the high voltage electrode.

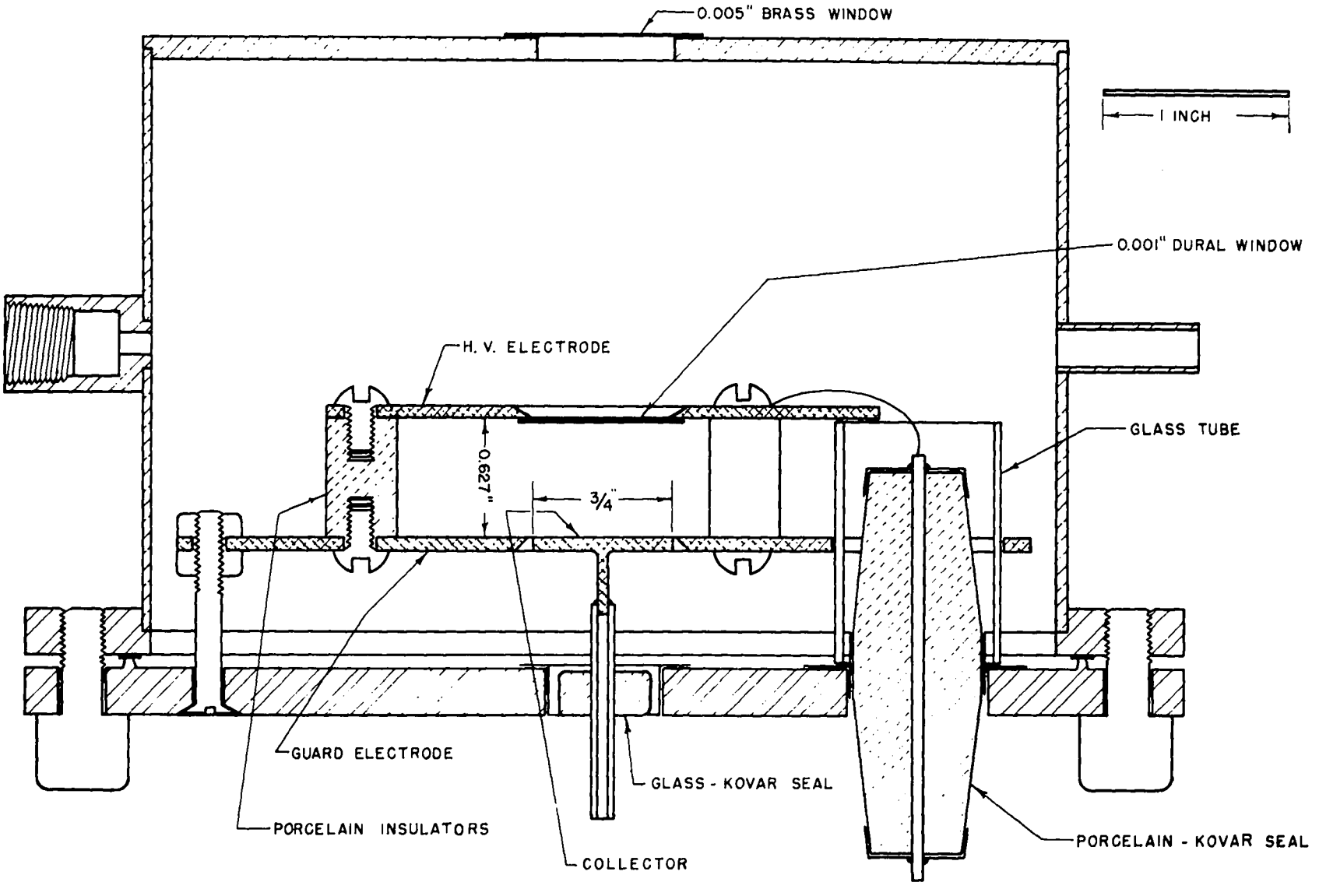


APPROVED FOR PUBLIC RELEASE

Figure 13.

Oscilloscope record obtained with the arrangement shown in Figure 10. The total duration of the sweep is approximately 1.5 $\mu$ seconds. Repetition rate about 100/sec. Exposure about 2 seconds.
The small oscillation at the beginning of the pulse is caused by electric pick up from the circuit which turns on the x-ray beam.

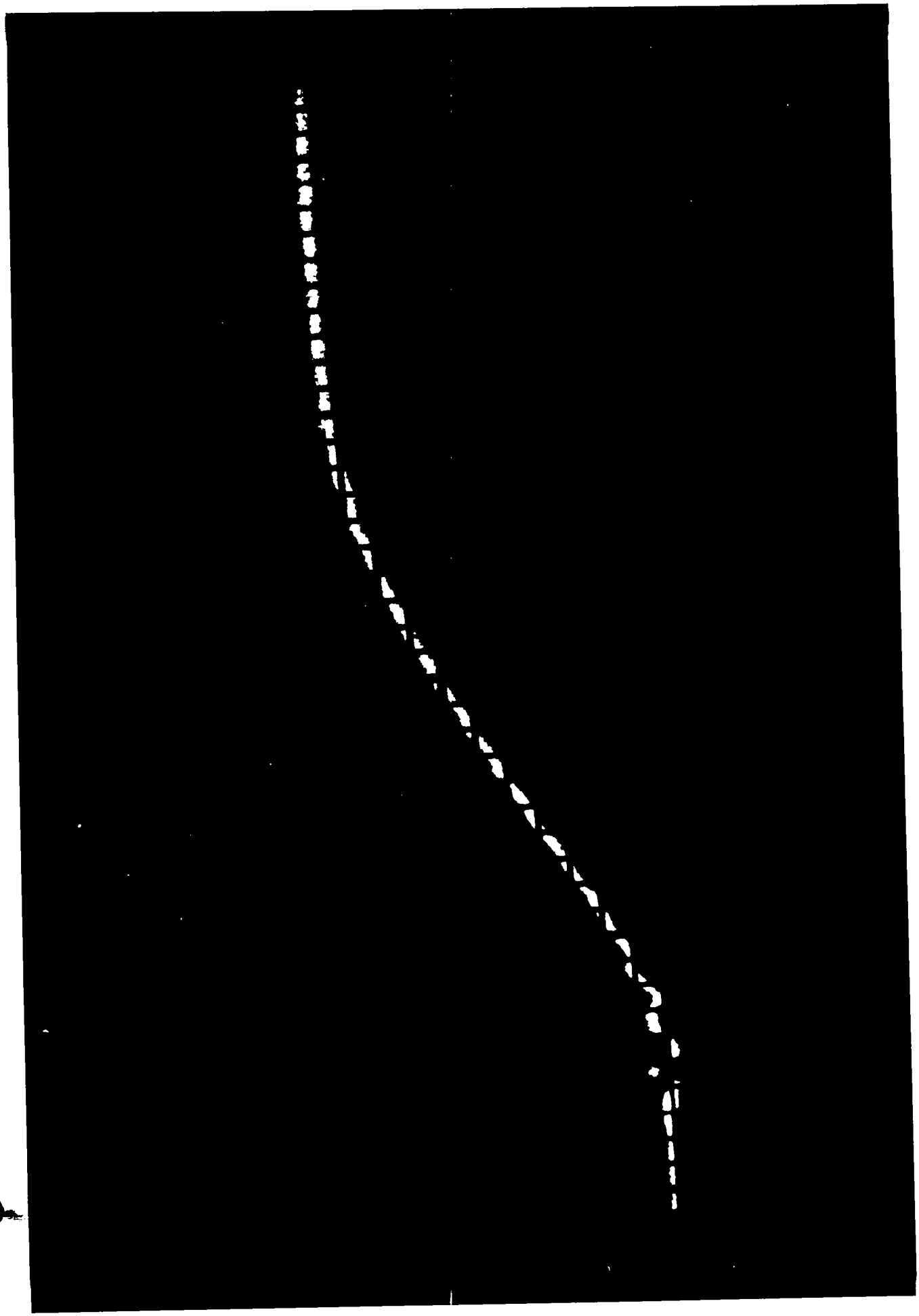

resolving time of which was approximately $2.4 \times 10^{-7}$ seconds. One sees that the agreement between experimental and theoretical pulse shapes is satisfactory, if not perfect. A possible explanation for the difference between curves (2) and (3) may be found in the edge effects (see Section 7), since, as it is apparent from the design of the chamber (Figure 12) the gas was irradiated up to the boundary of the sensitive volume. Should the experiment be repeated, this source of error could be minimized by providing uniform irradiation of the gas not only within the sensitive volume, but also outside of this volume, up to a distance from its boundary comparable with the separation of the plates.

The experiment described may be considered as a check of the theoretical predictions on the operation of the chamber or, alternately, as a method for the determination of the drift velocity of electrons. The values of the drift velocity obtained with this method are included in the graphs given in Figure 8.3.

The pulsed x-ray equipment was also used for the determination of the fraction of electron current in cylindrical ionization chambers filled with mixtures of argon and $CO_2$ (see Section 12.4). The experimental results were in very good agreement with the theoretical predictions, indicating that the electron attachment was negligible.

## 10.9 STATISTICAL FLUCTUATION OF THE IONIZATION CURRENT

When a chamber is connected to a fast amplifier and irradiated with a strong source, the output voltage exhibits fluctuations which are considerably larger than those due to the tube noise. These fluctuations are caused by statistical fluctuations in the intensity of the ionization current. An approximate estimate for their magnitude can be obtained as follows: Let $\tau$ be the resolving time of the detecting equipment which, as we have seen, is determined by the time for collection of the electrons in the chamber, by the input time constant RC, and by the frequency response of the amplifier. We may assume that the instantaneous value of the output voltage is proportional to the number of ion pairs produced in the chamber in the time equal to $\tau$, and this number, in turn, is proportional to the number of ionizing particles

Figure 14.

Comparison between computed and observed pulse shapes for the parallel plate chamber represented in Figure 12. A constant source of ionization is turned on at the time t = 0. Curve (1) gives the electron current in the chamber, computed for a drift velocity of $1.35 \times 10^6$ centimeters per second (separation of the plates; 1.57 cm.). Curve (2) gives the voltage at the output of the amplifier, computed for a value RC = 0.24 $\mu$ seconds of the input time constant and by taking into account the frequency response of the amplifier. Curve (3) gives the observed output voltage (from Figure 13).

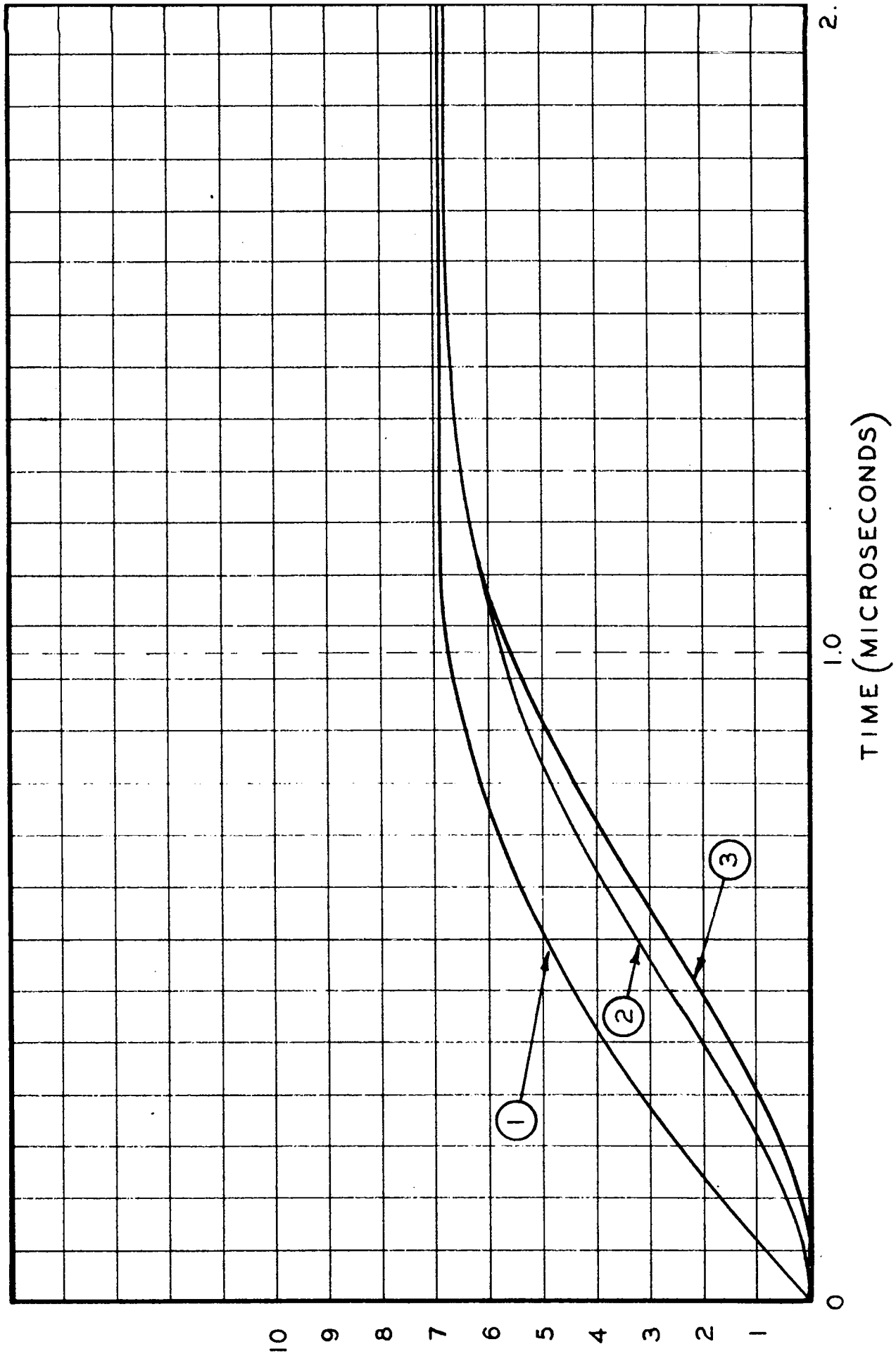

traversing the chamber during the time $\tau$ . If I is the intensity of the ionization current and m is the average number of ion pairs produced by each particle in the chamber, the average number of particles traversing the chamber during the time $\tau$ is given by $I\tau/me$. This number undergoes statistical fluctuations, the root mean square of which has the relative value $1/\sqrt{I\tau/me}$. This quantity represents also the relative value of the root mean square fluctuation of the output voltage, which we will indicate with $\Delta V/V$. Hence we have

$$\Delta V/V = \sqrt{me/I\tau} \qquad (40)$$

Some experiments were carried out for the purpose of checking the above relation. In these experiments, eight cylindrical chambers of the type which will be described in Section 12.4 were used. These chambers were 18 inches in length, 2 inches in diameter and were filled with a mixture of argon and carbon dioxide to a pressure of 4.5 atmospheres. They were all connected in parallel and their total capacity, including that of the connecting cables and of the amplifier input, was approximately 100 micromicrofarad... The leak resistor had a value of 1000 ohms, hence the input time constant was $10^{-7}$ seconds. The chambers were irradiated with a strong $\gamma$-ray source. A galvanometer, in series with the leak resistor and by-passed by a large condenser, was used for measuring the ionization current. The voltage drop across the resistor was applied to the input of a fast amplifier (70 per cent gain at 4 megacycles). The variable component of the output voltage was measured by means of a bolometric arrangement, which gave directly the mean square value of the fluctuations.

The experimental results are summarized in Figures 15 and 16. Figure 15 represents the mean square value of the fluctuations as a function of the current in the chambers. The voltage across the chambers was 2000 volts, and the ionization current was changed by varying the distance between the source and the bank of chambers. According to Equation 40, $(\Delta V)^2$ is given by the expression:

$$(\Delta V)^2 = V^2 \frac{me}{I\tau} = RI \frac{me}{\tau} \qquad (40')$$

Figure 15.

Average square fluctuation of the output voltage $(\triangle V)^2$ as a function of the intensity I of the ionization current. Eight cylindrical chambers in parallel (see description in Section 12.4) operated at 2000 volts.

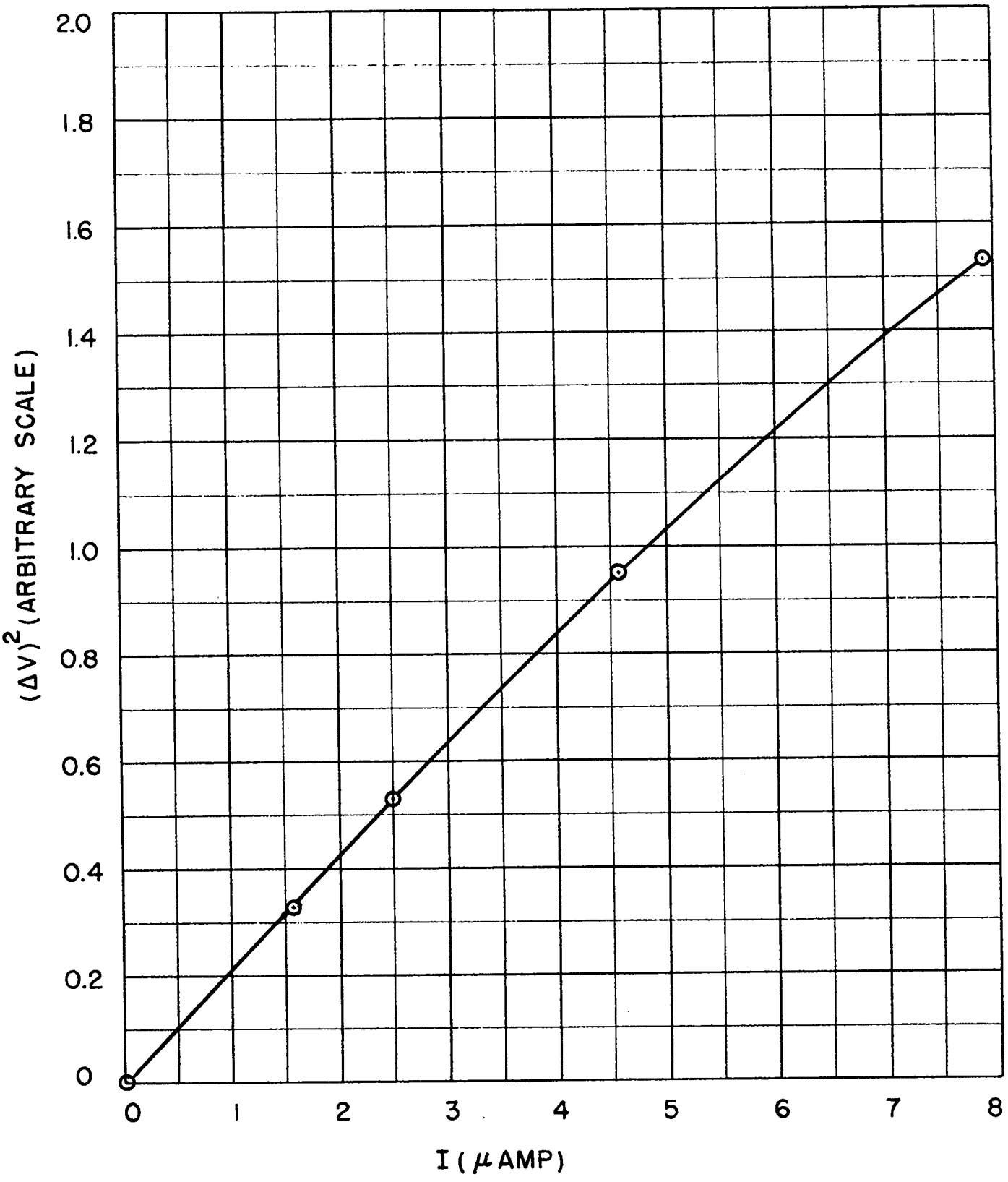

Figure 16

Average square fluctuation of the output voltage $(\Delta V)^2$ as a function of the voltage $V_o$ across the chambers for two different intensities of radiation. In both cases the ionization currents reach their saturation values ( $I_s = 0.54$ and $I_s = 0.19$ micro-amperes, respectively) in the neighborhood of 400 volts.

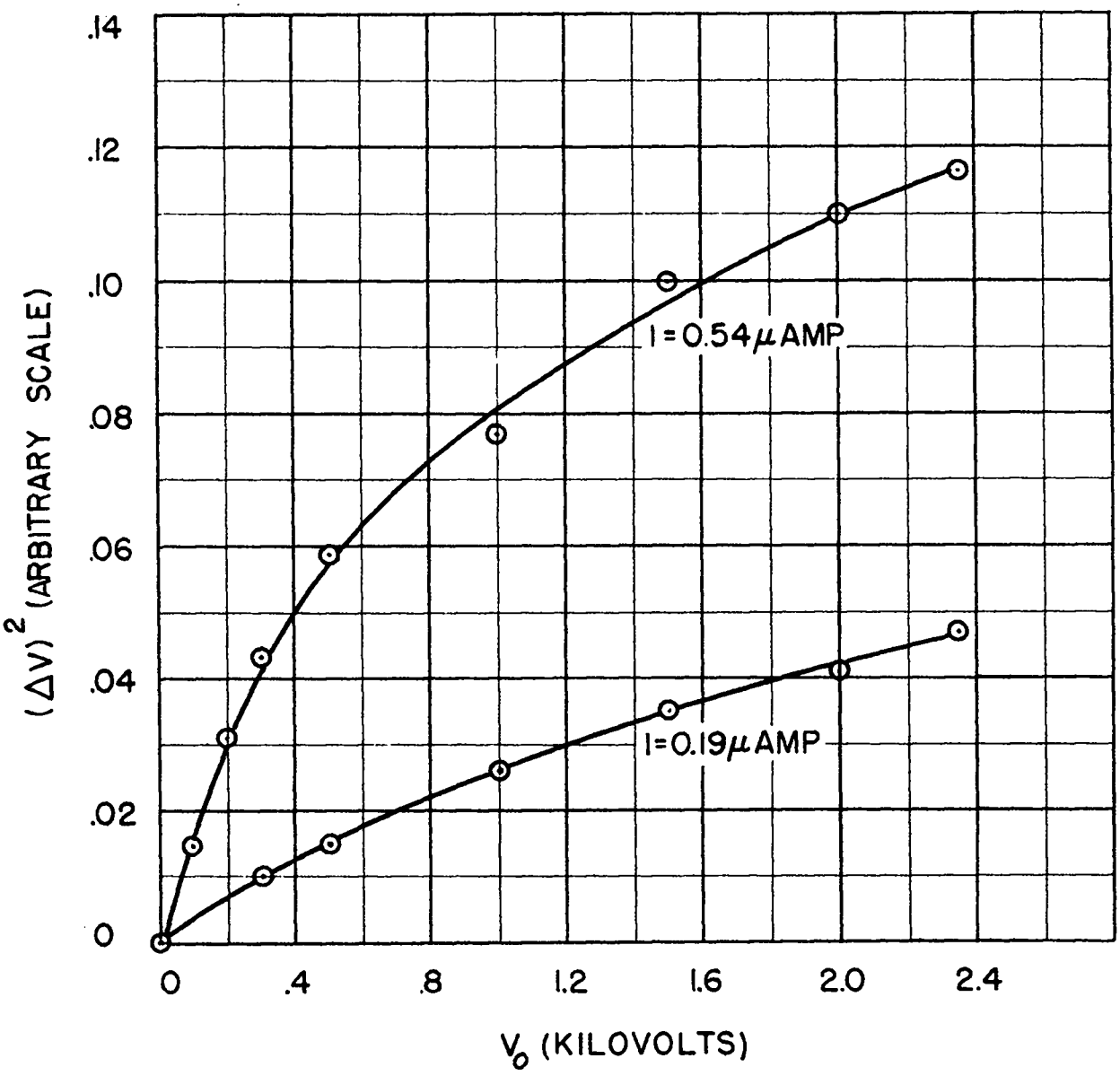

which indicates that $(\Delta V)^2$ should be proportional to I, if $\tau$ is constant. The curve in Figure 15 shows that this is approximately the case at leastso long as the ionization current is not too large. For large values of the ionization current, a deviation from the proportionality law becomes apparent. It is possible that this deviation may be caused by space charge effects which decrease the field in the chambers, thereby increasing the time of collection of electrons.

Figure 16 gives $(\Delta V)^2$ as a function of the voltage applied to the chambers for two fixed positions of the $\gamma$-ray source. In both cases, the ionization currents reached their saturation values at about 400 volts. These saturation values were 0.19 and 0.54 microamperes respectively. The dependence of $(\Delta V)^2$ on the chamber voltage shown in Figure 16 can be understood qualitatively if one considers that in the case in question the resolving time $\tau$ was mainly determined by the time of collection of the electrons, since this was long compared with both the input time constant and the time of rise of the amplifier. Hence, the observed increase of $(\Delta V)^2$ with voltage reflects the increase of the average drift velocity of electrons in the chambers.

Equation 40 may be expected to give the correct dependence of $\Delta V$ on I and $\tau$ but cannot be used for an accurate calculation of $\Delta V$, because of the simplifying assumptions which have been made in its derivation. However, if one takes $\tau$ as equal to the time of rise of the output pulse, and if one calculates m by assuming that all particles have in the chamber a track length equal to the chamber diameter, the calculated value of $(\Delta V)^2$, calculated from Equation 40, is within a factor of two of the observed value.

## 10.10 LIMITS OF VALIDITY OF THE THEORY

The method developed in Section 1 for the computation of the signal obtained from an ionization chamber breaks down when the ionization current varies very rapidly with time. Two assumptions were implicitly made in the argument leading to the fundamental equation, Equation 8, namely:

(1) The variations of the ionization current in a time of the order of the

transit time of an electromagnetic disturbance through the chamber are negligible. If it were not so, the signals obtained from various portions of the chamber would not simply add up, as Equation 8 implies. This condition may be expressed by the inequality

$$\frac{\ell}{c}\,\frac{dI}{dt} \ll I \qquad (41)$$

where $\ell$ represents the largest linear dimension of the chamber and $c$ is the velocity of light.

(2) The variations of the magnetic energy must be sufficiently small so that they may be neglected in the energy balance. If $W_m$ represents the magnetic energy, this condition is expressed by the inequality

$$\frac{d W_m}{dt} \ll V_o I \qquad (42)$$

Now $W_m$ is of the order of $h \ell^2 H^2$ where h represents the separation of the electrodes, $\ell$ their linear dimension, and H is some average value of the magnetic field. H, in turn, is of the order of $\ell ej/c = I/\ell c$. (For instance, $\pi \ell ej/c$ is the field at the edge of a circular parallel plate chamber of diameter $\ell$, in which the ionization current has a constant density ej.) Hence the condition given in Equation 42 may be rewritten as follows:

$$(h/c^2)\ (dI^2/dt) \ll V_o I$$

or

$$(\ell^2/c^2)\ (dI/dt) \ll V_o \ell^2/h \qquad (42')$$

It is easy to show that if Equation 41 is satisfied, then Equation 42' is satisfied as well, at least in all practical cases. In fact the condition given in Equation 41 gives $(\ell^2/c^2)\ (dI/dt) \ll (\ell/c)\ I$. The quantity $(\ell/c)\ I$ represents the charge carried by the ionization current during the transit time of an electromagnetic disturbance through the chamber. This is always small compared with the quantity $(\ell^2/h)\ V_o$ which represents, apart from a numerical factor, the charge

present on the electrodes on account of the field existing between them. Therefore we conclude that condition (1) is not only necessary, but in all pratical cases, also sufficient for the validity of the theory developed.

As we have seen in Chapter 8, the drift velocities not only of ions but also of free electrons are always very small compared with the velocity of light. This means that in the case of an instantaneous burst of ionization, the ionization current will set in suddenly but will subsequently vary with time at a sufficiently slow rate so as to insure the validity of our approximation. It follows that even though the theory developed does not enable one to calculate the current I for a time of the order of $l/c$ after the production of the ionization burst, it will give correct results for all subsequent times.

## 10.11 VERY RAPIDLY RISING IONIZATION PULSE

The theory is inadequate for the solution of a practical problem only in case one wants to calculate the signal produced by a source of ionization, the intensity of which keeps increasing very rapidly with time. In this case one has to start from the Maxwell equations, which read:

$$\begin{aligned} \text{curl } \vec{E} &= -\frac{1}{c}\frac{\partial \vec{H}}{\partial t} \\ \text{curl } \vec{H} &= \frac{1}{c}\frac{\partial \vec{E}}{\partial t} + 4\pi e\,(n^+ \vec{w}^+ - n^- \vec{w}^-) \\ \text{div } \vec{E} &= 4\pi e\,(n^+ - n^-) \\ \text{div } \vec{H} &= 0 \end{aligned} \tag{43}$$

The following simplifying assumptions will be made:

(1) The electromagnetic signal produced by the ionization is small compared with the pre-existing static electric field. This means that $\vec{w}^+$ and $\vec{w}^-$ may be considered as given functions of the position.

(2) Recombination and attachment are negligible. This condition becomes less restrictive as the pulse becomes faster. It means that the ion and electron

densities $n^+$, $n^-$, and the corresponding drift velocities, $\vec{w}^+$ and $\vec{w}^-$ are related by the equations

$$\frac{\partial n^+}{\partial t} = n_o - \text{div} \left[ n^+ \vec{w}^+ - D^+ \text{ grad } n^+ \right]$$
$$\frac{\partial n^-}{\partial t} = n_o - \text{div} \left[ n^- \vec{w}^- - D^- \text{ grad } n^- \right] \qquad (44)$$

where $n_o$ represents the number of ion pairs produced per second and per unit volume at a given position. As a consequence of the first assumption, Equations 44 are not connected with Equations43 and may be solved separately, with the boundary conditions that $n^+ = 0$ at the positive electrode, and $n^- = 0$ at the negative electrode. The values thus found can then be introduced in Equations43.

As an example, let us consider the case that the intensity of the ionizing radiation increases exponentially with time so that

$$n_o (x, y, z, t) = \psi (x, y, z) \; e^{t/\tau}$$

Since Equations44 are linear in $n^+$ and $n^-$, and since the only term which depends on the time explicitly is an exponential function of the time, there exist solutions in which $n^+$ and $n^-$ depend on the time as $e^{t/\tau}$. These solutions satisfy the correct initial conditions if we assume that $n^+$ and $n^-$ are zero before the beginning of the ionization pulse ( $t = -\infty$). This means that the only terms which depend explicitly on time in Maxwell's equations (Equation 43) are again exponential functions of the type $e^{t/\tau}$. As a consequence, the vectors $\vec{E}$ and $\vec{H}$, which describe the electromagnetic disturbance produced by the pulse, also vary with time as $e^{t/\tau}$, if we only assume that they are zero before the ionization pulse begins. We conclude that, under the very mildly restrictive conditions set forth above, a source of ionization, the intensity of which increases exponentially with time, will always produce in an ionization chamber a signal which exhibits the same time dependence as the intensity itself.(1)

(1) It can be shown easily that, while the absence of recombination is an essential condition for the validity of this result, the absence of attachment is not.

In many practical cases, diffusion may be neglected. If the signal is very short, the terms div $(n^+ \vec{w}^+)$ and div $(n^- \vec{w}^-)$ in Equation 44 may also be neglected and $n^+$ and $n^-$ are then given by the equations

$$n^+ (x, y, z, t) = n^- (x, y, z, t) = \int_0^t n_0 (x, y, z, t_1)\, dt_1 \qquad (45)$$

if we assume that they are both zero at the time t = 0. This means that in Maxwell's equations we may consider the density of charge as zero and the density of current as a given function of time and position.

As a practical application, let us consider the following problem. A coaxial line of infinite length consisting of two conducting cylinders is filled with a gas, so that it forms an ionization chamber. The two cylinders are at different voltages with the outer cylinder, for instance, positive.

For the description of the field, a cylindrical system of coordinates $(r, \varphi, z)$ will be used, with the z axis along the axis of the line.

Let us assume that a section of the line of very small length $\Delta$ and situated at z = 0 is uniformly ionized by an external agent. Furthermore, let us assume that the drift velocities of ions and electrons are proportional to the electric field, and therefore inversely proportional to the r coordinate. This means that the current density in the ionized layer is inversely proportional to r, so that its absolute value is given by an expression of the form

$$e\, j = e \left| \vec{j}^+ - \vec{j}^- \right| = \frac{a}{r}\, e\, j_a \qquad (46)$$

where a is the radius of the inner tube and $j_a$ is the value of j at the surface of this electrode. If $w_a^+$ and $w_a^-$ are the absolute values of the drift velocities at the same place, $j_a$ is given by

$$j_a (t) = (w_a^+ + w_a^-) \int_0^t n_0 (t_1)\, dt_1 \qquad (47)$$

Now it is well known that in a coaxial line made of two perfectly conducting cylinders separated by an uncharged dielectric of dielectric constant equal to 1, Maxwell's equations have solutions in which the electric vector has only an r-component $E_r$, while the magnetic vector has only a $\theta$-component, $H_\theta$. $E_r$ and $H_\theta$ are equal in magnitude and are given by equations of the type

$$E_r = H_\theta = (1/r)\ f_1\ (t - z/c) \tag{48}$$

or

$$E_r = -H_\theta = (1/r)\ f_2\ (t + z/c) \tag{49}$$

Equation 48 represents a transverse wave propagating with light velocity, c, in the direction of the positive z axis. Equation 49 represents a transverse wave propagating with the same velocity in the negative direction.

It is easy to show that, under the assumptions made above, the ionization pulse will produce two waves of this type propagating in opposite directions from the ionized layer. For this purpose, we only need to prove that the boundary conditions at $z = 0$ can be satisfied by assuming that the electromagnetic field is represented by equations of the type in Equation 48 for $z > 0$, and by equations of the type in Equation 49 for $z < 0$. These boundary conditions state that $\vec{E}$ is continuous across the ionized layer, while the value of $\vec{H}$ changes by $4\pi/c$ times the surface density of current in the ionized layer. Since we have assumed that the outer conductor is positive, this current points towards the inner conductor and the boundary condition give the following equations

$$(1/r)\ f_1\ (t) - (1/r)\ f_2\ (t) = 0$$

$$(1/r)\ f_1\ (t) + (1/r)\ f_2\ (t) = (4\pi/c)\ \Delta\ (a/r)\ e\ j_a$$

These equations may be satisfied for all values of z if one takes

$$f_1\ (t) = f_2\ (t) = (2\pi/c)\ \Delta\ a\ e\ j_a\ (t)$$

The solution of our problem is therefore:

$$E_r = H_\varphi = (2\pi/c)\,\Delta\,(a/r) \cdot j_a\,(t - z/c) \qquad \text{for } z>0$$
$$E_r = -H_\varphi = (2\pi/c)\,\Delta\,(a/r) \cdot j_a\,(t + z/c) \qquad \text{for } z<0 \tag{50}$$

The current, I, in the inner tube can be calculated from the equation

$$4\pi I = 2\pi r\, H_\varphi \tag{51}$$

Together with Equation 50 this gives

$$I\,(z,t) = (\pi/c)\,\Delta\, a\, e\, j_a\,(t - z/c) \qquad \text{for } z>0$$
$$I\,(z,t) = -(\pi/c)\,\Delta\, a\, e\, j_a\,(t + z/c) \qquad \text{for } z<0 \tag{52}$$

The quantity $2\pi a \Delta j_a$ represents the total charge flowing from the ionized layer into the inner conductor per unit time. Hence, Equations 52 simply mean that the current entering the pipe at $z = 0$ splits into two equal parts which propagate with light velocity in the two opposite directions.

If the ionized layer is not infinitely thin, as it is assumed above, then the solution of the problem can be obtained by subdividing the ionized layer into an infinite number of infinitely thin layers and taking the sum (i.e., the integral) of the solutions corresponding to the elementary layers.

LOS ALAMOS TECHNICAL SERIES

VOLUME I

EXPERIMENTAL TECHNIQUES

PART II

CHAPTER 11

# GAS MULTIPLICATION

by

BRUNO ROSSI AND HANS STAUB

# CHAPTER 11

# GAS MULTIPLICATION

## 11.1 GENERAL CONSIDERATIONS

When in a portion of the volume of an ionization chamber, the electric field strength exceeds a certain value, the electrons which penetrate this volume will acquire, between collisions, a sufficient energy to ionize the gas molecules. Thus more electrons will be liberated, which in turn will produce more ionization by collision, until finally all electrons, whether directly produced by the external ionizing agent or generated by secondary collision processes, reach the positive electrode.

The phenomenon described above is called "gas multiplication" , and it is often used for the purpose of amplifying the effects of weakly ionizing radiations. The chambers to be operated with gas multiplication are usually in the shape of a hollow cylinder, with a thin wire stretched along the axis. The wire is always positive with respect to the cylinder and, when the difference of potential between the two electrodes is sufficiently large, there exists around the wire a cylindrical region where gas multiplication takes place. The diameter of this cylindrical region is usually a small multiple of the diameter of the wire. Hence, its volume is very small compared with the volume of the chamber, and the probability of an electron being produced in it by the primary ionizing radiation is negligible. The electrons produced outside of the region where gas multiplication takes place produce, on the average, the same number of ion pairs by collision before reaching the wire. Let us denote this number by n-1, so that n represents the total number of electrons per primary ion pair in what we may call the "initial avalanche". In addition to the electrons set free by collisions, electrons may be produced also by photoelectric effect, because ionization and excitation of the gas molecules by electron collision result in the emission of photons. Since the excitation energy is always smaller than

the ionization energy, when the counter is filled with a pure gas, photo-electric effect can only occur on the cathode. When, however, the counter is filled with a gas mixture, photons emitted by molecules of one kind may be able to ionize molecules of another kind. Let $\gamma$ be the average number of photoelectrons produced per ion pair generated in the gas (where always $\gamma \ll 1$ ). Then the initial avalanche of n electrons will be accompanied by the production of $\gamma n$ photoelectrons, which will produce a secondary avalanche of $\gamma n^2$ electrons. The argument may be repeated and one finally obtains the following expression for the total number M of electrons set free in the chamber when one ion pair is produced by an external agent:

$$M = n + \gamma n^2 + \gamma^2 n^3 \ldots . \qquad (1)$$

The value of $\gamma$ depends on the voltage applied. When the voltage is sufficiently low so that $\gamma n < 1$, we say that the chamber is operated as a "proportional counter". The number M is called the "gas multiplication" and its value is given by:

$$M = \frac{n}{(1 - \gamma n)} \qquad (1')$$

This equation shows that if n is sufficiently small, M is practically equal to n, which means that the photoelectric effect can be neglected.

If the voltage is such that $\gamma n \geq 1$, then Equation 1 gives $M = \infty$, which physically means that an electric breakdown occurs in the chamber. A chamber operated under these conditions is called a "discharge counter". The discharge may be inherently unstable, or may be quenched by external means. Not much development work on discharge counters was carried out at the Los Alamos project. Hence, we shall limit our considerations to the counters operating in the proportional region.

First, it should be pointed out that a proportional counter as defined above is not necessarily "proportional". In fact, the gas multiplication is a constant, i.e., independent of the primary ionization, only as long as one can neglect the modification of the electric field near the wire caused by the space charge. This is the case when both the primary ionization and the gas multiplication are suffi-

ciently small. Let us assume for the moment that this condition is fulfilled, and let us assume, moreover, that no electron attachment takes place. Then the gas multiplication M, for a given gas, will be a function of the diameter a of the wire, of the diameter b of the cathode, of the pressure p, of the voltage $V_o$ across the counter. It will also depend on the nature of the cathode, if the photoelectric effect plays a role. If, however, the phtoelectric effect is negligible, which is always the case for sufficiently low values of the gas multiplication, then the nature of the cathode is immaterial, and all significant phenomena take place at a small distance from the wire. Hence M will not change, if $V_o$ and b are changed in such a way as not to alter the field at the wire. Moreover, M will remain unchanged if a and b are multiplied by a common factor k, p is divided by the same factor, and if $V_o$ is kept constant. In fact, by so doing all linear dimensions, including the mean free paths, are multiplied by the same factor k, while the electric field strength is divided by k. Hence the energy gained by the electrons between collisions at corresponding points of the two counters is the same, and the number of collisions for electrons travelling between two corresponding points of the two counters is also the same. It follows that M can be expressed as a function of the ratio $V_o / \log (b/a)$ and of the product pa:

$$M = M\left( \frac{V_o}{\log(b/a)} , pa \right) \qquad (2)$$

We want now to discuss qualitatively the <u>time dependence</u> of the pulse given by a proportional counter. For simplicity, we shall assume that the wire is grounded through a resistance R, sufficiently large so that the product RC of this resistance times the combined capacity C of the collecting electrode plus the input of the amplifier represents a time long compared with the duration of the pulse. Suppose now that $N_o$ ion pairs are produced simultaneously at a given point of the counter. The electrons will drift toward the wire, causing its potential to vary by a small amount. As soon as the electrons reach the neighborhood of the wire, gas multiplication takes place.

In a very short time all the electrons formed by collision will reach the wire, and during this time the potential of the wire will undergo an appreciable change. At the same time, the positive ions will start drifting away from the wire at first rapidly, then more and more slowly as they go into the region where the field is weaker. Thus the potential of the wire will continue to change after all electrons have been captured, first fairly rapidly, then very slowly. Hence the pulse of the proportional counter may be expected to exhibit a shape of the type shown in Figure 1. The "delay" $t_1$ in the beginning of the pulse depends of course on the distance from the wire at which the original ions are formed. If this distance is of the order of one cm, $t_1$ may be expected to be a few tenths of a microsecond. The time interval $t_2 - t_1$ in which the gas multiplication takes place and the electrons are swept away is only a small fration of a microsecond.. The total time for the positive ions to reach the cathode is of the order of a millisecond, but most of the pulse due to the motion of the positive ions takes place in a much shorter time, while the positive ions travel in the intense field near the wire. The contribution of the electrons to the pulse is in general smaller than the contribution of the positive ions, because the ionization by collision takes place usually at a distance from the wire smaller than the wire radius.

In the case that the primary ions are not produced all at the same place, but are distributed along a track of finite length, the electrons from the various sections of the track will reach the region where multiplication occurs at various times. This modifies the shape of the initial part of the pulse in a manner which depends on the position and on the orientation of the track. However, the shape of the pulse, after a time long compared with the time of collection of electrons, will not be appreciably affected. Also, as long as space charge effects can be neglected, the pulse shape, for a given gas multiplication, will be independent of the number of primary ions.

Usually, the time constant RC, or more generally, the resolving time of the ampli-

Figure 1

Schematic representation of the shape of the pulse of a proportional counter.

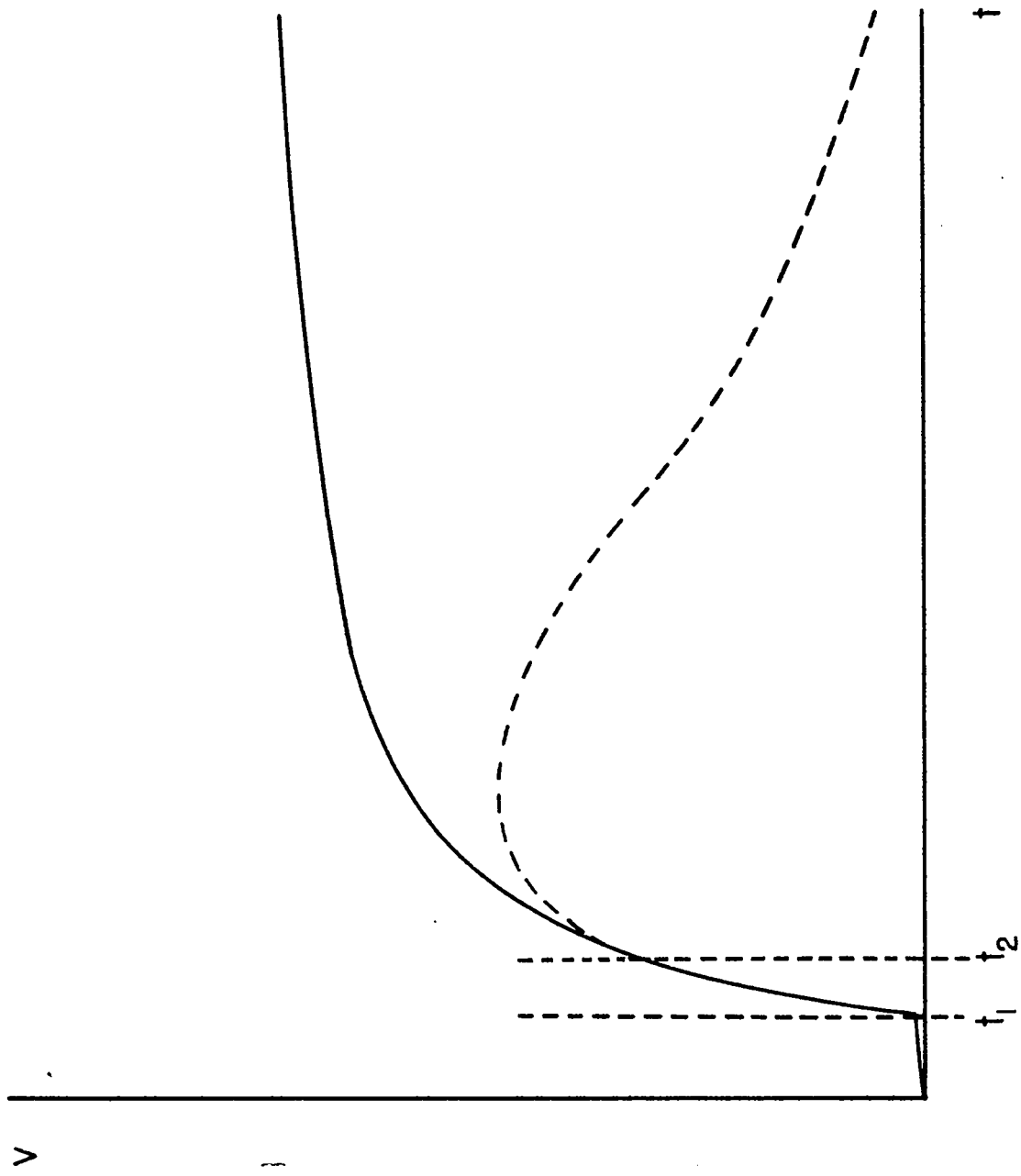

fier is chosen so as to be large compared with the time $t_2$ for the collection of electrons, but short compared with the total time for the collection of positive ions. The observed pulse shape will then be of the type represented by the dotted line in Figure 1. The pulse height will depend somewhat on the value of the resolving time but will be independent of the position of the track because this only affects the shape of the initial part of the pulse, as pointed out above.

Again, under the assumption that space charge effects can be neglected, the time dependence of the current, through the counter, when a continuous source of ionization is suddenly turned on or off, is identical to the time dependence of the voltage of the wire when a number of ion pairs is produced simultaneously in the counter, exactly as in the case of an ionization chamber without gas multiplication (see Section 10.4).

The analysis of the operation of a proportional counter, when space charge effects cannot be neglected is hopelessly complex. The effect of the positive space charge left near the wire after the removal of the electrons is to weaken the field near the wire, thereby decreasing the value of the gas multiplication. Possibly the size of the effect could be calculated in the case of a uniformly irradiated chamber. Such a calculation, however, would have little bearing on the problem, which is practically more important, of determining the effect of the space charge in a proportional counter used for the detection of individual ionizing particles. In this case, the total number of ion pairs produced per second in the counter is not the only factor to be considered. The gas multiplication for a given particle will be influenced by the space charge produced by particles which have penetrated the counter at earlier times, as well as by the space charge produced by the particle under consideration. These two effects require separate investigation. The second effect will depend, among other things, on the orientation of the track, because this determines both the length of the wire over which the space charge is distributed and the time interval during which the space charge is produced.

In conclusion, it does not seem practically possible to predict theoretically the conditions under which space charge effects start to become noticeable, nor to describe accurately the operation of proportional counters when this occurs. Whenever proportional counters are to be used for quantitative measurements, it is advisable to test their operation by checking the uniformity of the pulses produced by particles dissipating a given amount of energy in the counter, and possibly by determining whether or not the gas multiplication is independent of the primary ionization.

## 11.2 EXPERIMENTAL VALUES OF THE GAS MULTIPLICATION FOR VARIOUS GASES

It has been shown in the preceding section that, for sufficiently low values of the gas multiplication M, this quantity, for a given gas, may be expected to be a function of the two variables $V_o/\log(b/a)$ and pa only. Therefore it will be possible to calculate M for any set of values of $V_o$, p, a, and b if M has been measured as a function of $V_o$ and p with a given counter (a and b constant).

Measurements of the gas multiplication as a function of voltage and pressure were carried out for a number of gases in the following way. Alpha-particles from a polonium source were introduced in the counter and the pulses, after suitable amplification, were observed on the screen of an oscilloscope. Then the voltage across the counter was reduced until the counter was operating as an ionization chamber without gas multiplication, and the gain of the amplifier was increased until the output pulses had again the same amplitude. The increase in the gain of the amplifier was taken as a measure of the gas multiplication. This procedure would be rigorously correct only if the resolving time of the amplifier was large compared with the duration of the pulses. Actually, its value was approximately 100 microseconds, which is long compared with the time for the collection of electrons but short compared with the time for the collection of the positive ions. The error thus introduced, however, is not very serious because when the counter is used without gas multiplication, the pulse is

mainly due to the motion of the electrons (see Section 10.6), and when it is used with gas multiplication, the main part of the voltage change caused by the motion of the positive ions takes place in a time short compared with 100 microseconds. Moreover, this error does not affect the relative values of M because the pulse shape of a proportional counter does not change appreciably with gas multiplication.

Some of the gases investigated are listed below, along with the references to the figures which summarize the experimental results. It must be emphasized that no effort was made to reach any high degree of accuracy in obtaining the experimental data here presented:

| | |
|---|---|
| Fig. 2 | Tank Hydrogen |
| Fig. 3 | Methane |
| Figs. 4 & 5 | Tank Argon |
| Fig. 6 | Spectroscopic Nitrogen |
| Fig. 7 | Boron Trifluoride |
| Fig. 8 | 90% Hydrogen, 10% Methane mixture |
| Fig. 9 | 98% Argon, 2% $CO_2$ mixture |
| Fig. 10 | 90% Argon, 10% $CO_2$ mixture |
| Fig. 11 | 84% Argon, 16% Propane mixture |

From an examination of the experimental results summarized in Figures 2 to 11, one can draw the following conclusions:

(1) In most cases, the gas multiplication is, over a wide region, an approximately exponential function of the voltage.

(2) The slope of the curve which represents log M as a function of $V_o$ increases with decreasing pressure and decreasing wire diameter. For low pressures of hydrogen, argon, or nitrogen, the gas multiplication changes so rapidly with voltage that the counter is difficult to use. The addition of a small amount of

Figure 2

Tank hydrogen 99.97% pure. Wire diameter 2a = 0.010"; cylinder diameter 2b = 0.87". Gas multiplication M vs voltage for pressures of 10 and 55 cm Hg.

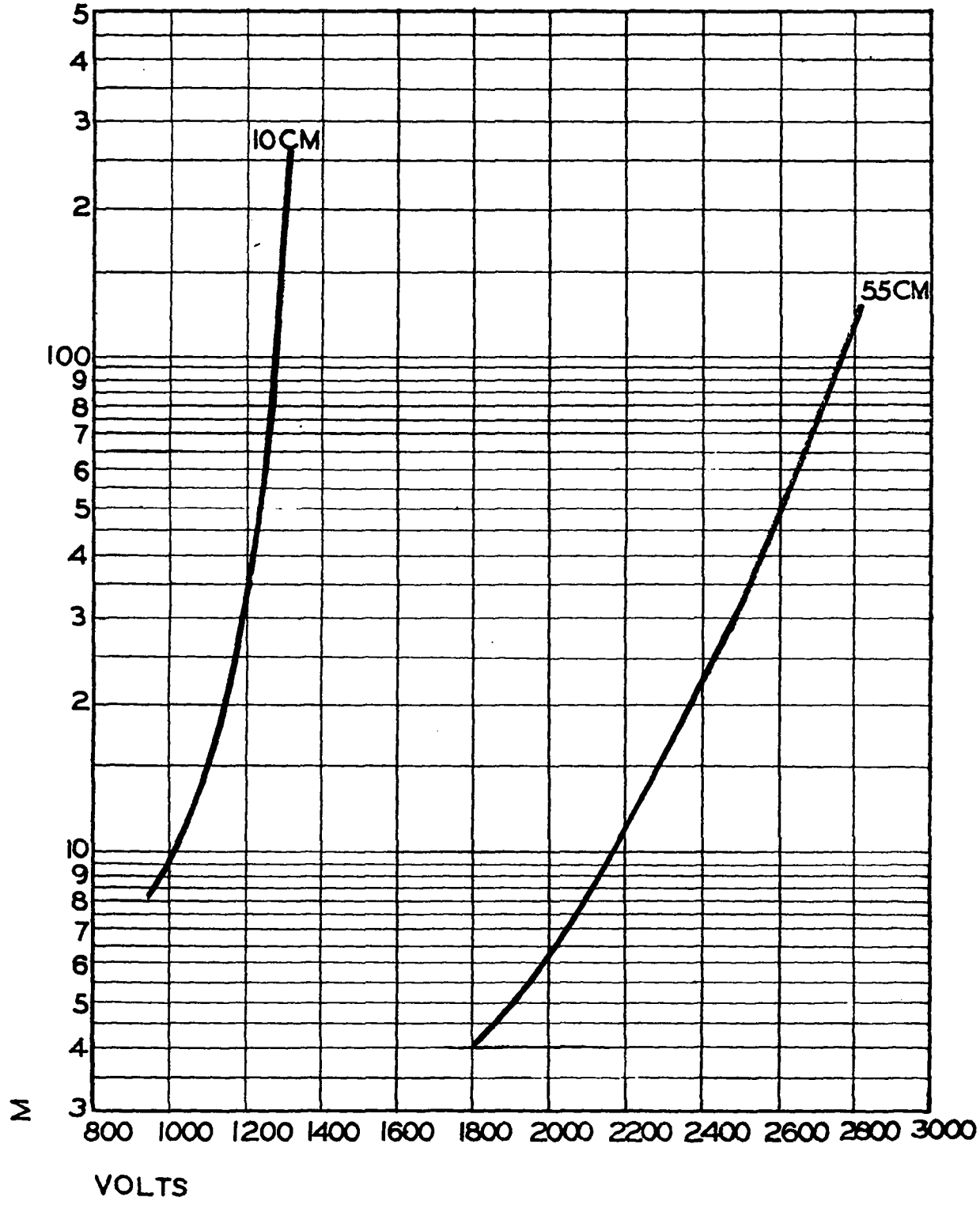

Figure 3

Methane 85% pure. Wire diameter: 2a = 0.010"; cylinder diameter 2b = 0.87". Gas multiplication M vs voltage for pressures of 10 and 40 cm Hg.

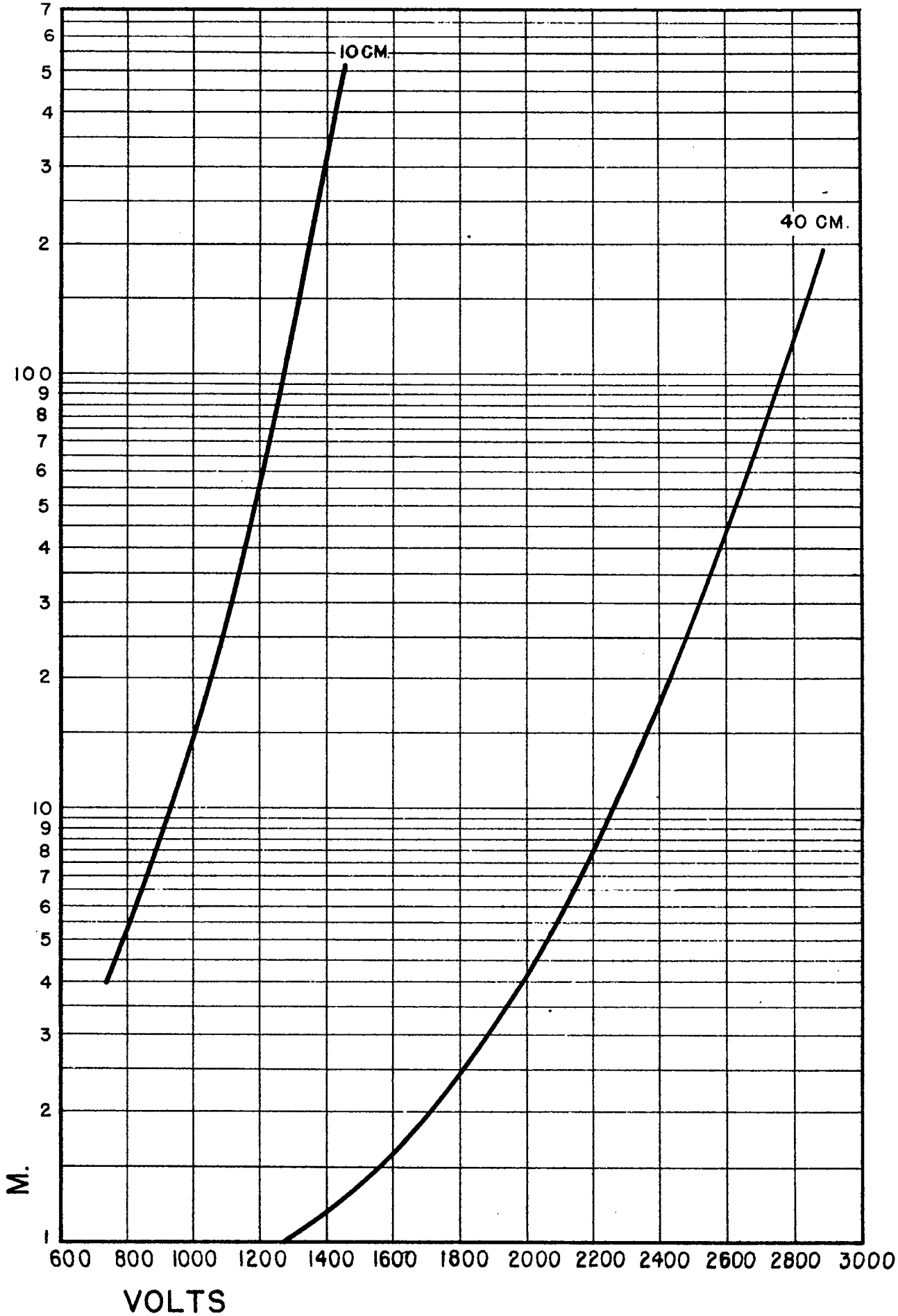

Figure 4

Tank argon 99.6% pure. Wire diameter 2a = 0.01"; cylinder diameter 2b = 0.87". Gas multiplication M vs voltage for pressures of 10 and 40 cm Hg.

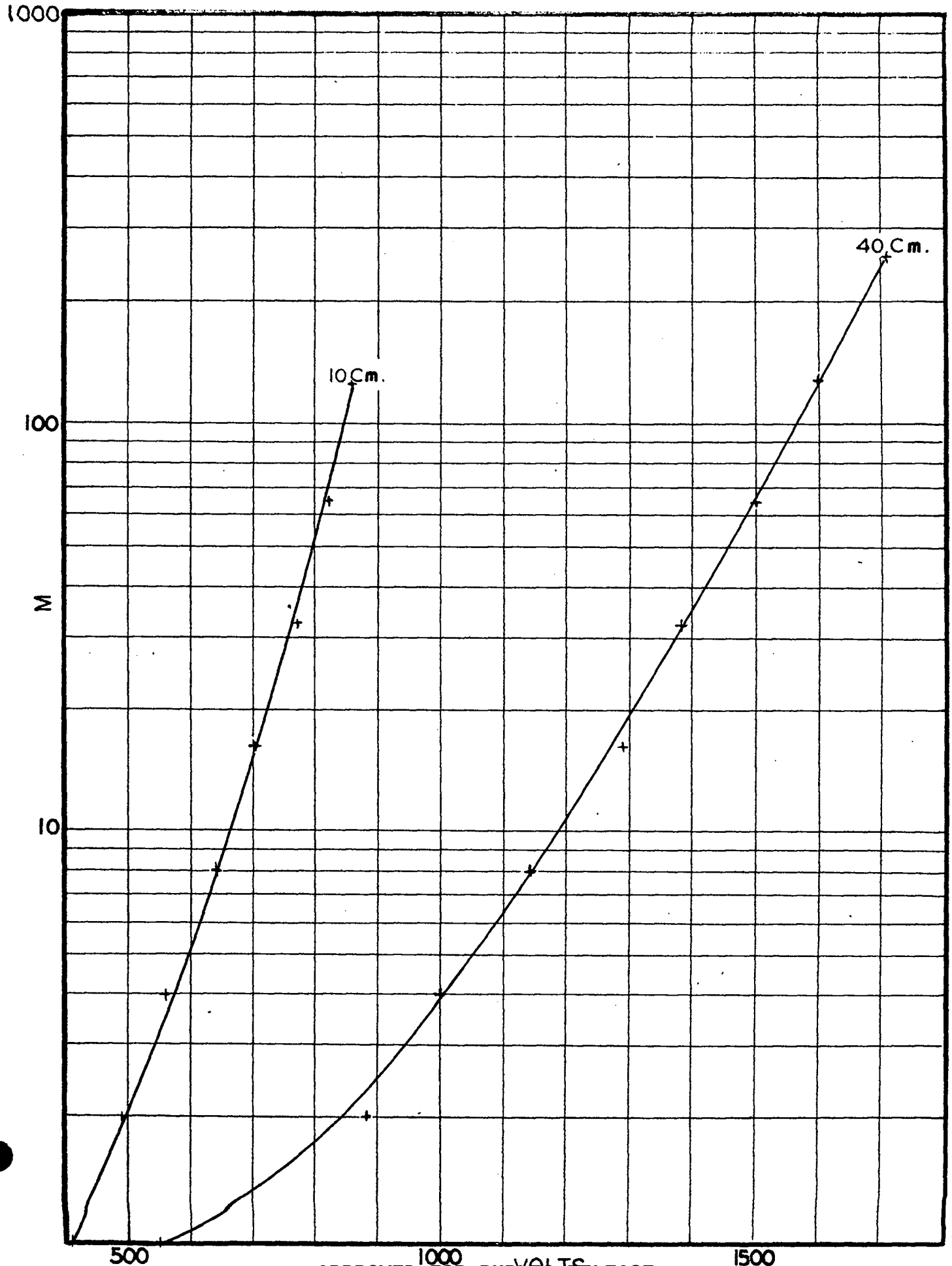

Figure 5

Tank argon 99.6% pure. Wire diameter 0.001"; cylinder diameter 1.56". Gas multiplication M vs voltage for a pressure of 6.8 atmospheres.

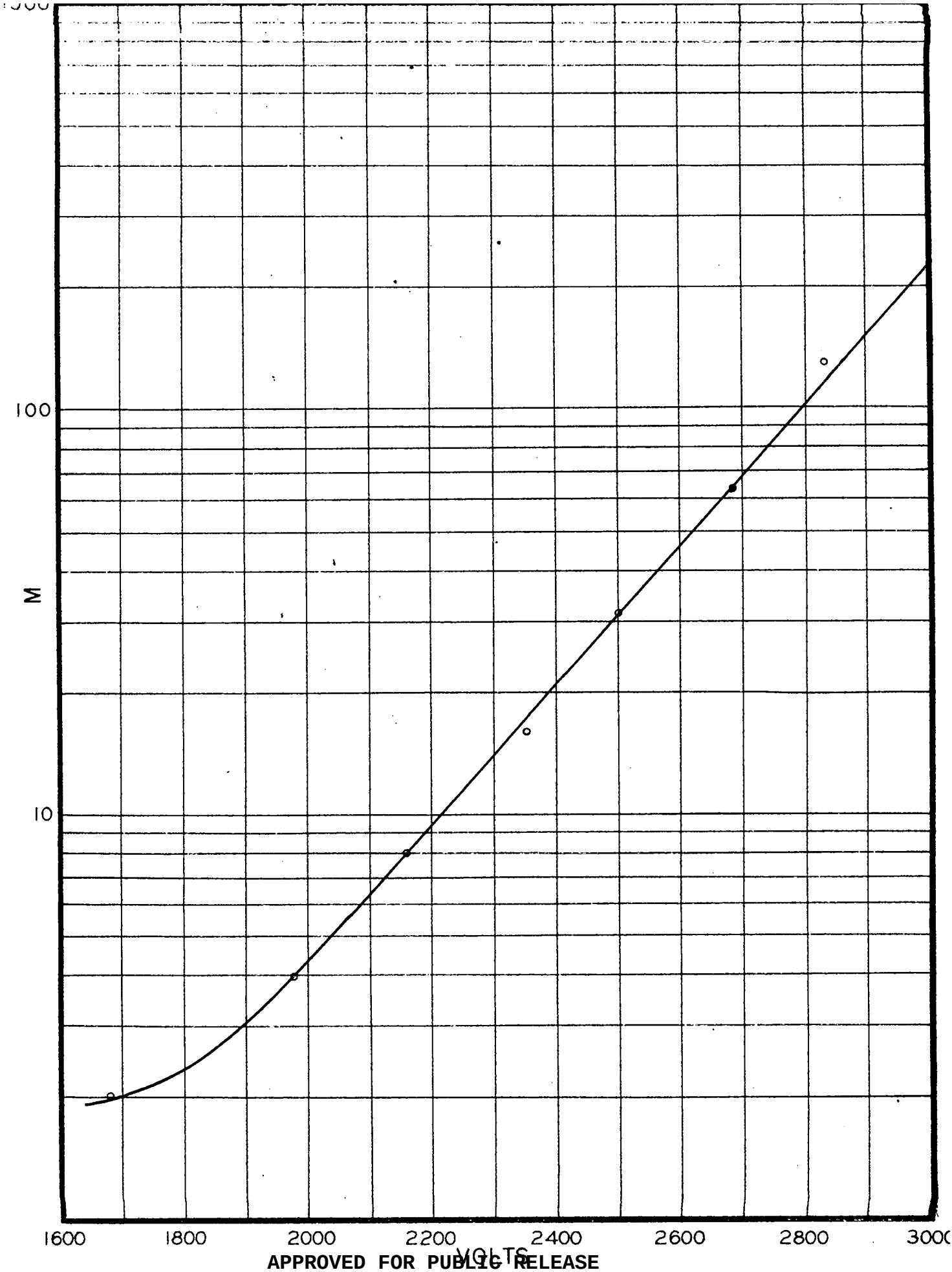

Figure 6

Spectroscopic nitrogen. Wire diameter 2a = 0.001"; cylinder diameter 1.56". Gas multiplication M vs voltage for pressures from 0.79 to 4.25 atmospheres.

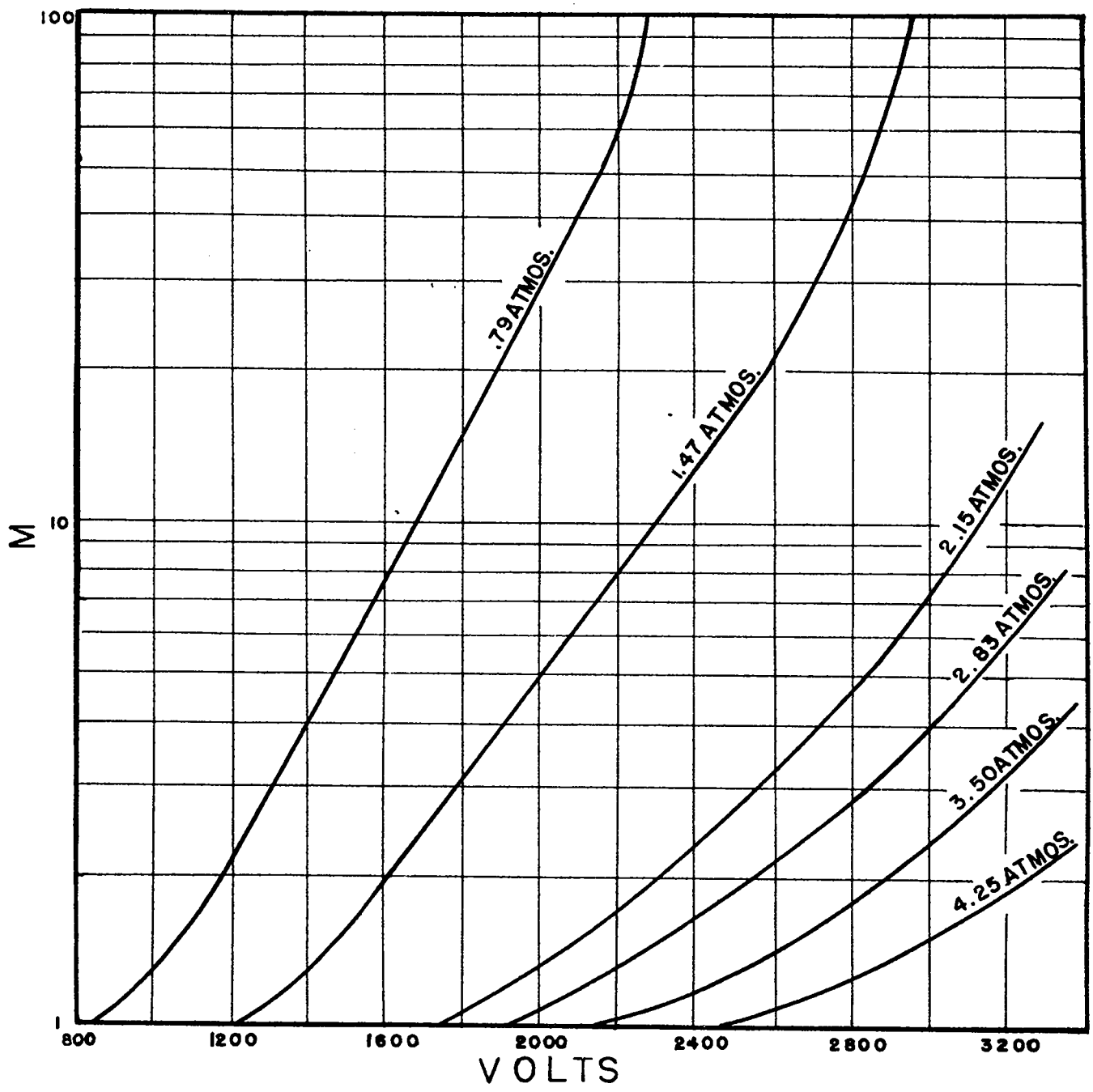

Figure 7

Boron trifluoride. Gas multiplication M vs voltage. Curve A: wire diameter 2a = 0.010"; cylinder diameter 2b = 1.50"; pressure p = 10 cm Hg. Curve B: wire diameter 2a = 0.001"; cylinder diameter 1.56"; pressure p = 80.4 cm Hg.

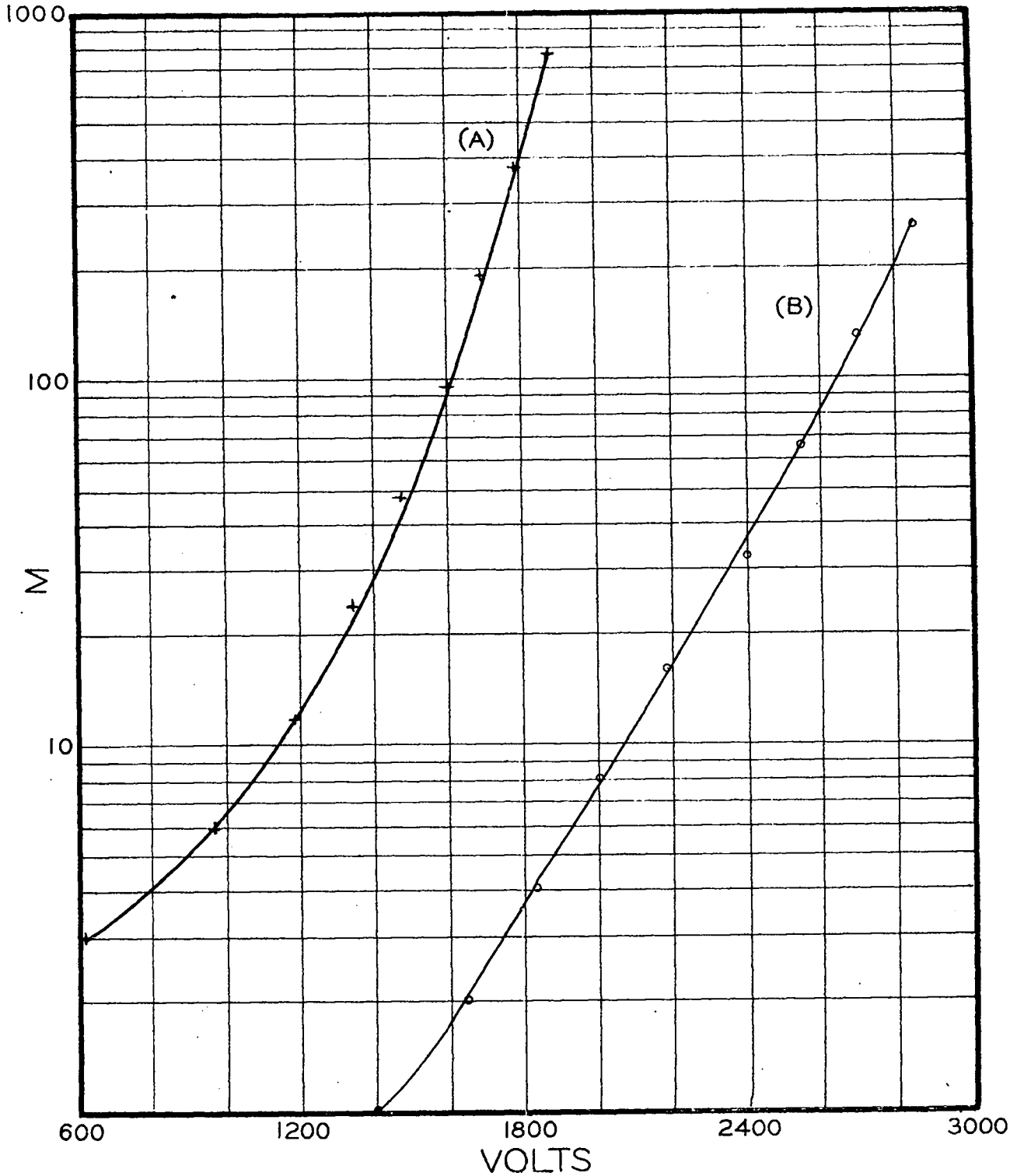

Figure 8

90% hydrogen, 10% methane mixture. Wire diameter 2a = 0.010"; cylinder diameter 2b = 0.87". Gas multiplication M vs voltage for pressures of 10 and 40 cm Hg.

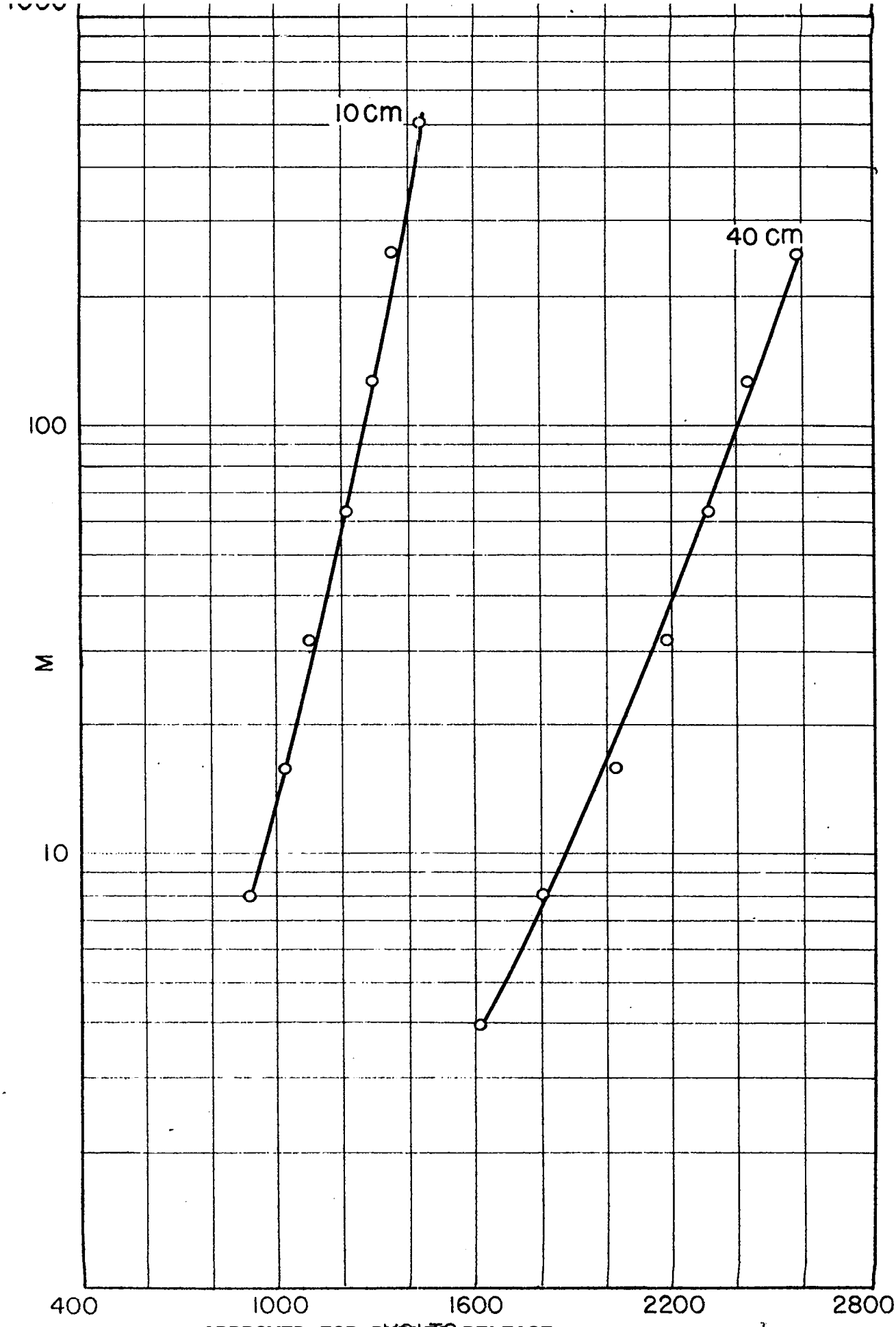

Figure 9

98% argon, 2% $CO_2$ mixture. Wire diameter 2a = ~~0.14"~~ 0.010"; cylinder diameter 2b = 0.87". Gas multiplication M vs voltage for pressures of 10 and 40 cm Hg.

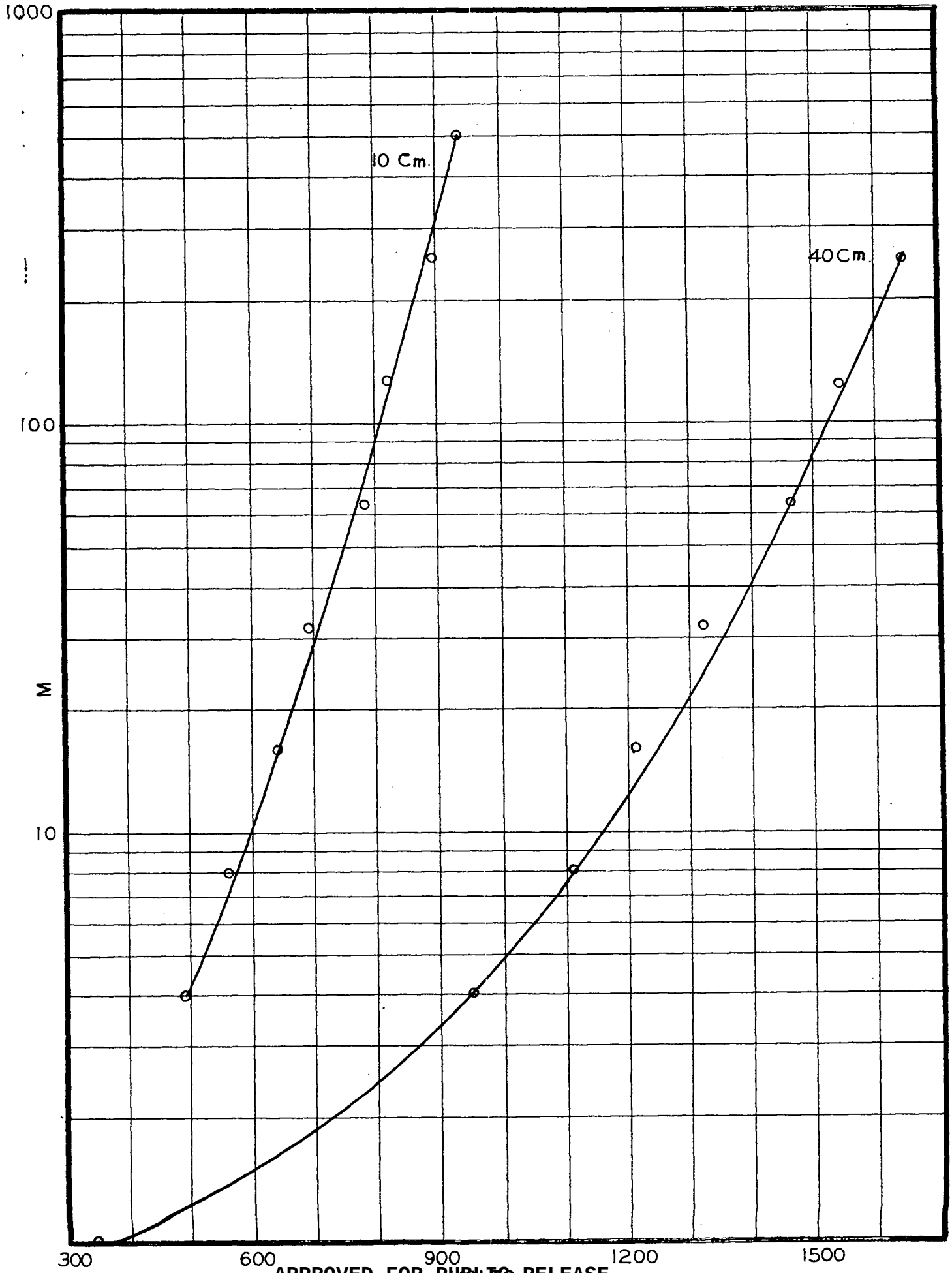

Figure 10

90% argon, 10% $CO_2$ mixture. Wire diameter 2a = 0.005"; cylinder diameter 2b = 1.50". Gas multiplication M vs voltage for pressures of 1.13, 2.15 and 3.5 atmospheres.

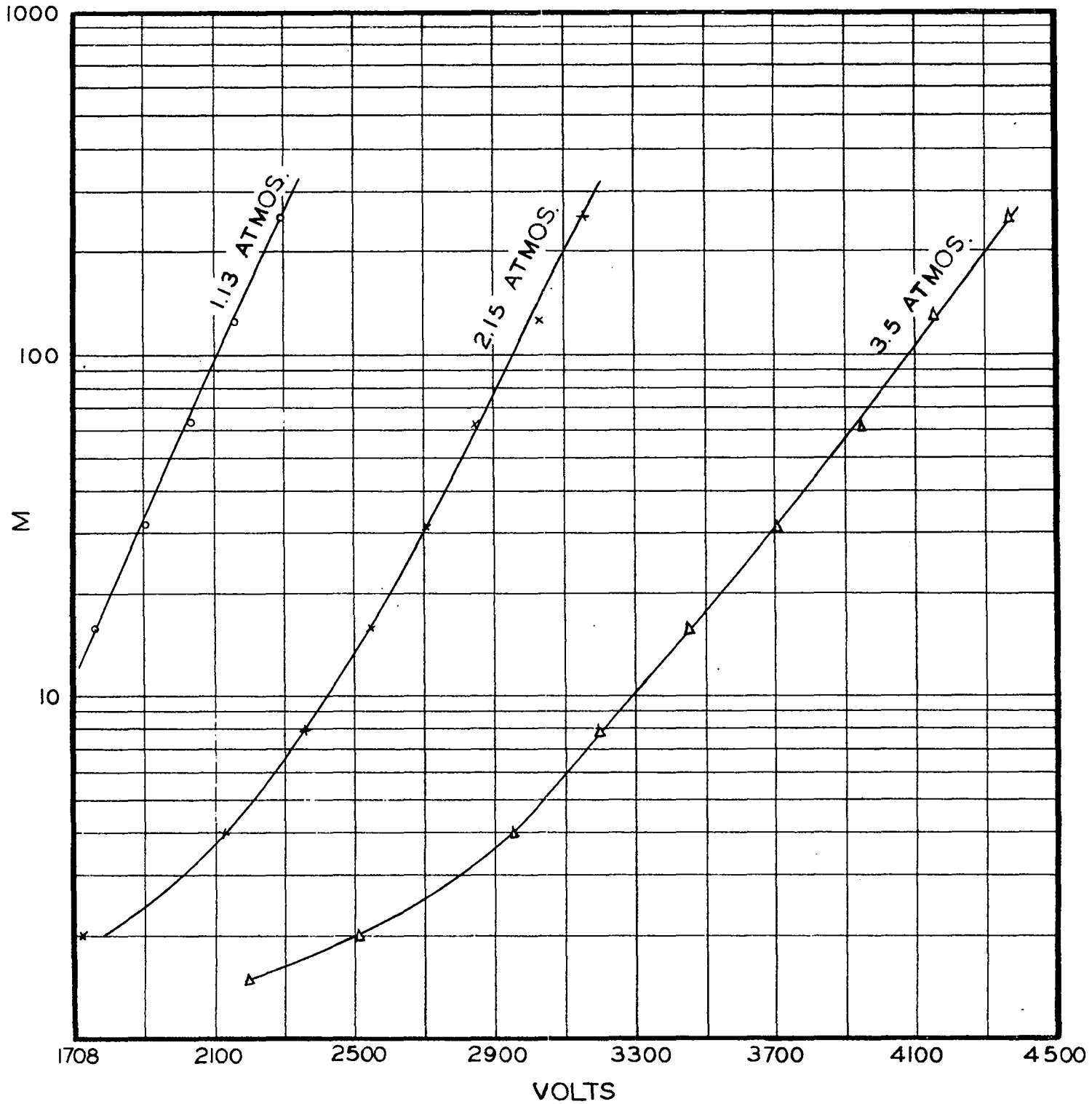

Figure 11

84% argon, 16% propane mixture. Wire diameter 2a = 0.001"; cylinder diameter 2b = 1.50". Gas multiplication M vs voltage at a pressure of 0.83 atmospheres.

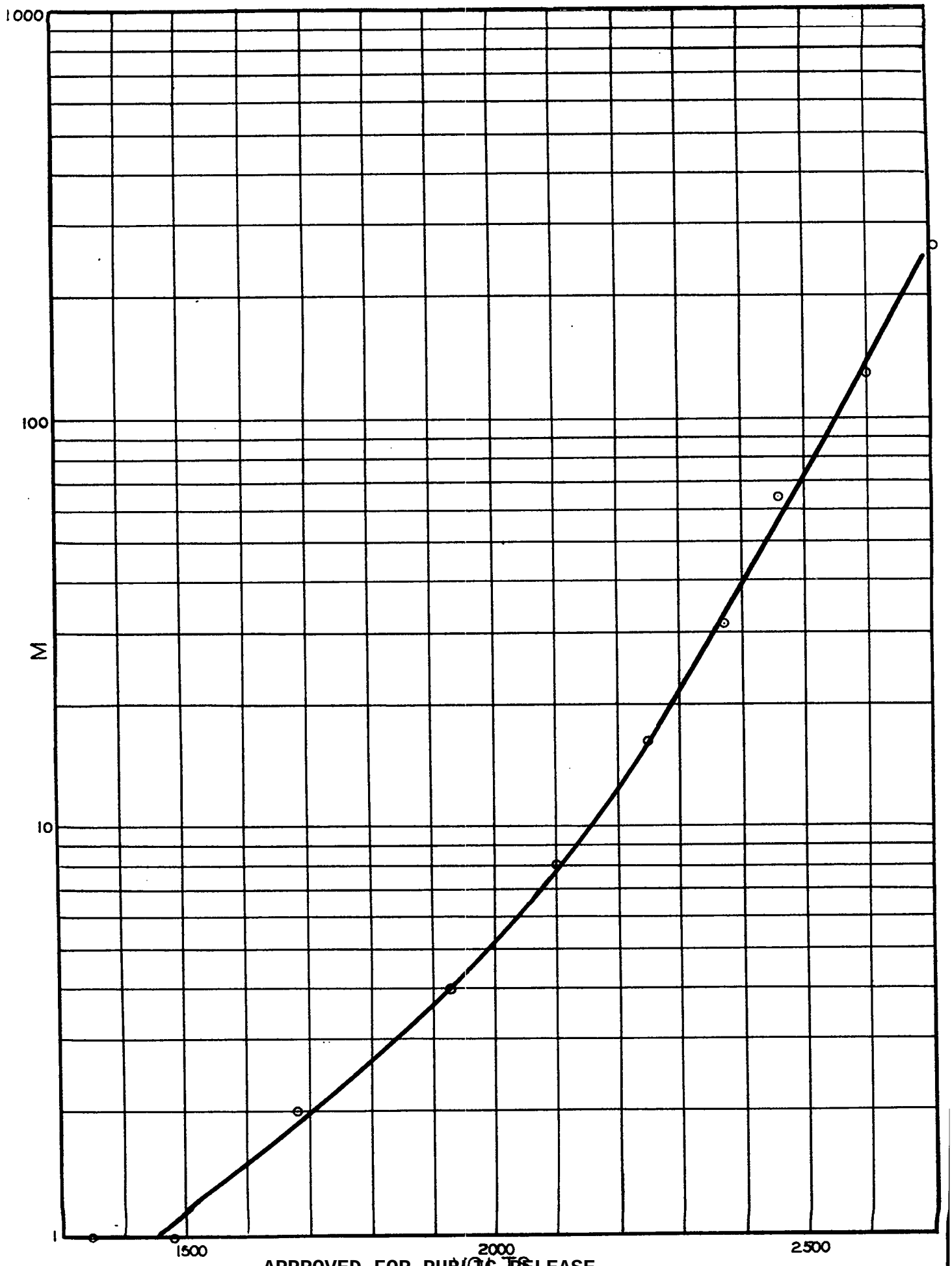

carbon dioxide to argon or of methane to hydrogen makes the dependence of M on $V_o$ at low pressures much less critical.

It may be added that an attempt was made to verify experimentally the relation expressed by Equation 2 by comparing the curves of $V_o$ vs p at constant M with argon filled counters of different dimensions, namely, 2a = 0.010", 2b = 0.87"; 2a = 0.001", 2b = 1.50"; 2a = 0.002", 2b = 1.50"; 2a = 0.005", 2b = 1.50". Discrepancies of the order of 10 per cent were found between the values of $V_o$ observed with a given counter and those computed by means of Equation 2 from the results obtained with a counter of different dimensions. It is difficult to decide whether or not the observed discrepancies are significant. They may well be due to errors in the measurement of the wire diameter.

11.3 THE SHAPE OF PROPORTIONAL COUNTERS

The shape of pulses from a proportional counter was investigated by determining the intensity of current as a function of time immediately after a constant source of ionization is suddenly turned off. For this test, the pulsed x-ray equipment described in Sec. 10.8 was used. The counter had an inner diameter of 0.75". The wire was 0.010" in diameter and 6" in length. The x-ray beam was admitted into the counter through a thin brass window. The irradiated section of the counter was 1.5" in length. The counter was connected in the same way as the ionization chamber shown in Figure 10.11. The resolving time of the amplifier was 0.8 microseconds.

Some of the results obtained with a gas filling of 30 cm Hg of argon and $CO_2$ (98% argon, 2% $CO_2$ ) are shown by the photographic records reproduced in Figure 12. The length of the sweep was 67 microseconds. Trace (a) was obtained with 300 volts across the counter, at which voltage no gas multiplication occurs. Under these conditions, the current through the counter was

Figure 12

Photographic records of pulses of a cylindrical chamber upon sudden interruption of constant source of ionization.

a. without gas multiplication
b. with gas multiplication
c. calibration pulse

The gain for (b) and (c) was about 30 times smaller than for (a). The total duration of the sweep was 67 microseconds.

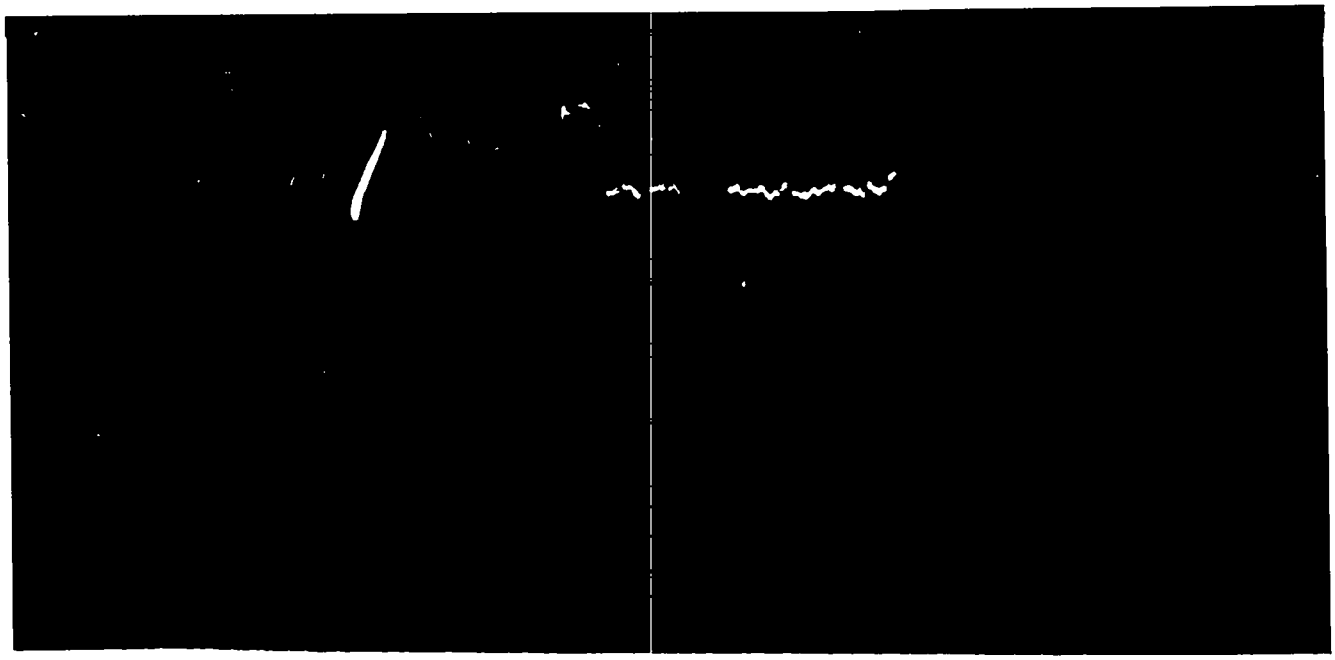

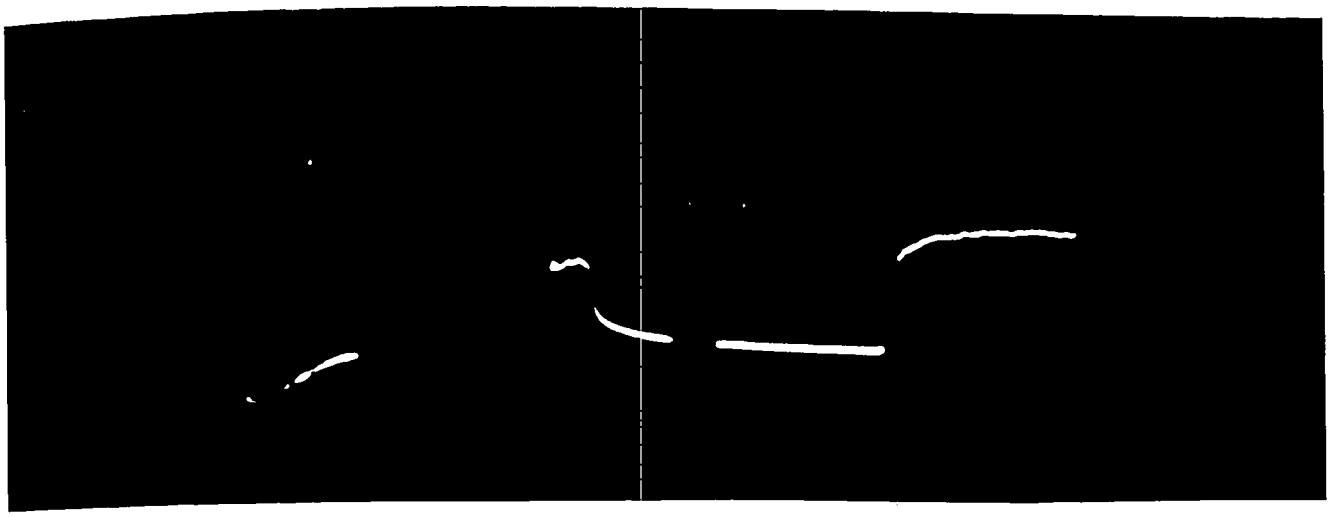

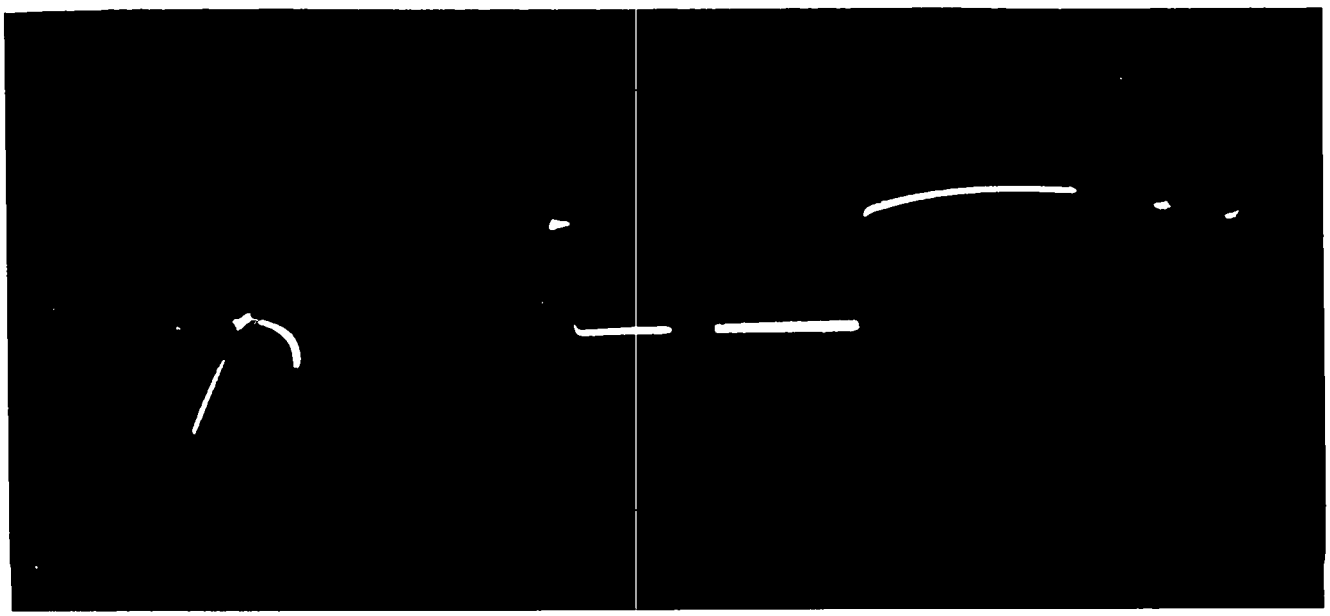

$1.3 \times 10^{-8}$ amperes. Trace (b) was obtained with 1000 volts across the counter, at which voltage the gas multiplication was about 30, giving a current through the counter of $0.5 \times 10^{-7}$ amperes. Trace (c) represents a calibration pulse obtained by sending through the leak resistor of the counter a current of $0.5 \times 10^{-7}$ amperes and then cutting it off electronically (see Section 10.2). The gain of the amplifier was of course much lower for the traces (b) and (c) than it was for trace (a). Figure 13 gives the current as a function of time, as obtained from the counter pulse shown in trace (b) of Figure 12 and from the calibration pulse shown in trace (c). One recognizes that the shape of the pulse exhibits the features which one may expect from a qualitative analysis of the operation of the counter, as discussed in Section 1.

Experiments were carried out with different values of the x-ray intensity at pressures from 20 cm Hg to 76 cm Hg, and of the multiplication from 20 to 300. No large differences in the pulse shapes were detected.

## 11.4 DEPENDENCE OF THE PULSE HEIGHT ON THE DISTANCE OF THE TRACK FROM THE WIRE

It has been pointed out in Section 1 that the height of the pulses of a proportional counter should be independent of the distance of the ionizing track from the wire, provided no electron attachment takes place. This was tested experimentally for a number of gases, at pressures both above and below atmospheric. The measurements at pressures below atmospheric were carried out by shooting polonium $\alpha$-particles parallel to the axis and close to the cylinder or close to the wire respectively. The measurements at pressures above atmospheric were carried out by using two polonium sources, one deposited on the inner surface of the cylinder, the other deposited on the wire (the range of the $\alpha$-particles, at the pressures used, was small compared with the diameter of the counter). Some of the observed ratios $\rho$ between the pulse heights obtained with tracks located near the wall and near the wire, respectively, are

Figure 13

Current as a function of time in a proportional counter upon sudden interruption of a constant source of ionization (from trace (b), Figure 12)

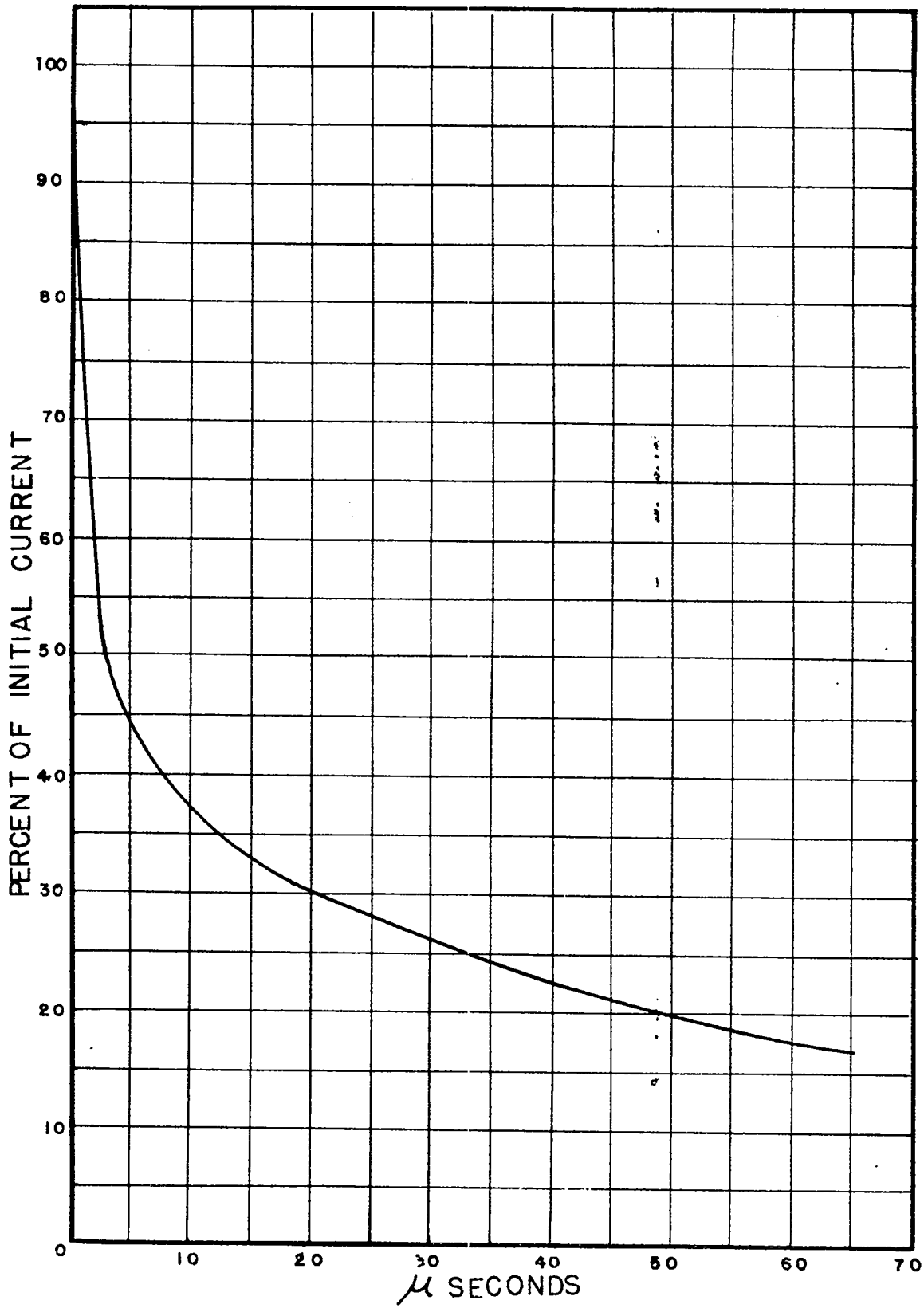

listed in Table 11.4-1 along with the data describing the experimental conditions under which the measurements were taken. The value of $\rho = 1$ found

Table 11.4-1

Ratio between the pulse heights corresponding to the same primary ionization produced near the wall and near the wire, respectively, in a proportional counter.

p = pressure

2a = wire diameter

2b = cylinder diameter

M = gas multiplication

$\rho$ = Ratio between the pulse heights

| Gas | p | 2a (inches) | 2b (inches) | M | $\rho$ |
|---|---|---|---|---|---|
| $H_2$ | 22 cm Hg | 0.010 | 1.5 | 250 | 1.0 |
| A (99.6% pure) | 6.8 atm. | 0.001 | 1.56 | 128 | 1.0 |
| $CH_4$ | 22 cm Hg | 0.010 | 1.5 | 57 | 1.0 |
| $BF_3$ | 10 cm Hg | 0.010 | 1.5 | 80 | 1.0 |
| $BF_3$ | 1.05 atm. | 0.001 | 1.56 | 128 | ~0.02 |
| $BF_3$ | 1.05 atm. | 0.001 | 1.56 | 1000 | 0.15 |
| 84% argon and 16% propane (commercial) | 6.8 atm. | 0.001 | 1.56 | 128 | 0.2 |

for these ratios in the case of argon and hydrogen is in agreement with the fact already mentioned that no appreciable attachment takes place in these gases (see Section 8.4; however, hydrogen was only tested at low pressure). The behavior of $BF_3$, for which $\rho = 1$ when a low pressure and a comparatively thick wire are used, and for which $\rho \ll 1$ when a high pressure and a very thin wire are used, can be understood if one considers: (a), that for

$BF_3$ the electron attachment decreases with increasing E/p, while for a given value of E/p, it is proportional to the pressure; and (b), that the field strength near the cylinder wall, for a given gas multiplication, is weaker the thinner is the wire.

## 11.5 END EFFECTS; ECCENTRICITY OF THE WIRE

The central wire of a proportional counter is often connected at both ends to metal rods sufficiently thicker than the wire itself so that no gas multiplication takes place at their surface. The wire supports are in this case a part of the collecting electrode (see(a) in Figure 14). In some counters, the wire may be supported by and insulated from two metal tubes which form guard electrodes (see (b) in Figure 14). In both cases, the electric field near the ends of the wire is different from the field near the center. The modification of the field has two separate effects. The lines of force near the ends of the wire are not radial, so that the "sensitive volume" is not a rectangular cylinder, but has roughly the shape shown in (a) of Figure 14. By "sensitive volume" we understand here the region where electrons are produced which give rise to gas multiplication. Also the field strength at the surface of the wire is weaker near the ends and reaches its normal value only at some distance from the ends. This causes the gas multiplication to decrease gradually as one approaches either end of the wire. The end effects were investigated by shooting $\alpha$-particles in a direction perpendicular to the wire, at various distances from the ends of the wire. The wire was 0.010" in diameter and supporting rods 0.025" and 0.040" in diameter respectively, were used. The results are shown in Figure 15. It is seen that the normal gas multiplication is reached only at a considerable distance from the ends of the wire, a distance which increases with the thickness of the supporting rods. On the other hand, if the supporting rods are part of the collecting electrode, they cannot be made too thin, lest gas multiplication takes place at

Figure 14

Different ways of supporting the central wire in a proportional counter. Shaded areas represent insulators.

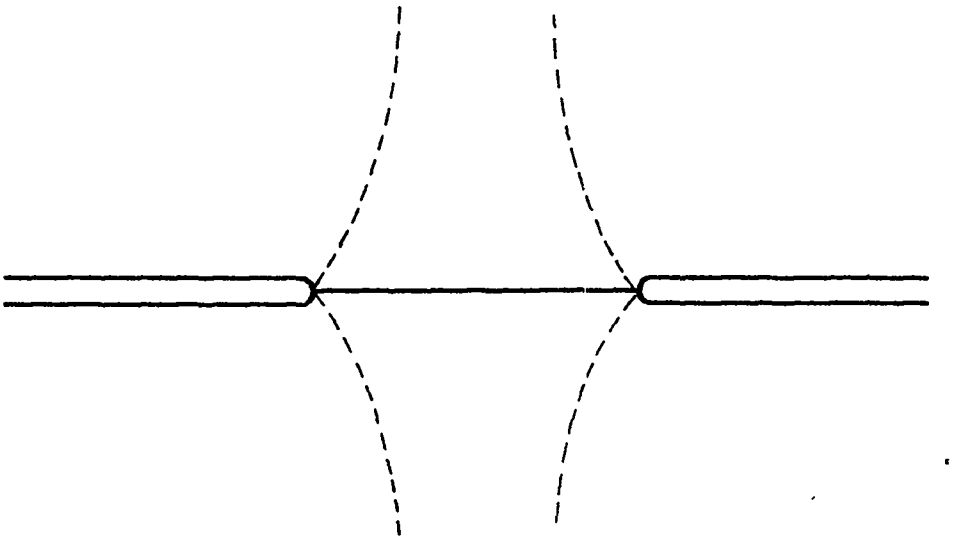

(a)

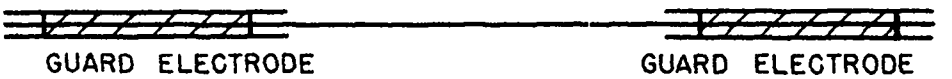


(b)

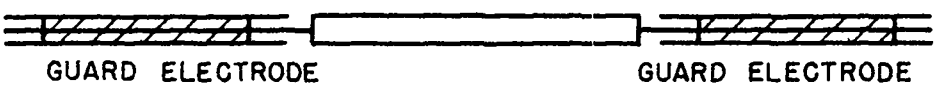


(c)

Figure 15

End effects in a proportional counter for two different thicknesses of the wire support. Wire diameter 0.010 inch; cylinder diameter 0.87 inch ; gas filling 22 cm Hg. of $H_2$; gas multiplication 250.

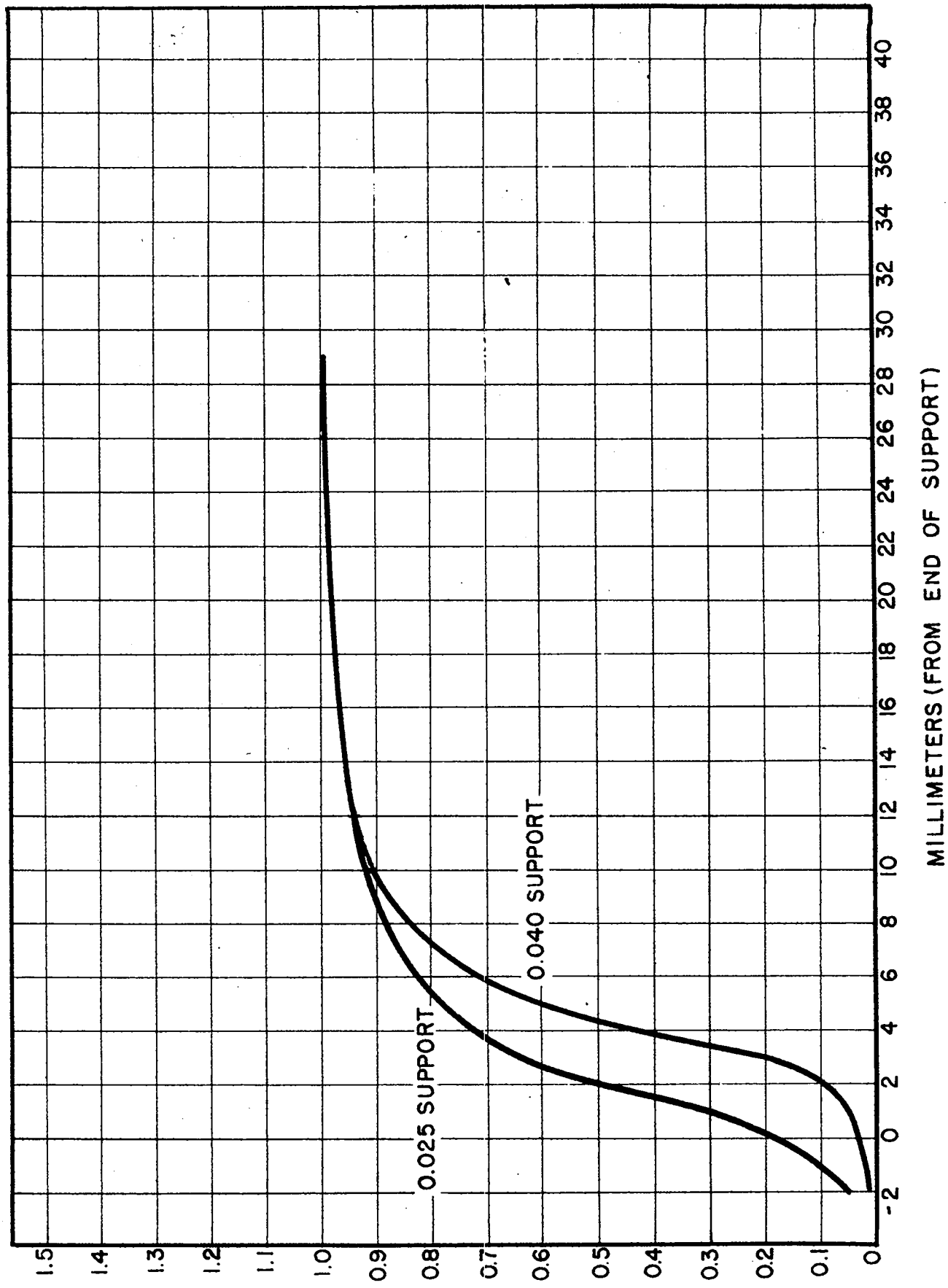

their surface. (It may be pointed out that in the measurements mentioned above, when 0.025" diameter supporting rods were used and the gas multiplication at the wire was 250, a gas multiplication of about 10 was observed at the rods.)

The end effects may be avoided by supporting the collecting wire by means of guard electrodes of the same diameter as the wire, as indicated in (c) of Figure 14. A counter designed according to this principle will be described in Section 14.15.

It has been implicitly assumed so far that the two electrodes of a proportional counter are exactly coaxial cylinders. The effect of a small eccentricity of the wire shall now be investigated. We will assume therefore that the inner and outer electrodes are cylinders with their axes parallel but not coincident. The problem of determining the electric field between the two cylinders may be solved by considering the field produced by two straight parallel filaments of infinite length, uniformly charged with equal and opposite linear densities of charge. If we denote with $\lambda$ and $-\lambda$ the densities of charge, with $r_1$, and $r_2$ the distances of a point P from the positive and the negative filament, respectively, the potential at the point P has the expression:

$$V = 2\lambda \log m + k \qquad (3)$$

where $m = r_2 / r_1$, and k is a constant.

It can be shown easily that the equipotential surface corresponding to a given value of the voltage V and therefore of the parameter m is a circular cylinder of radius:

$$r = d \frac{m}{m^2 - 1} \qquad (4)$$

the axis of which is in the plane of the two filaments, at a distance:

$$\delta = \frac{d}{m^2 - 1} \qquad (5)$$

from the positive filament. In the above equations, d indicates the distances between the two filaments.

Suppose now that the counter is formed by two cylinders of radii a and b respectively, the axes of which are at a distance $\Delta$ apart. The field between the two cylinders will be identical to the field produced by two straight filaments, arranged in such a way that the surfaces of the two electrodes are equipotential surfaces ( see Figure 16). The distance d between the two filaments and the values $m_a$ and $m_b$ of the parameter m at the surface of the electrodes are determined by the following equations:

$$a = d\,\frac{m_a}{m_a^2 - 1} \qquad b = d\,\frac{m_b}{m_b^2 - 1} \tag{6}$$

$$\Delta = \delta_b - \delta_a = d\left[\frac{1}{m_b^2 - 1} - \frac{1}{m_a^2 - 1}\right]$$

The potential V in the space between the two cylinders is given by Equation 3 where the constant $\lambda$ and k are determined by the boundary conditions,

$V = 0$ for $m = m_a$ (i. e., at the surface of the inner electrode)

$V = -V_o$ for $m = m_b$ (i. e., at the surface of the outer electrode)

One thus obtains:

$$V = -V_o\,\frac{\log(m/m_a)}{\log(m_b/m_a)} \tag{7}$$

The electric field strength $\vec{E}$ is computed as the negative gradient of V.

$$\vec{E} = \frac{V_o}{\log(m_b/m_a)}\,\text{grad}(\log m) \tag{8}$$

As an example, let us calculate the magnitude of E for points of the plane which contain the axes of the two cylinders as well as the two fictitious line charges. In this plane the following relation holds

$$m = r_2/r_1 = \frac{d \mp r_1}{r_1}$$

where the plus sign refers to points of the plane for which $r_2 > d$, and the

Figure 16

Diagram for the calculation of the field in a counter with eccentric wire.

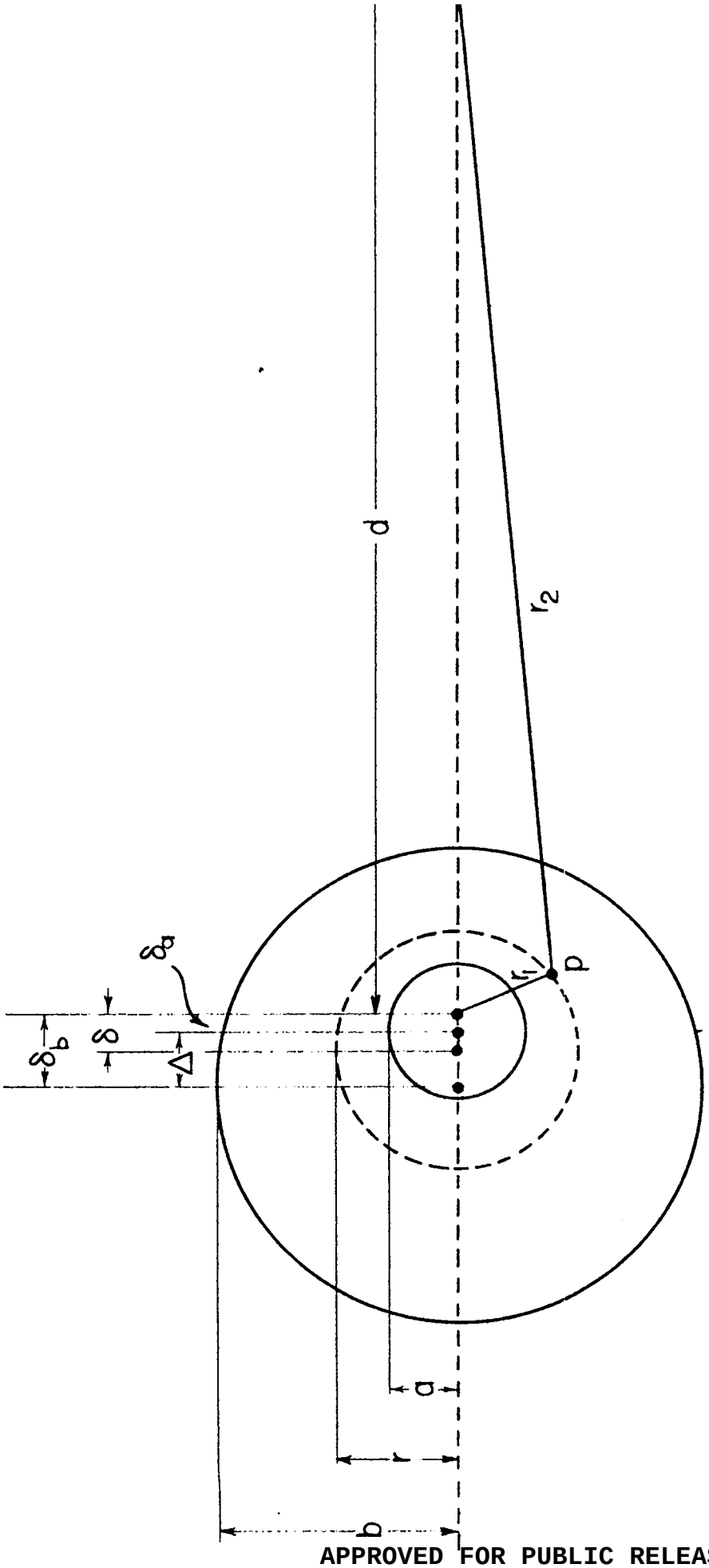

minus sign to points of the plane for which $r_a < d$.

From Equation 8 it follows

$$\vec{E} = \frac{V_o}{\log(m_b/m_a)} \cdot \frac{d}{r_1(d \mp r_1)} \tag{9}$$

If we apply the above equation to points at the surface of the inner electrode ($r_1 = a - \delta_a$, $r_1 = a + \delta_a$), we obtain the values of the maximum and minimum field strengths at the surface of this electrode. These values are given by

$$\left.\begin{matrix} E_{max} \\ E_{min} \end{matrix}\right\} = \frac{V_o}{\log(m_b/m_a)} \cdot \frac{d}{(a \mp \delta_a)[d \mp (a \mp \delta_a)]} \tag{10}$$

We now assume that the eccentricity of the wire is small. Since, when the eccentricity vanishes, d becomes infinity and $\delta_a$ becomes zero, we can assume that $d \gg a$ and $\delta_a \ll a$. The maximum relative variation of the field at the surface of the inner electrode as given by Equation 10 may then be written as follows

$$\frac{\delta E}{E} = 2\left(\frac{\delta_a}{a} + \frac{a}{d}\right) \tag{11}$$

If $b \gg a$ and under the assumption of a small eccentricity, Equations 11 and 6 yield

$$\frac{\delta E}{E} = 4 \frac{a\Delta}{b^2} \tag{11'}$$

From this equation and from the experimentally determined dependence of the gas multiplication on electric field strength at the inner electrode, one can easily determine the spread in gas multiplication caused by a given eccentricity of the wire. For instance, in the case of a 1" counter ($2b = 1"$) with a 0.010" wire ($2a = 0.010"$), 0.010" off center ($\Delta = 0.010"$) Equation 11' yields $\frac{\delta E}{E} = 8 \times 10^{-4}$. If the counter is filled with hydrogen at 55 cm pressure and operated at a gas multiplication of about 100, such a variation of the electric field strength will produce a change in gas multiplication of the order of one per cent.

## 11.6 SPREAD IN PULSE HEIGHT

There are several reasons for which tracks, producing the same amount of

ionization in the sensitive volume of a proportional counter, may fail to give rise to pulses of equal height. Some of these reasons have already been mentioned and include space charge effects (see Section 1), electron attachment (see Section 4), end effects (see Section 5), and eccentricity of the wire (see Section 5). Other possible causes of spread in pulse height are inequalities in the diameter of the wire and particles of dust present on the wire. These effects are likely to be particularly troublesome in the case that a very thin wire is used, which it is necessary to do in order to keep the operating voltage within reasonable limits when the gas pressure in the counter is high. Actually with a given counter ($2a = 0.001"$, $2b = 1.56"$, gas filling 6.8 atmospheres of an argon-propane mixture, polonium source on the wire) a spread in the pulse height of the order of 50 per cent was observed before the wire was cleaned. After the wire had been carefully cleaned, the spread in pulse height was reduced to about 10 per cent.

A typical pulse height distribution curve is shown in Figure 17. Similar curves were obtained with reasonably monoenergetic sources of $\alpha$-particles whenever carefully cleaned counters were used, and care was taken to avoid the disturbing influence of end effects or electron capture. Under these conditions, the width of the pulse height distribution, defined as the pulse height interval which contains 50 per cent of all the observed pulses, was found to be between 8 and 10 per cent of the average pulse height. This represents an upper limit for the spread inherent in the gas multiplication, because it is likely that at least part of the observed spread may be caused by lack of monochromaticity of the sources used.

## 10.7 MULTIPLE WIRE COUNTER

A proportional counter, in which a grid formed by a number of parallel and equidistant wires takes the place of the single wire used in the conventional counters, was developed at the Los Alamos Laboratories. The diagram of such a

Figure 17

Typical spread in pulse height for a proportional counter. Wire diameter 0.010 inch; cylinder diameter 1.5 inch; gas filling 39 cm Hg of $H_2$ + 1 cm Hg of $CH_4$; gas multiplication 620. The experiment was performed by shooting a collimated beam of $\alpha$-particles through the counter, in a direction perpendicular to the axis. The output pulses of the amplifier were analysed by means of an electronic discriminator. The curve gives number of pulses against bias voltage. The width of the pulse height distribution is $\Delta V/V_B = 0.06$.

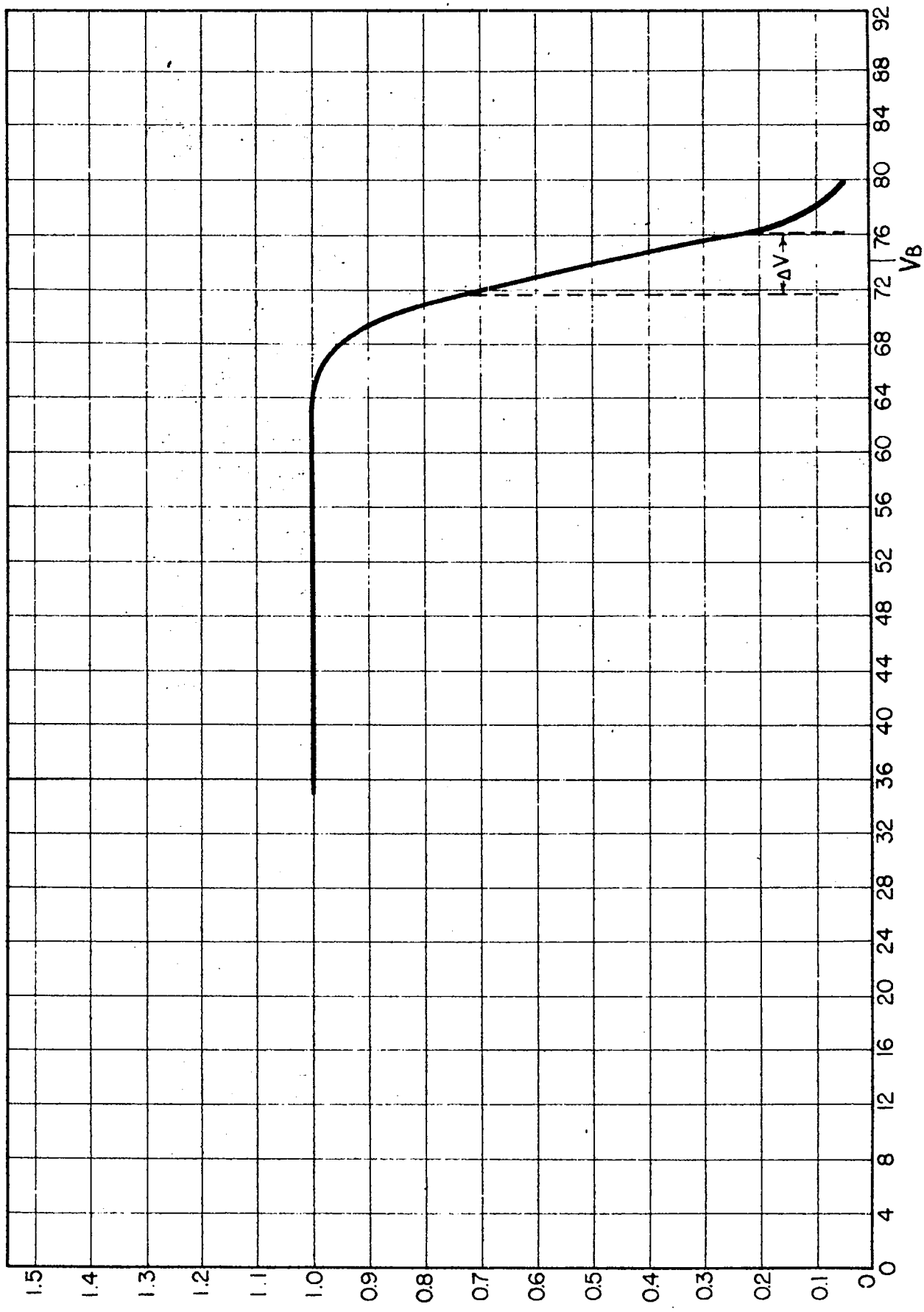

Figure 18

Schematic diagram of a multiple wire proportional counter. $S_1$, $S_2$ form the high voltage electrode; W is the collecting electrode. The arrow P represents the direction of the beam of ionizing particles.

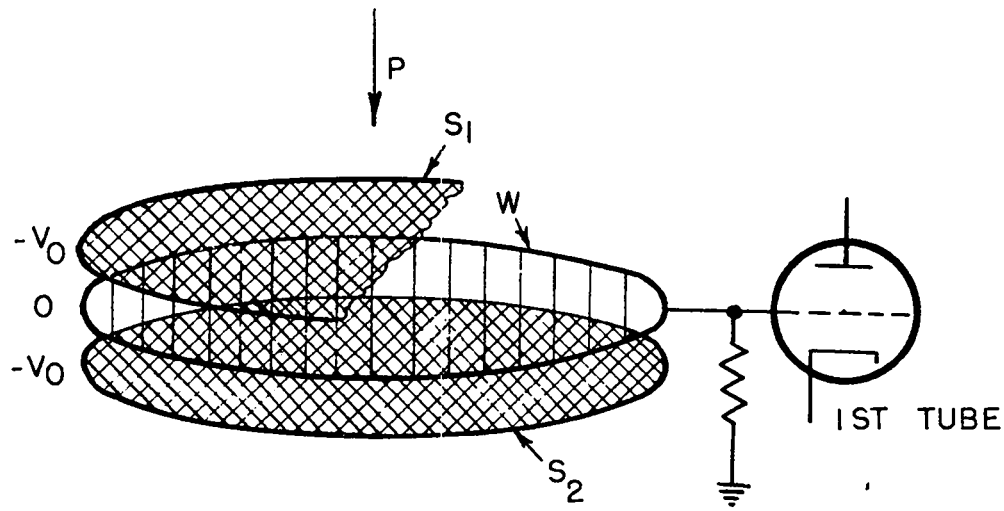

counter is schematically represented in Figure 18. The grid W is mounted rigidly between two screens, $S_1$ and $S_2$, of high transparency. The grid W is grounded through a resistor and connected to the input of the amplifier. The screens $S_1$ and $S_2$ are connected to the negative high voltage supply. The ionizing particles are admitted into the sensitive volume of the counter through one of the screens. The electrons liberated by an ionizing particle between the screens drift toward the wires, in the neighborhood of which gas multiplication takes place.

For testing purposes a counter was built containing two separate elements of the type described above. The details of the construction are shown in Figure 19. The two counting grids and the three high voltage screens are mounted on invar rings and stretched tight by differential thermal contraction. Collimated beams of $\alpha$-particles, from polonium sources placed in the guns A and B, respectively, can be directed into the counter through either of two sets of holes (0.026 inch in diameter, 0.5 inch length, 2 millimeters separation). The holes normal to the plane of the wires are drilled in a row making an angle of $31.5^{\circ}$ with the direction of the wires, so that five positions of the beam may be obtained between two neighboring wires. The counter was filled with a mixture of 97 per cent argon (99.6 per cent purity) and 3 per cent $CO_2$.

The shortest time constant of the amplifier used for the tests with the counter described above was 100 microseconds.

The gas multiplication as a function of voltage was measured at pressures of 4 cm Hg and 29 cm Hg. The results are presented in Figure 20. At 29 cm pressure the measurements were carried out, as described in Section 2, by comparison of pulse heights with and without gas multiplication. At 4 cm pressure, the primary ionization in the counter was too small to permit observation of ionization pulses without gas multiplication, so that the gas multiplication is plotted on an arbitrary scale (by taking M=1 for the lowest

Figure 19

Construction of a double multiple wire proportional counter.

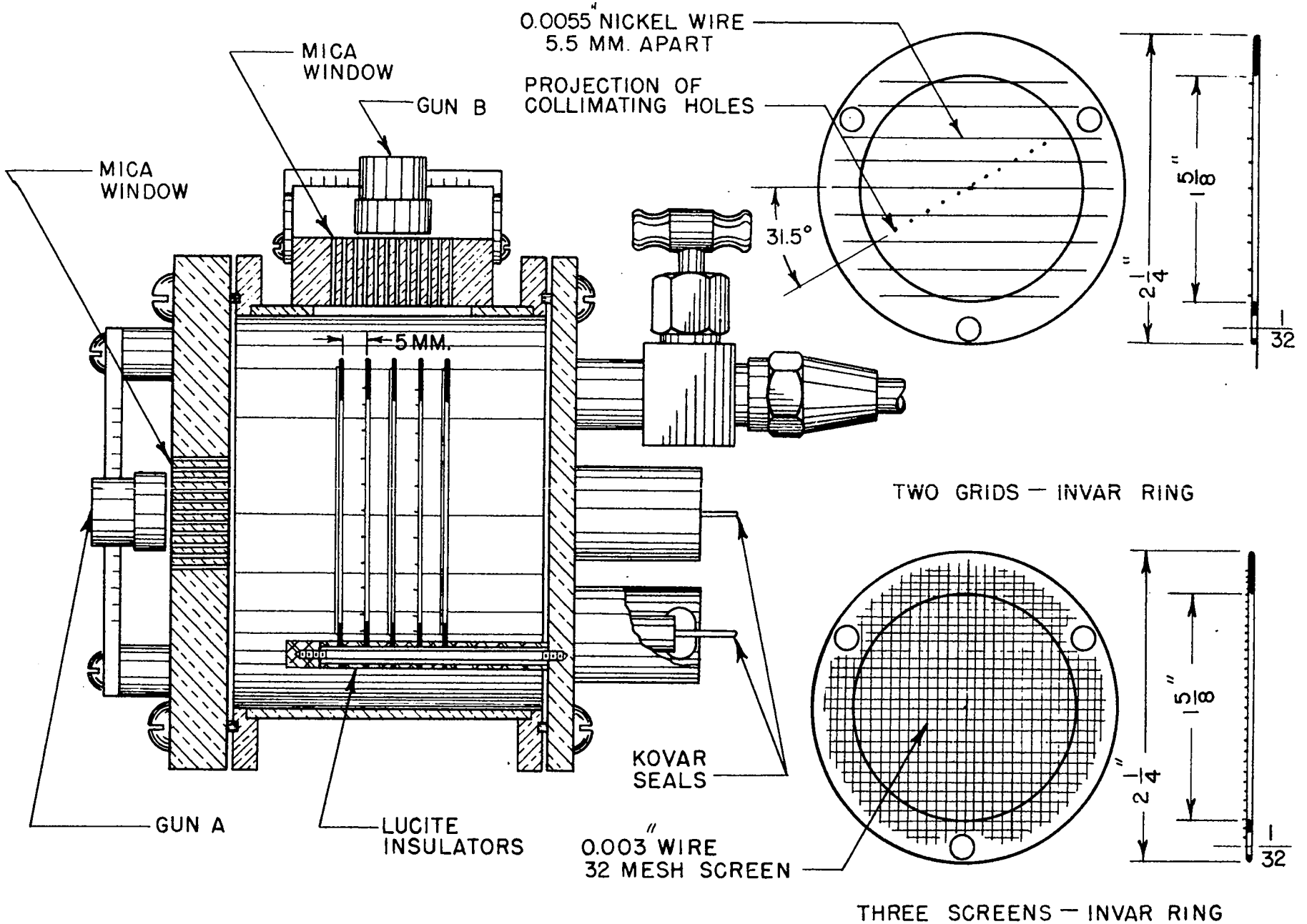


APPROVED FOR PUBLIC RELEASE

Figure 20

Gas multiplication M vs voltage for the multiple wire proportional counter represented in Figure 19. Gas filling 97 per cent argon; 3 per cent $CO_2$ at total pressures of 4 cm Hg and 30 cm Hg. The gas multiplication for the lower pressure is plotted on an arbitrary scale.

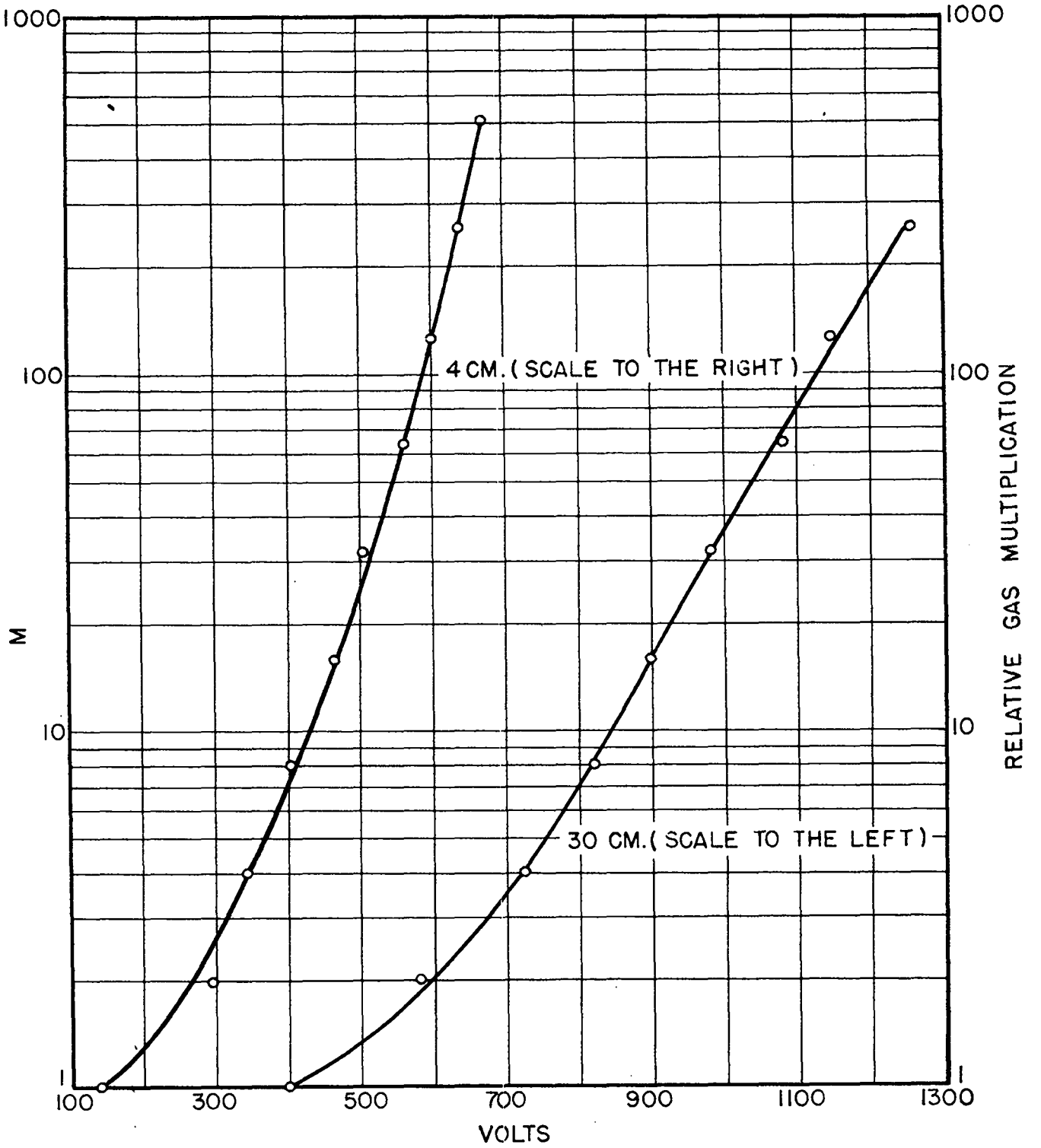

gas multiplication which gave measurable pulses).

The variation of the pulse height with the distance of the track from the counting wires was investigated by shooting $\alpha$-particles perpendicularly to the plane of the wires, through the holes in front of the gun A. A continuous and periodic variation of pulse height was observed as the $\alpha$-particle beam was displaced with respect to the wires. The pulse height reached a maximum when the $\alpha$-particles passed near one of the wires and a minimum when the $\alpha$-particles passed midway between wires. The difference between maximum and minimum was about 11 per cent.

The spread in pulse height observed with the $\alpha$-particle source in a given position was 13 per cent, i. e., it was of the same order of magnitude as with a conventional proportional counter operated under similar conditions.

The two counting units had one common high voltage electrode represented by the middle screen. The question was investigated whether or not the pulses in one of the units would be picked up by the collecting electrode in the other unit. This was done by shooting $\alpha$-particles in a direction parallel to the screens, through the holes in front of the gun B. No induced pulse was observed and if any was present it was certainly smaller than 0.2 per cent of the genuine pulse. The experiment also showed that the sensitive volume of each counter was sharply defined by the screens and no appreciable variation of pulse height was observed as the $\alpha$-particle beam was moved across the sensitive volume.

LOS ALAMOS TECHNICAL SERIES

VOLUME I

EXPERIMENTAL TECHNIQUES

PART II

CHAPTER 12

# BETA RAY, $\gamma$-RAY AND X-RAY DETECTORS

by

BRUNO ROSSI AND HANS STAUB

# CHAPTER 12

# BETA RAY, $\gamma$-RAY AND X-RAY DETECTORS

## 12.1 GENERAL CONSIDERATIONS

All of the instruments described in the present section are essentially detectors of high energy electrons. Gamma and x-rays (both referred to in what follows as "$\gamma$-rays") act upon the detector through the intermediary of secondary electrons generated in the walls or in the gas of the chamber.

Unless a very high pressure is used, individual electrons produce only a small number of ions in a chamber, because of their small specific ionization. For this reason the electron detectors used in the Los Alamos project were limited to two categories: (a) discharge counters (Geiger-Mueller counters) in which the primary ionization produced by the electron is used to initiate an avalanche; and (b) integrating chambers, by which the ionization current produced by a large number of electrons is recorded.

Because of the small range of electrons in solid matter, $\beta$-ray detectors must have very thin walls, or be provided with thin windows, at least if one does not want to place the source inside the counter.

Gamma ray detectors, instead, generally have walls of a thickness greater than the maximum range of the secondary electrons, yet not so large as to produce any appreciable attenuation of the primary $\gamma$ radiation.

## 12.2 YIELD OF $\gamma$-RAY COUNTERS

In discussing the response of discharge counters, we may assume that these counters record all electrons which traverse their sensitive volume, at least if the pressure is sufficiently high and the counting rate sufficiently low. Hence these counters have practically 100 per cent detection efficiency for $\beta$-rays. In

the case of $\gamma$-rays, the counting yield $\eta$ of a discharge counter, defined as the ratio of the number of counts to the number of photons traversing the counter, is given by the probability that at least one secondary electron be produced by the photon in the wall and emerge from the wall into the sensitive volume of the counter. (Production of secondary electrons in the gas can usually be neglected.) The thickness of the effective layer, i.e., the layer from which secondary electrons may emerge into the counter, increases with the "range" of the electrons, and the number of electrons produced in this layer is proportional to its thickness and to the cross-section for production of electrons by $\gamma$-rays in the wall material. As for the dependence on the angle of incidence $\vartheta$ of the photons upon the wall, if the secondary electrons proceed in the direction of the incoming photons, the yield will be independent of $\vartheta$. This is so because the thickness of the effective layer is proportional to $\cos\vartheta$, while the path of the photons in this layer is proportional to $1/\cos\vartheta$. In the opposite limiting case; i.e., when the electrons are completely scattered so as to be isotropically distributed, the yield will be proportional to $1/\cos\vartheta$. This is so because the thickness of the effective layer, in this case, is independent of $\vartheta$, while the path of the photon in this layer is proportional to $1/\cos\vartheta$. A semiempirical expression for the yield $\eta$ was derived under the assumption of complete scattering, a condition which is fairly well verified for elements of high atomic number and for comparatively small electron energies. (Metallurgical laboratory report). For perpendicular incidence the following relation holds

$$\eta = 0.135\,(\mu_{ph}R_{ph} + \mu_c R_c + 2\mu_{pr} R_{pr}) \qquad (1)$$

where $\mu_{ph}$, $\mu_c$ and $\mu_{pr}$ are the absorption coefficients of $\gamma$-rays in the wall material relative to photo effect, Compton effect, and pair production respectively, and $R_{ph}$, $R_c$ and $R_{pr}$ are the extrapolated ranges of monokinetic electrons of energy corresponding to the mean energies of the secondary electrons for the three processes indicated. The factor 2 which multiplies the last term corresponds to

the fact that when a photon undergoes materialization two secondary electrons are produced. The numerical factor 0.135 is chosen empirically for the best fit with the experimental results.

It may be noted that according to the assumption of complete scattering, the number of electrons emerging from a given surface is independent of the orientation of this surface in the $\gamma$-ray beam. Hence the yield of a counter of any shape can be calculated by multiplying the expression for $\eta$ given in Equation 1 by the ratio of the total wall area to the cross-sectional area of the counter perpendicular to the direction of the $\gamma$-ray beam. For a cylindrical counter with its axis perpendicular to the direction of incidence, this factor is $\pi$. Figure 1 gives the calculated yield as a function of energy for a cylindrical counter with copper and bismuth walls under the conditions specified above. The behavior indicated by these curves was experimentally checked by W. C. Peacock.[1]

---

(1) Massachusetts Institute of Technology Thesis, 1944.

---

Admittedly, the assumption of complete scattering is very crude and the reason why it leads to results in fairly good agreement with the experimental facts is that it does not enter very critically in the computation of the yield of a counter if the walls, from which secondary electrons are emitted, present all possible orientations to the incident $\gamma$-rays, as is true in most practical cases.

The variation of $\eta$ with energy and with atomic number, as represented by Figure 1, can be readily understood, at least qualitatively, by considering the dependence of the $\mu$'s and the R's on the two above quantities.

A completely theoretical determination of the yield for a parallel plate lead counter was attempted at Los Alamos, but these calculations apply to energies higher than those at which Equation 1 may be expected to hold.

Some simplifying assumptions were made concerning the energy distribution of the secondary electrons arising from the various processes. Moreover, it was

Figure 1

Counting yield $\eta$ of cylindrical counters with bismuth and copper walls as a function of $\gamma$-ray energy.

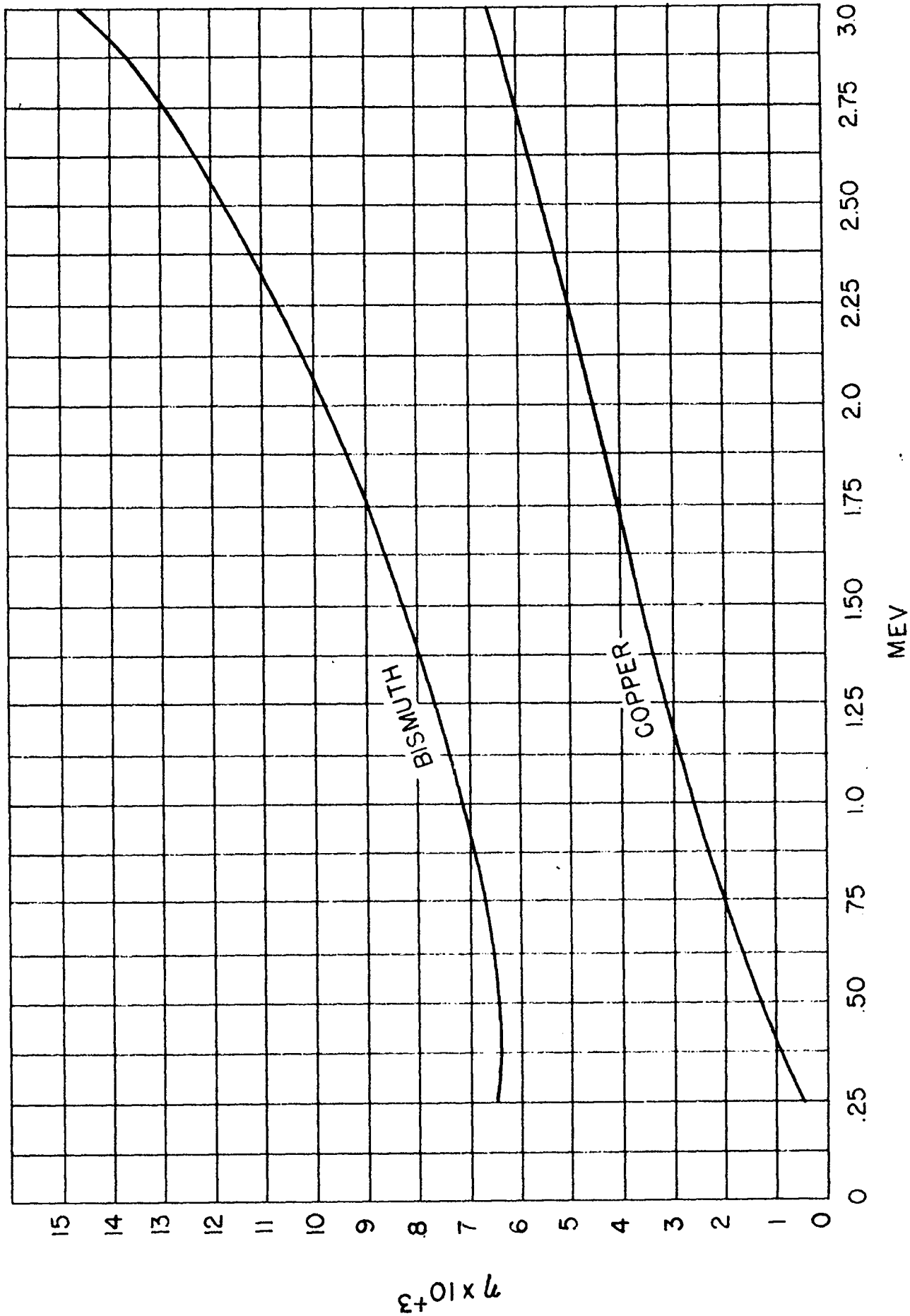

Table 12.2-1

AVERAGE NUMBER OF ELECTRONS EMERGING FROM A LEAD PLATE WHEN A PHOTON FALLS PERPENDICULARLY UPON THE PLATE

| PHOTON ENERGY (Mev) | LEAD THICKNESS (cm) 0.1 | 0.2 | 0.3 | 0.4 | 0.5 | 0.6 | 0.7 | 0.8 | 0.9 | 1.0 |
|---|---|---|---|---|---|---|---|---|---|---|
| 5 | .027 | .030 | .028 | .027 | .027 | .025 | .025 | .023 | .021 | .021 |
| 6 | .036 | .043 | .041 | .039 | .038 | .035 | .033 | .032 | .029 | .027 |
| 7 | .048 | .058 | .059 | .054 | .052 | .050 | .045 | .042 | .042 | .037 |
| 8 | .057 | .072 | .071 | .068 | .064 | .061 | .059 | .055 | .052 | .047 |
| 9 | .065 | .088 | .089 | .084 | .079 | .074 | .069 | .066 | .062 | .057 |
| 10 | .075 | .102 | .106 | .101 | .096 | .088 | .085 | .079 | .074 | .070 |
| 12 | .088 | .129 | .141 | .136 | .127 | .121 | .112 | .105 | .097 | .090 |
| 14 | .100 | .150 | .170 | .169 | .161 | .149 | .139 | .129 | .120 | .112 |
| 16 | .109 | .172 | .200 | .203 | .195 | .182 | .168 | .156 | .145 | .136 |
| 18 | .117 | .189 | .226 | .236 | .228 | .214 | .198 | .183 | .169 | .157 |
| 20 | .124 | .205 | .249 | .264 | .259 | .245 | .226 | .209 | .193 | .178 |


APPROVED FOR PUBLIC RELEASE

assumed that all secondary electrons are produced in the forward direction. The energy loss of electrons by ionization and radiation, as well as their scattering by nuclear collision, was taken into account. Pair production by the secondary photons was neglected. The results are summarized in Table 12.2-1, which gives the average number of electrons emerging from a lead plate of a given thickness when a photon of a given energy falls perpendicularly upon it. Where this number is small compared with one, it also represents the yield $\eta$ as defined above; i.e., the probability of at least one electron emerging from the plate.

## 12.3 RESPONSE OF AN INTEGRATING CHAMBER

The intensity of the ionization current in an integrating chamber irradiated with $\gamma$-rays can be calculated accurately only in the case that the walls and the gas of the chamber have at least approximately the same atomic number. In this case the ionization of the gas in the sensitive volume of the chamber is the same as if the gas were surrounded by more gas of the same nature rather than by the chamber's walls. The whole energy E of a photon which suffers an absorption or a scattering process goes into secondary electrons or into photons of low energy. It is eventually dissipated over a distance short compared with the mean free path of the primary photon, thereby producing $E/W_o$ ion pairs, where $W_o$ is the energy per ion pair. Hence, a $\gamma$-ray flux of n photons per $cm^2$ will produce a number $n\mu E/W_o$ ion pairs per $cm^3$ of the gas, where $\mu$ is the total absorption coefficient of photons in the gas. The ionization current in the chamber, which is here supposed to be uniformly irradiated throughout its volume, will then by given by:

$$I = en\mu \frac{E}{W_o} A \qquad (2)$$

where e is the charge of the electron and A the volume of the chamber. If e is measured in electrostatic units, the quantity $e\mu E/W_o$ represents the number of roentgens per incident photon produced in the gas of the chamber.

When the walls of the chamber are made of a material appreciably different in atomic number from the gas, then the ionization cannot be calculated with

Equation 2. An approximate expression for the total number of ion pairs per second produced in the chamber is $N\eta\,(\nu)_{av.}$ where N is the number of photons per second falling on the chamber, $\eta$ is the yield as defined above and $(\nu)_{av.}$ is the average number of ion pairs produced by each secondary electron in the chamber. The ionization current is then given by the equation:

$$I = e\,N\,\eta\,(\nu)_{av.} \qquad (3)$$

The value of $(\nu)_{av.}$ may be computed from the specific ionization of the secondary electrons and from their average path length in the chamber. In the computation of the latter quantity one must take into account the detour factor: i.e., the increase in path length caused by multiple scattering (see, for instance, H. P. der Physics, 22,2, pp. 26-28). It may be noted that when the detour factor is small and when the pressure in the chamber is sufficiently low, so that the range of the secondary electrons is large compared with the linear dimensions of the chamber. $(\nu)_{av.}$ is practically independent of energy. Hence, the ionization current in the chamber shows the same dependence on the $\gamma$-ray energy as the yield $\eta$ of a counter with the same wall material.

The response of an ionization chamber irradiated with a $\gamma$-ray source of variable intensity has been discussed in detail in Section 10.4. It has been shown there that the total ionization current follows faithfully the variations of intensity of the ionizing radiation only if these variations are comparatively slow; more precisely, if the time during which an appreciable variation takes place is long compared with the time of collection of ions. In the case of variations which take place in times short compared with the time of collection of ions, however, only the electron current follows the changes of the ionizing radiation, while the intensity of the ion current remains practically constant.

Hence the chambers to be used for studying a rapidly varying $\gamma$-radiation must be filled with a gas in which the electrons remain free, and in order to avoid contamination of the gas, which may lead to electron attachment, sealing waxes and

organic insulators must be avoided in the chamber construction.

The relation between the observed output voltage and the number of ion pairs per second produced in the chamber is given by Equation 10.26

$$V_e(t) = e \int_0^{\infty} N(t - t_1)\ \chi(t_1)\ dt_1 \qquad (4)$$

where $\chi(t)$ represents the transient response of the detecting equipment including both the ionization chamber and the amplifier. The function can be determined by means of a pulsed X-ray source, as described in Section 10.8.

## 12.4 CYLINDRICAL $\gamma$-RAY IONIZATION CHAMBER

Figure 2 represents a cylindrical $\gamma$-ray integrating ionization chamber 2 inches in diameter, 29 inches effective length, which has proved very useful both in laboratory and in field work. The gas filling consists of an argon - $CO_2$ mixture (generally 96 per cent argon, 4 per cent $CO_2$) at a total pressure of about 4.5 atmospheres. It was found that a sufficient purity of the gas can be achieved by keeping the chamber under vacuum for about 12 hours, filling it with the appropriate argon-$CO_2$ mixture through a dry ice trap and then letting the gas circulate through a calcium purifier heated at 150°C for about 4 hours. It was found that this operation does not reduce the $CO_2$ content unduly. The construction of the purifier used for this purpose, which is capable of handling eight chambers simultaneously, is shown in Figure 3. Usually in the chambers thus prepared, no appreciable electron attachment can be detected even after several months. The volume of the chamber is 1410 $cm^3$. The capacity of the collecting electrode is 12.7 micromicrofarad. The chamber is normally operated at -2000 volts. Saturation is reached at about -400 volts, and with 1 gram of radium at 1 meter distance, the saturation current was found to be approximately 6 x $10^{-10}$ amperes. The chamber was primarily designed for measuring rapid variations of the $\gamma$-ray intensity, but it was also widely used for static measurements.

For a cylindrical geometry and under the assumption that no negative ions are formed, the fraction of electron current is given by the equation (see Section 10.6)

Figure 2

Cylindrical $\delta$-Ray ionization Chamber (see Section 4)

(1) and (2) Brass end pieces

(3) Brass cylinder 2" o.d., 1/32" wall thickness; it represents the high voltage electrode.

(4) 0.025" diameter kovar wire; it represents the collecting electrode and has an active length of 29".

(5) and (6) Kovar pieces supporting the collecting electrode by means of glass insulators. These pieces are grounded during operation of the chamber and act as guard electrodes.

(7) Circular holes (1/2" diameter) covered with a 0.003" brass foil to admit x-rays into the chamber for testing purposes.

(8) and (11) Couplings for connecting the chamber to the filling system.

(9) and (10) Needle valves

(12) Male amphenol connector, insulated from the end pieces by a lucite plate. The pin of the connector is attached to the collecting electrode; the case is attached to the guard electrode (5) and to ground.

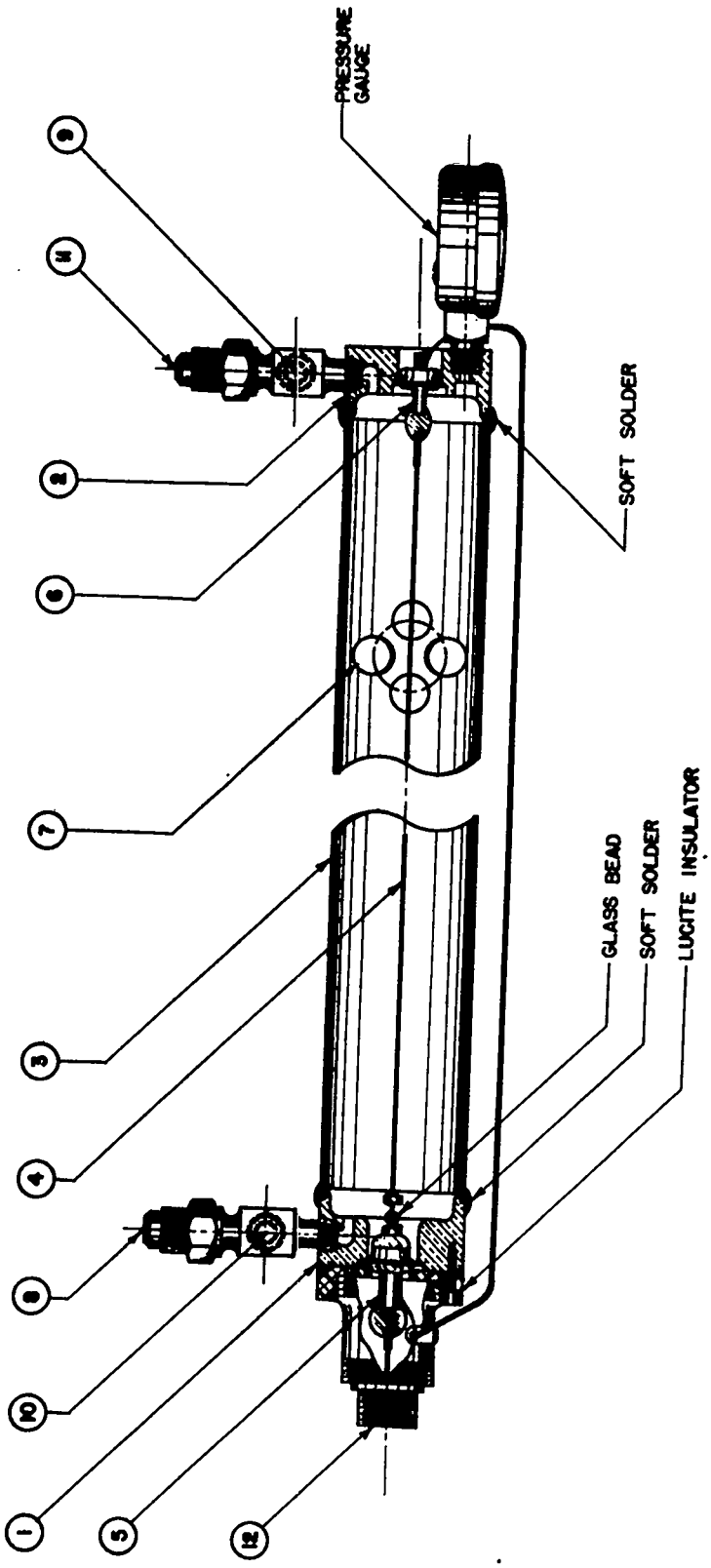

Figure 3

Hot calcium purifier

(1) Steel end plate

(2) Steel flange

(3), (4) Brass cylindrical sections, 1/8" wall

(5) Brass rings, 1/4" thickness

(6) Steel cylinder, 1/8" wall

(7) Gasket made of 1/32" copper sheet

(8) 1/4" steel rod

(9) Brass baskets, provided with copper screens on the bottom and lined on the side with copper sheet.

(10) Packless valves

The heating element (about 300 watts power) is wound around the steel cylinder. The calcium, in the form of turnings, is placed in the baskets (9) by removing the end plate (1) and extracting the inner assembly formed by the steel rod (8) and the baskets (9). The connection to the pump is made by means of a 1" copper tube soldered to the brass cylinder (4). All joints are hard soldered.

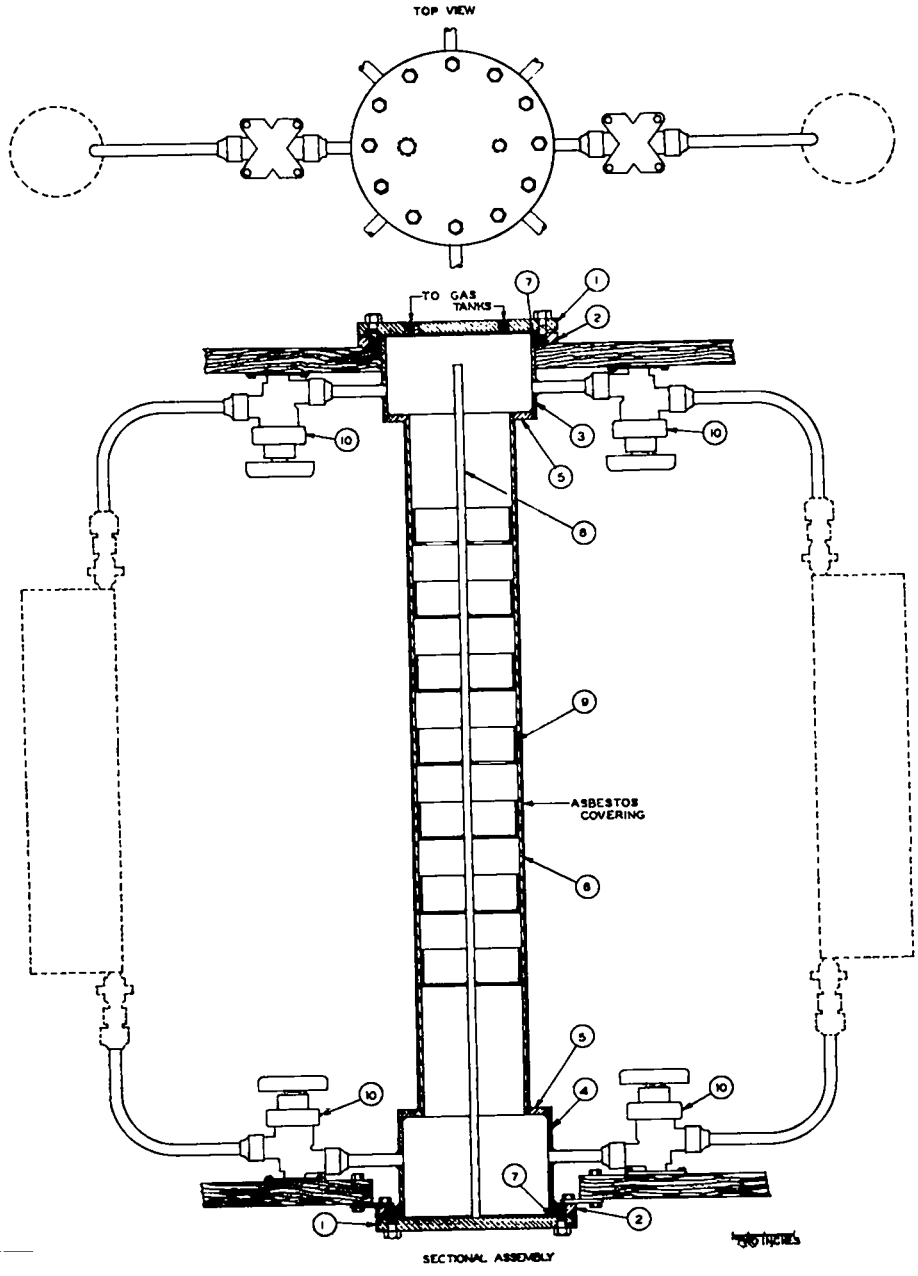

$$I_o^-/I_o = 1 - \frac{1}{2 \log b/a} \qquad (5)$$

where a is the radius of the inner electrode and b the (inner) radius of the outer electrode. It is here assumed that $b >> a$ and that the outer cylinder is kept at a negative potential with respect to the collecting electrode. For the chamber under consideration, Equation 5 gives $I_o^-/I_o = 0.886$.

Experiments were carried out to check the theoretical value of the electron current and also to determine the transient response of the ionization chamber. These experiments were performed with the pulsed X-ray source described in Section 10.8 by observing the time dependence of the current subsequent to a sudden interruption of the x-ray beam. Measurements on many chambers of the type described gave values of $I_o^-/I_o$ which were usually within 1 or 2 per cent of the theoretical value, indicating the absence of any appreciable electron attachment.

The transient response of the chamber is illustrated in Figure 4. The curve marked $I^-/I_o$ gives the calculated intensity of electron current in terms of the initial total current $I_o$ as a function of time following a sudden interruption of the radiation. This curve was calculated under the assumption that the electrons in the chamber have a constant drift velocity equal to $4 \times 10^6$ centimeters per second. The curve marked $I^+/I_o$ gives the intensity of the positive ion current in terms of $I_o$ calculated by assuming a drift velocity proportional to the electric field strength. The curve marked $V/kI_o$ gives the voltage drop across the leak resistor R in terms of $RI_o$ calculated by neglecting the contribution of the positive ion current which can be considered as constant during the time of collection of the electrons. This curve was calculated by using a value of 0.48 microseconds for the product RC of this resistance times the capacity of the collecting electrode and the amplifier input, and by considering the amplifier as having infinite band width. The crosses are experimental points taken from the oscilloscope trace. The agreement with the calculated curve is very satisfactory. It appears from Figure 4 that the chamber described is capable of reproducing without much distortion

Figure 4

Response of the cylindrical ionization chamber (represented in Figure 2) to a sudden interruption of a constant source of ionization.

$I^-$ : electron current (calculated)
$I^+$ : positive ion current (calculated)
$I_o$ : total initial current
$V$ : voltage drop across the leak resistor R caused by the electron current (calculated for RC = C.48 microsecond)
X : Experimental values of V.

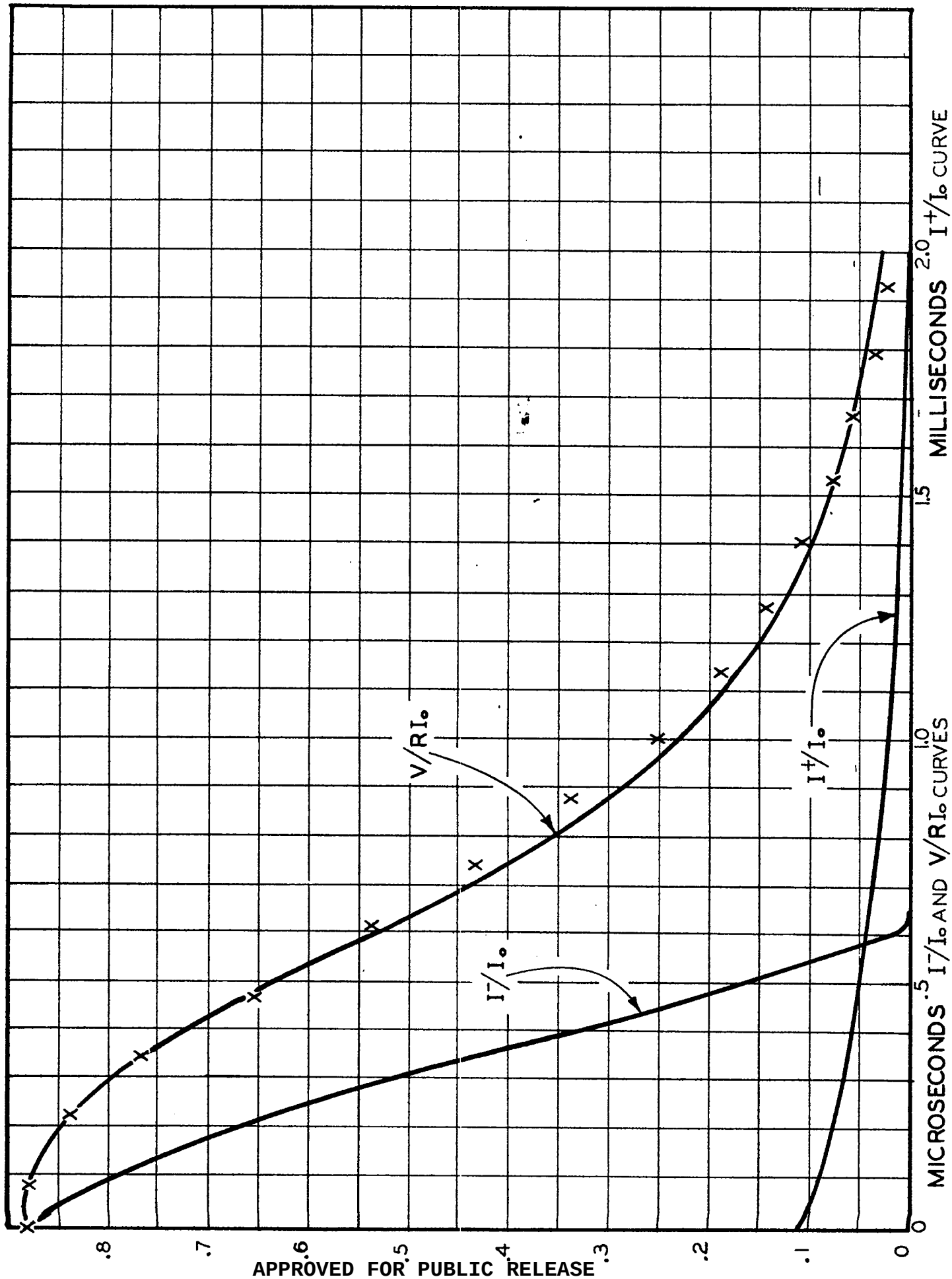

variations of $\gamma$-ray intensity taking place in times of the order of several microseconds.

## 12.5 MULTIPLE PLATE X-RAY IONIZATION CHAMBER

Figure 5 shows the construction of an ionization chamber which was used for measuring the time dependence of the intensity of very fast x-ray pulses. Only metal, porcelain and glass are in contact with the gas. The seal between the bottom plate and the case is made gas tight by means of a copper gasket. In order to increase the sensitivity, the electrode assembly consists of five circular aluminum discs connected alternately so that discs (2) and (4) form the collecting electrode, while discs (1), (3) and (5) form the high voltage electrode. The gas filling consists of an argon - $CO_2$ mixture (90 per cent argon, 10 per cent $CO_2$) at a total pressure of 100 cm Hg. The gas is purified by circulation over hot calcium.

The chamber is normally operated at 2000 volts. Under these conditions the drift velocity of electrons in the argon - $CO_2$ mixture is higher than $5 \times 10^6$ centimeters per second. Since the separation of the electrodes is 1 centimeter, the resolving time of the chamber may be estimated to be less than 0.2 microsecond. This chamber is therefore considerably faster than the cylindrical chamber described in Section 4. This is due to the uniformly high field provided by the parallel plate arrangement and to the small spacing of the electrodes. In Figure 6 two oscilloscope records obtained with 370 kilovolt X-ray pulses are reproduced, as an example of the performance of the chamber.

## 12.6 MULTIPLE PLATE $\gamma$-RAY IONIZATION CHAMBER

This chamber, similar in principle to that described in Section 5, was designed for the study of $\gamma$-ray pulses produced by a betatron. Its construction is shown in Figure 7.

The $\gamma$-ray beam is admitted into the chamber along its axis. A high sensitivity is achieved by the design of the electrode assembly, which consists of ten thin lead plates alternately connected to the high voltage supply and to the amplifier input.

Figure 5

Multiple Plate X-Ray Ionization Chamber.

(1,3,5) Dural discs, 1 mm thick, 3 1/2" in diameter, forming the high voltage electrode. They are connected by 3 threaded stems with brass spacers. These stems, of which two are shown in the drawing (6 and 7) , are placed near the edge of the discs, at an angular distance of 120°. Two of the stems are supported by porcelain insulators (8), one by the center piece of a kovar-glass seal (9), which provides electrical connection to the high voltage electrode. Discs 1 and 3 have central holes 5/8" in diameter to permit the passage of the stem (10) supporting discs 2 and 4.

(2,4) Dural discs, 1 mm thick, 3 1/2" in diameter, forming the collecting electrode. They are supported by a central threaded stem with brass spacer (10). This stem terminates in the center piece of a kovar glass seal (11), which provides electrical connection to the collecting electrode. The two discs have notches to avoid contacts with the stems supporting the discs 1, 3, 5, (see detail 4).

(12) Steel cylinder, 3/32" wall

(13) Steel plate, 1/8" thick

(14) Base steel plate 1/4" thick, supporting the electrode assembly

(15) Steel flange, 1/4" thick.

(16) Connection for pressure gauge

(18) One of the two gas inlets

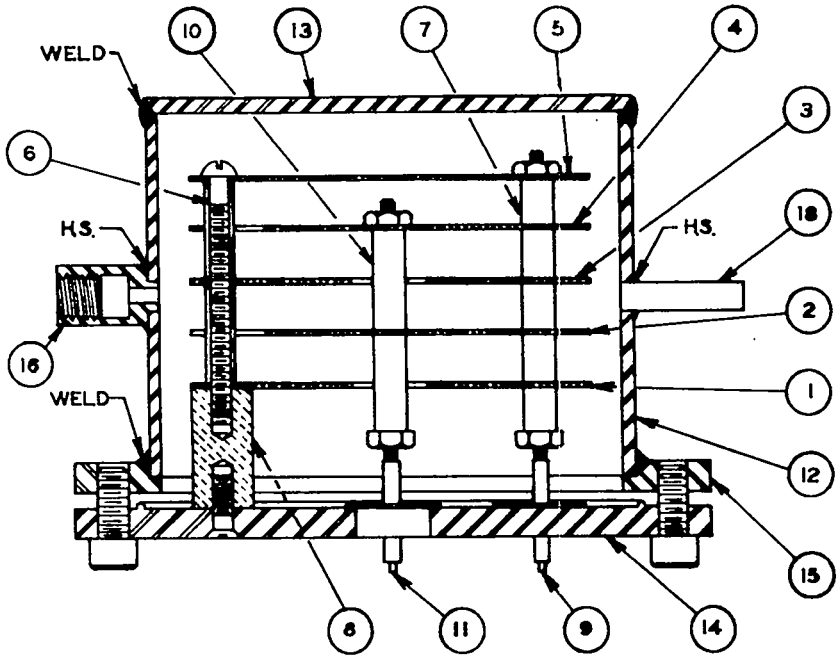


SECTION A-A

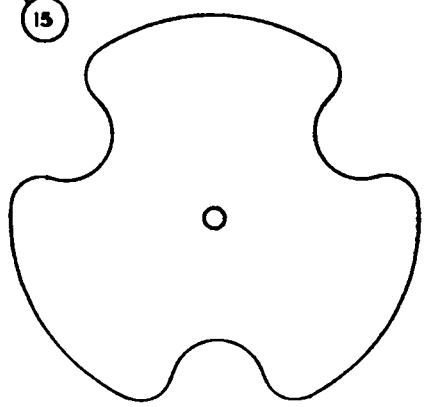

PART 4

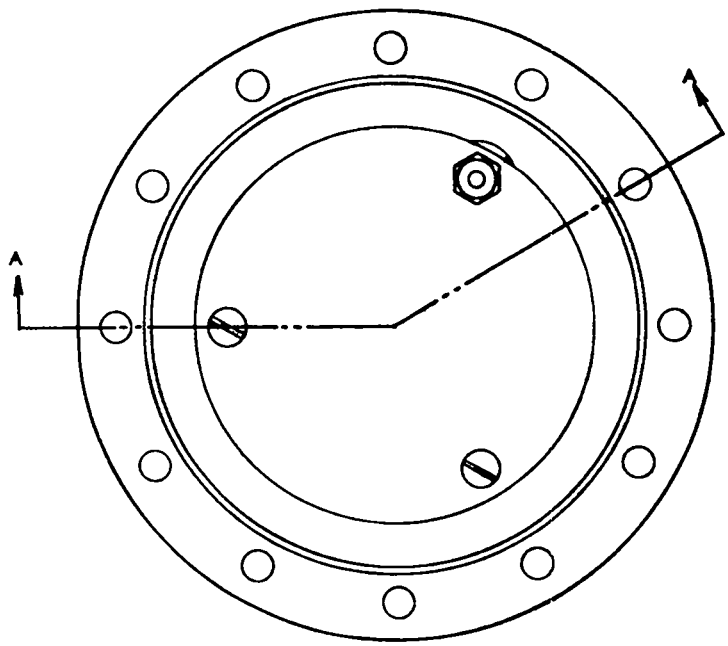


ONE INCH

TOP VIEW (COVER REMOVED)

Figure 6

Oscilloscope records of two x-ray pulses from a tube operated by a 370 kilovolt Westinghouse impluse generator. Total duration of the sweeps: 4.4 microseconds. X-ray tube 21 feet from the ionization chamber.

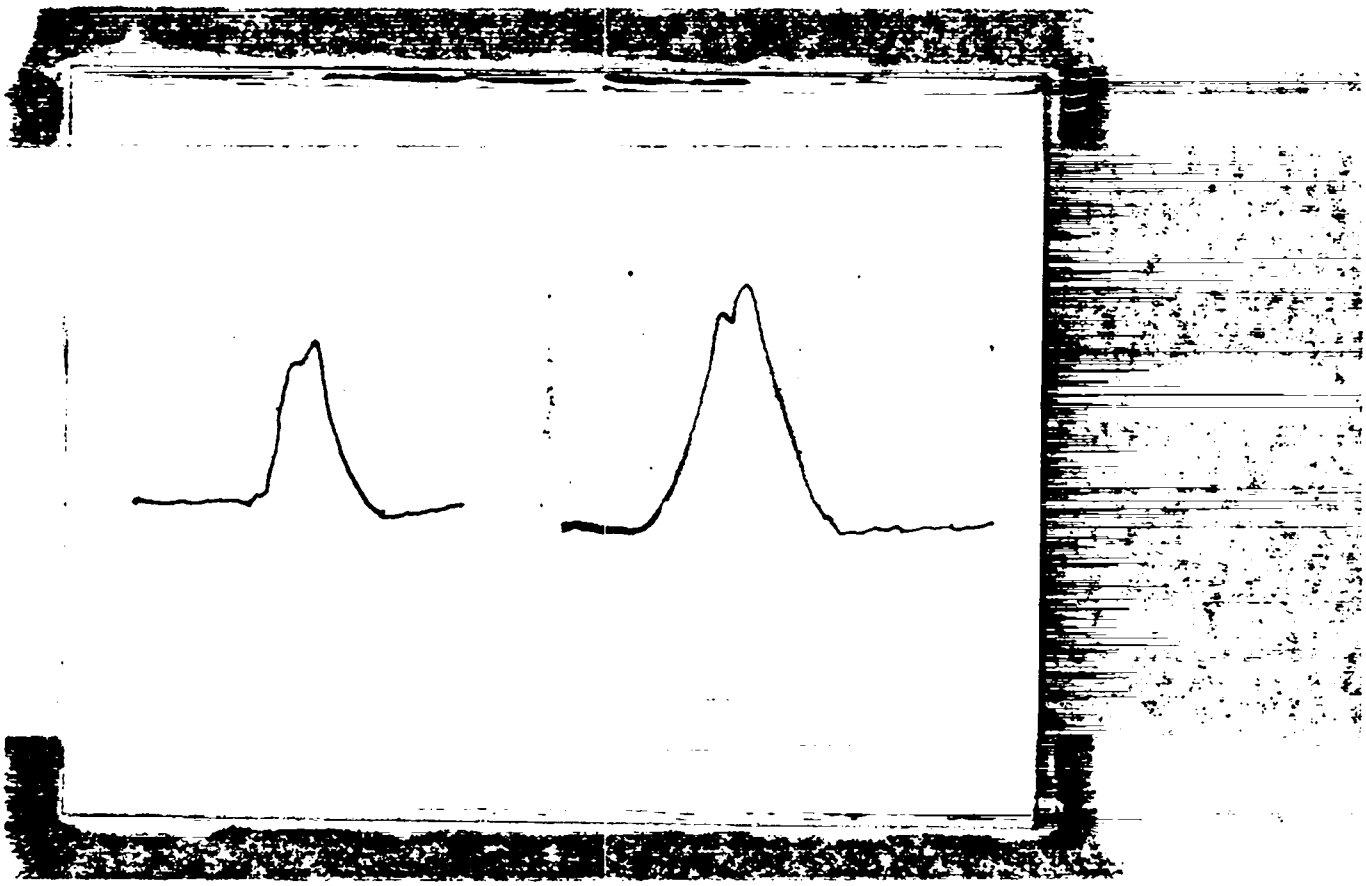

Figure 7

Multiple plate $\gamma$-ray ionization chamber (see Section 6)

(1) Brass cylinder 1" o.d., 0.025" wall.

(2) Kovar glass seal

(3) Brass cylinder 1" o.d., 0.010" wall

(4,5) Brass end plates

(7) Lead discs 0.040" thick, 0.9" in diameter, supported at the edges by 3 brass stems 0.047" in diameter and electrically connected to the outer brass case. Two of the stems are shown in the drawing (10). These discs have a central hole 0.350" in diameter to permit the passage of the rod (11) which is part of the collecting electrode.

(7) Lead discs, 0.040" thick, 0.8" in diameter, supported by the central brass rod (11) and forming the collecting electrode.

(8) Commercial Kovar glass seal. The kovar tube at the center of the seal supports the rod (11) bearing the collecting plates.

(9) Shield for lead to the collecting electrode.

(12) Gas outlet

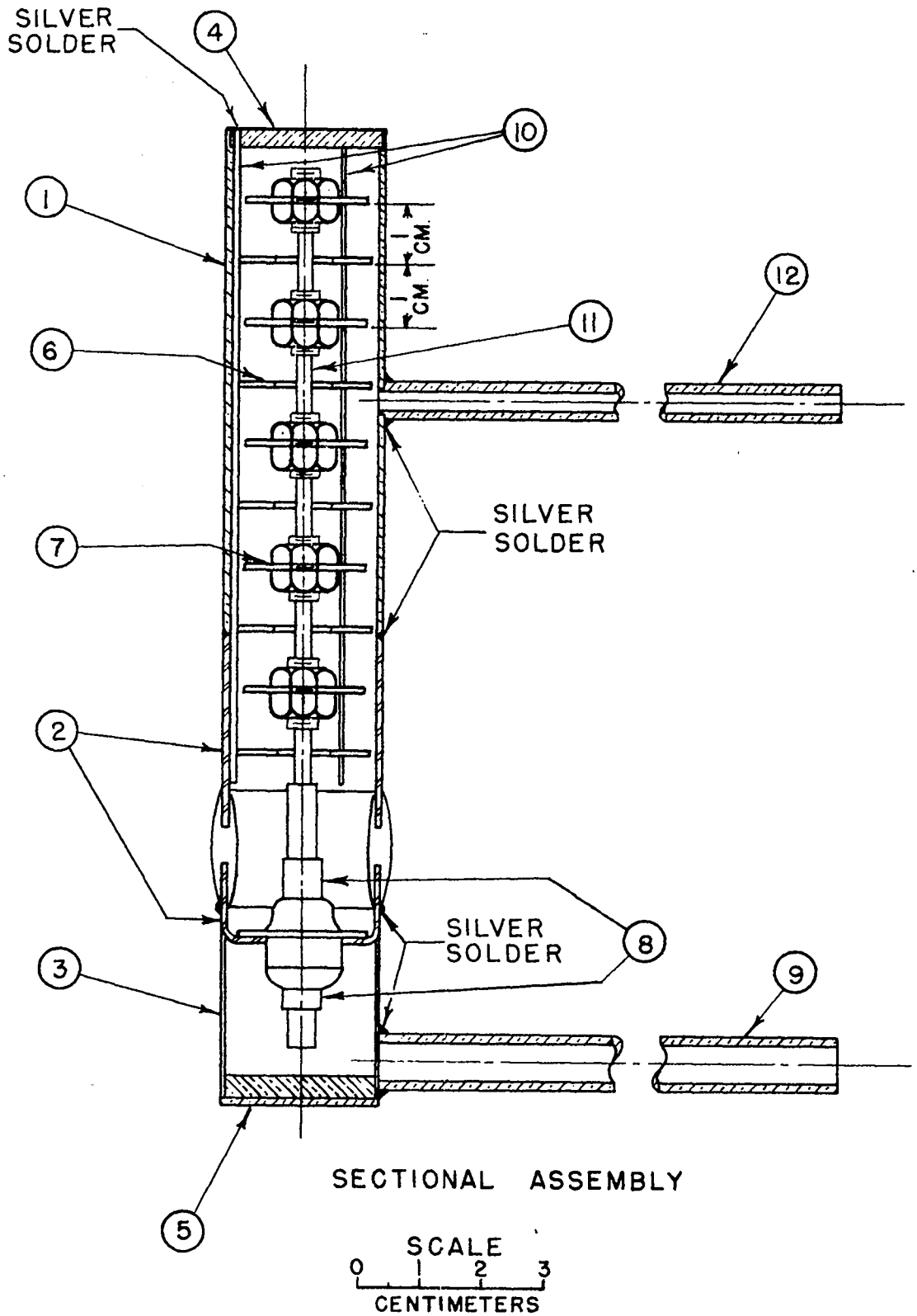

The brass cylinder which forms the outer case is kept at high voltage while the brass cylinder marked (3) is grounded. The chamber is filled with a mixture of 95 per cent argon, 5 per cent $CO_2$, the argon being purified by circulation over hot calcium before being admitted into the chamber. The total gas pressure is approximately 11 atmospheres. The chamber is operated at 2700 volts.

## 12.7 GAMMA-RAY IONIZATION CHAMBER WITH GAS MULTIPLICATION.

This chamber (see Figure 8) was designed for measurements of $\gamma$-ray pulses of low intensity. Its construction resembles that of the multiple wire proportional counter described in Section 11.7. The high voltage electrode consists of a set of lead plates. The collecting electrode consists of a set of brass diaphragms with circular holes. Across each hole, three thin steel wires are stretched at whose surfaces gas multiplication takes place. The ionization current corresponding to a given intensity of radiation is enhanced both by the gas multiplication and by the multiple electrode arrangement. The chamber is filled at 2 atmospheres with a mixture of 80 per cent argon, 20 per cent methane. Voltages up to 4000 volts can be used, giving a gas multiplication up to 400. Because of the peculiar transient response of chambers with gas multiplication (see Section 11.3), the current will not follow faithfully rapid variations of the $\gamma$-ray intensity. Therefore the most useful application of the chamber described above is in conjunction with an integrating circuit for the measurement of the integrated intensity of a $\gamma$-ray pulse.

## 12.8 GEIGER-MUELLER COUNTERS

Figure 9 shows the construction of a thin walled Geiger-Mueller counter designed at the Metallurgical Laboratory for use as a $\beta$-ray detector. The cylinder (A) is machined from a solid dural rod to a wall thickness of .004" to .005". The $\beta$-ray source is usually in the form of a foil which is wrapped around the cylinder. For many purposes it is important that the wall thickness be uniform so as to insure uniform absorption of the $\beta$-rays. Uniformity of wall thickness will also prevent the cylinder from collapsing when it is evacuated. The counter is assembled in the

Figure 8

Gamma ray ionization chamber with gas multiplication (see Section 7)

(1) Brass tube 3 3/4" o.d., 0.065" wall

(2) Brass end plate 1/4" thick.

(3) Brass end plate 1/4" thick

(4) Brass flange

(5) Fuse wire gasket

(6) Lead plates (.040" thick. They are supported by two steel rods with brass spacers of which one is shown in the diagram (7). These plates form the high voltage electrode.

(8) Brass diaphragms with circular holes as shown in detail in the section A-A. Three 0.003" steel wires are stretched across the opening 1/4" apart. The diaphragms are supported by the steel rods with brass spacers (9). These diaphragms form the collecting electrode.

(10,11) Porcelain insulators supporting the high voltage electrode and the collecting electrode, respectively. They are held in position by metal studs on the end plate (3).

(12,13) Porcelain insulators supporting the high voltage electrode and the collecting electrode, respectively. They are fastened with screws to the end plate (3).

(14,16) Kovar-glass seals providing electrical connection to the high voltage electrode and to the collecting electrode respectively.

(15) Gas inlet.

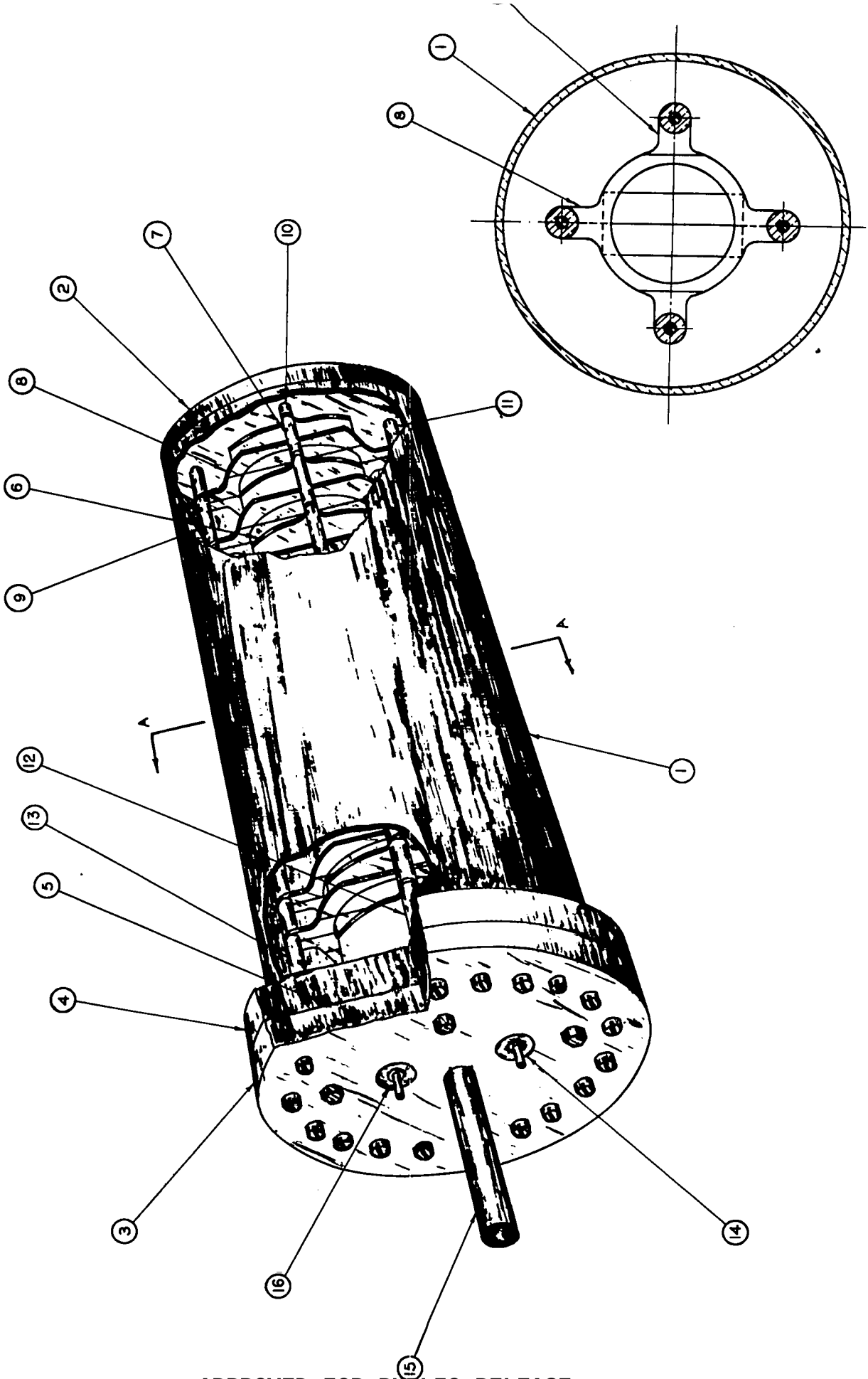

Figure 9

Beta ray counter (see Section 8)

(A) Dural cylinder, 0.004" to 0.005" wall thickness. It forms the high voltage electrode.

(B) Brass collar

(C) Brass end plate

(D) Neoprene gasket

(E) Glass-kovar seal

(F) Gas inlet

(G) Pyrex insulator

(H) bronze spring clip

(I) Kovar wire 0.005" diameter.

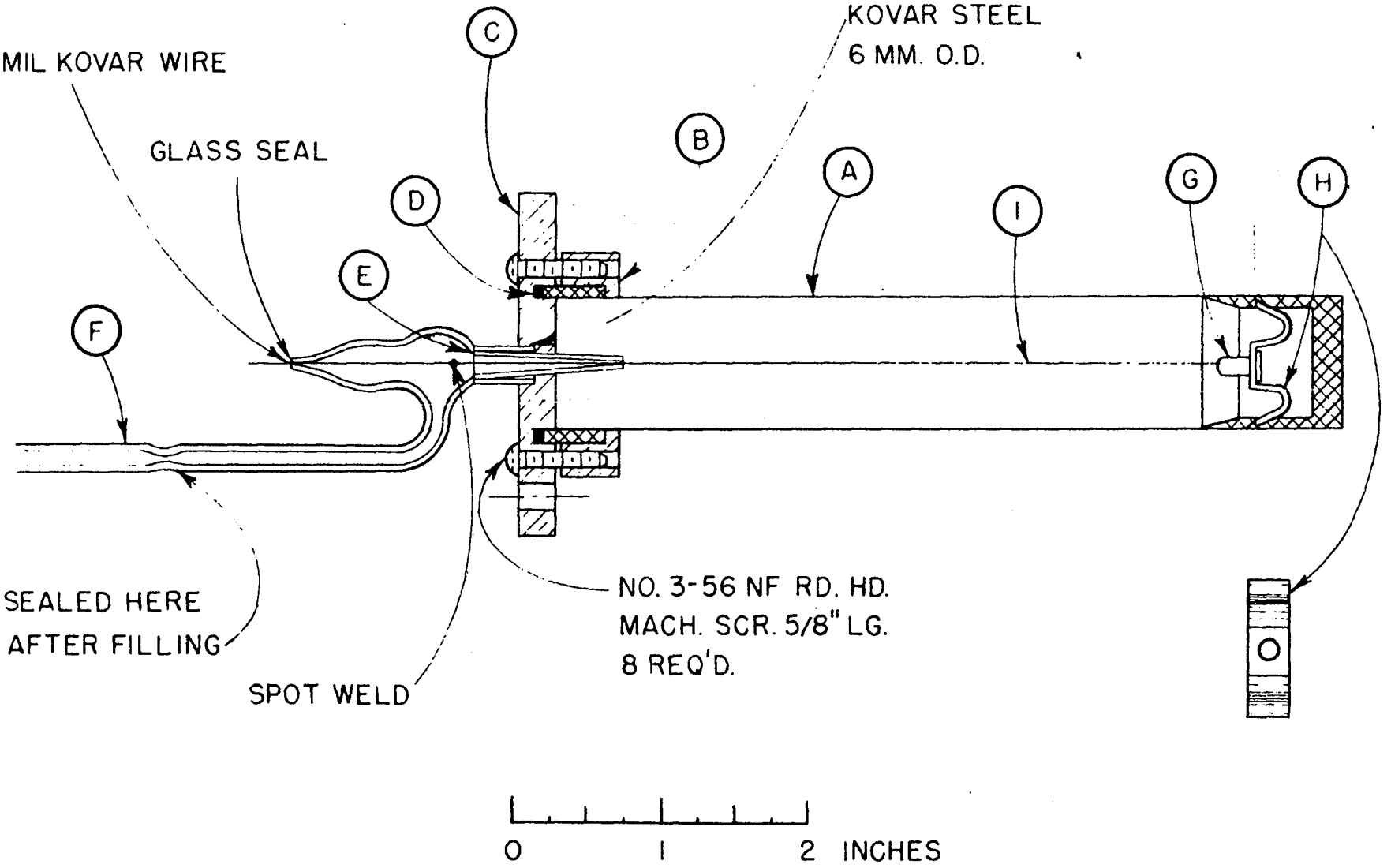




APPROVED FOR PUBLIC RELEASE

following way. First the glass-kovar seal (E) is soldered into the brass cap (C). The central wire assembly, including the pyrex end (G), is made and inserted into the bronze spring clip (H). This unit is then inserted into the dural tube (A) so that the ends of the spring fit into the groove cut in (A). The dural tube (A) is then clamped to the cap (C) by means of the collar (B), the kovar wire protruding through the open end of (E). The neoprene gasket (D) may be made of one piece or from a square strip of neoprene if the ends are carefully fitted together. Finally, the central wire, 0.[illegible] thick, is stretched ~~taught~~ taut and the kovar wire at the end is sealed to the glass end of (E). The desired tension on the wire may be obtained by clamping the counter in a vertical position and hanging a weight on the end of the wire. The counter is usually filled with a mixture of ethyl alcohol vapor (1 cm Hg pressure) and of argon (9 cm Hg pressure). With this mixture, it operates as a self quenching counter. It ordinarily has a threshold voltage of about 900 volts In the best counters, the counting rate at the plateau increases by 2 per cent when the voltage is increased by 160 volts.

Figure 10 represents a brass walled Geiger-Mueller counter of simple design used in the Los Alamos Laboratory as a $\gamma$-ray detector. The gas filling is the same as in the $\beta$-ray counter shown in Figure 9, namely 9 centimeters argon and 1 centimeter ethyl alcohol. The details of the construction are sufficiently clear from the figure.

## 12.9 MICA WINDOW GEIGER-MUELLER COUNTER

Figure 11 shows the construction of a mica window $\beta$-ray counter. The counter is prepared and assembled in the following way.

The copper cylinder is first washed with 5N nitric acid, then rinsed in distilled water and dried in the oven at 90° C for about 15 minutes. Then the cylinder is oxidized on the inside by mounting it on top of a test tube containing $Pb(NO_3)_2$. The test tube is heated with a gas burner until the fumes passing through the copper tube have caused its inner surface to acquire an even purple-brown coat.

The mica window is mounted with the following technique. The copper flange is

Figure 10

Gamma ray counter (see Section 8).

(1) Brass cylinder, 7/8" in diameter, 1/32" wall

(2) 0.005" Kovar wire

(3) Glass insulator

(4) Kovar-glass seal

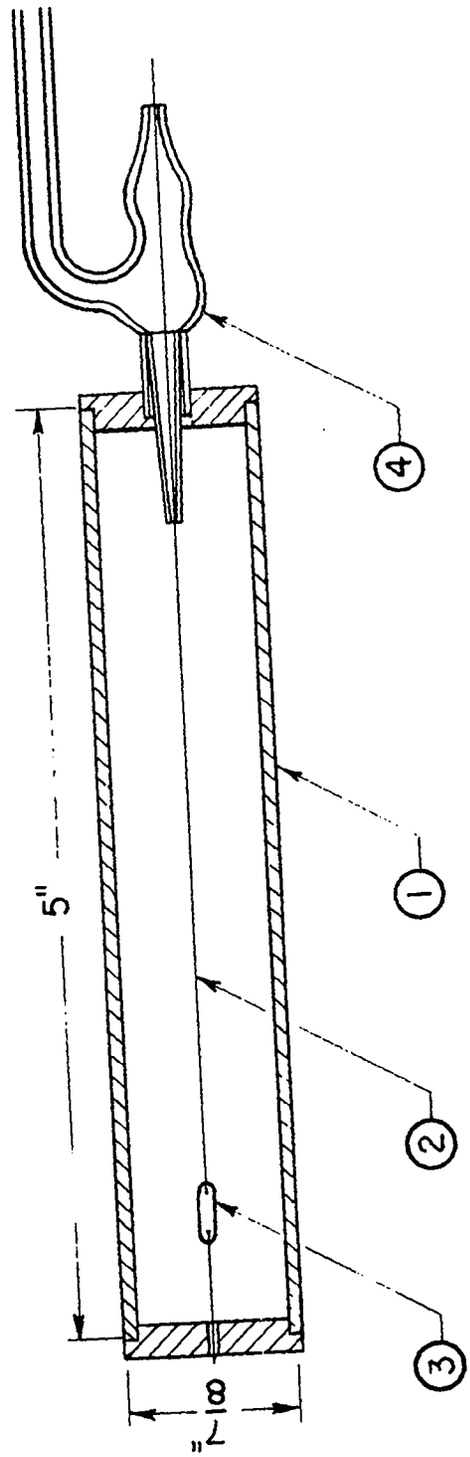

Figure 11

Mica window $\beta$ -ray counter (see Section 9)

(1) Copper cylinder 1 1/4" o.d., 1/32" wall.

(2) Copper flange, 1/16" thick.

(4) Pyrex glass piece, sealed to the copper tube with DuPont high temperature melting wax.

(6) Pyrex bead, about 0.020" diameter

(7) Mica sheet 3 to 5 mg/cm$^2$.

(8) Brass ring

(9) Stop cock.

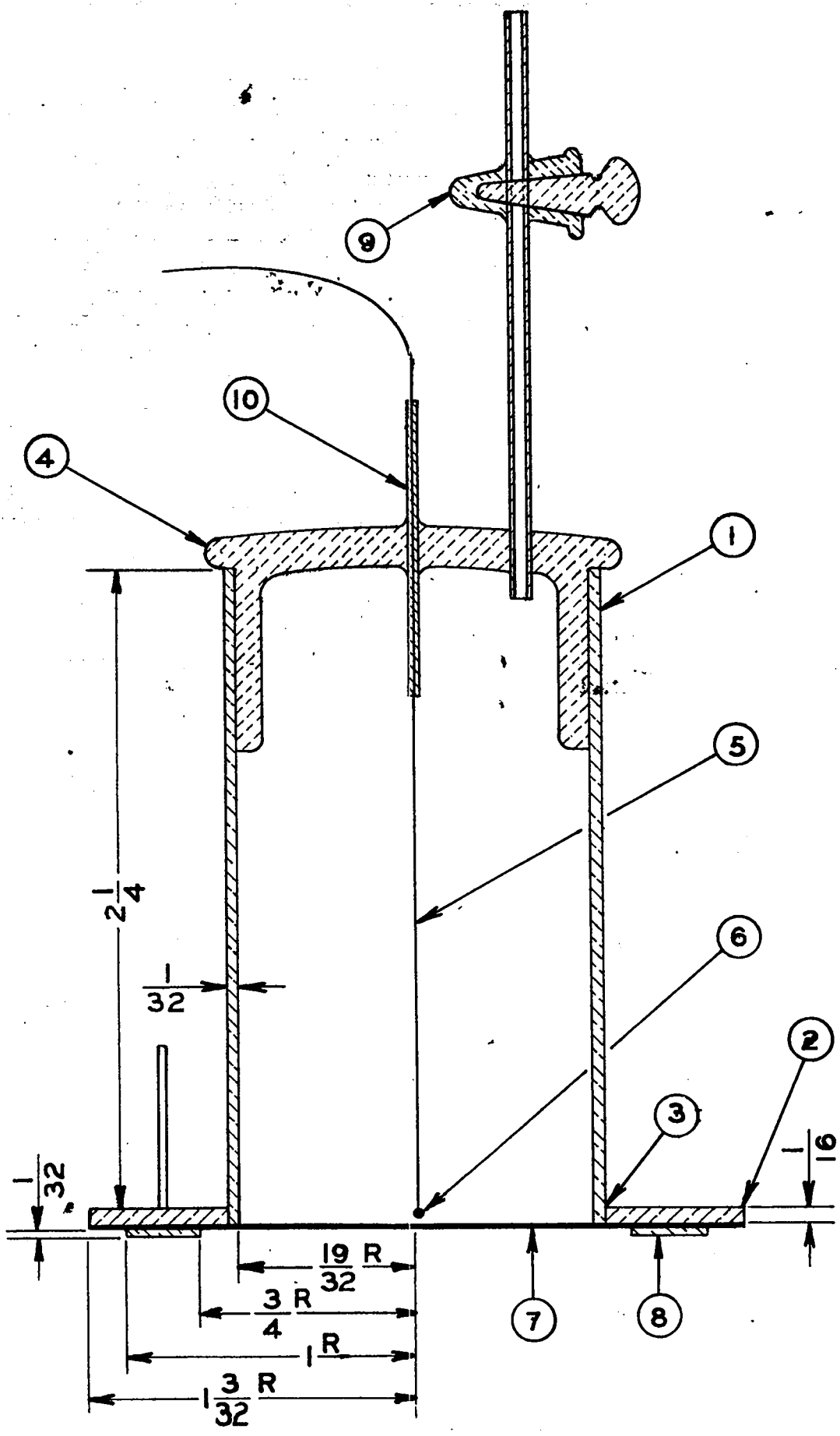

heated gently and a ring of high temperature melting DuFont "Parlon" wax is deposited about two-thirds of the way toward the outer edge. The mica is placed on a brass plate, which is uniformly heated electrically. The copper cylinder is set on the mica sheet and the brass plate is kept at a high temperature while the wax flows evenly as far as the outer edge of the flange. The brass ring (8) is also placed on the hot brass plate and covered with wax. The cylinder with the mica window is placed on top of the ring and allowed to cool slowly.

The counters are filled with 90 per cent argon, 10 per cent alcohol to a total pressure of 10 centimeters Hg. They usually have plateaus of about 200 volts.

## 2.10 PULSED COUNTERS

For some special experimental purposes a simple $\gamma$-ray detector was designed which answers the following requirements: (a) it has a very small active area; (b) it can be pulsed (i.e., it can be made sensitive for short predetermined time intervals of the order of 100 microseconds); (c) it provides a sufficiently large output pulse to operate recorders without need of further amplification, even through long cables.

The principle adopted in the design of the detector is based upon the fact that if one raises the voltage across a spark gap somewhat above the so-called sparking potential, no discharge actually occurs unless electrons are present between the electrodes.

The detector resembles physically a small Geiger-Mueller counter. It is operated with argon filling near atmospheric pressure. A direct current voltage below the sparking potential, applied between cylinder and wire, removes rapidly whatever electrons are liberated in the counter by cosmic rays or local radioactivity.

The voltage is raised above the sparking potential during the appropriate time interval by superimposing a square voltage pulse on the direct current voltage. If, during this time, electrons appear in the counter, they are accelerated toward the wire and initiate a discharge. Positive ions will not give rise to a discharge

unless they liberate electrons by striking the cathode, a process which is usually very unlikely. It follows that a discharge will occur only if an ionizing particle traverses the counter during a time which coincides approximately with the duration of the square voltage pulse. (The sensitive time does not coincide exactly with the duration of the pulse because of the finite transit time of electrons in the counter.)

The design of the counters is affected by the requirement that it should be possible to assemble units containing a large number of closely spaced individual counters. The design adopted is shown in Figure 12. The counter wall is a platinum cylinder of 0.125" inside diameter, and 0.005" wall thickness. The wire is made of tungsten and is 0.005" in diameter. It is supported by lucite caps, which are shaped so as to increase the leakage path along the insulating surface. The individual counter tubes were mounted between two lucite bars, with a spacing of 0.155" between the axes of neighboring counters.

The unit was assembled by first sliding the platinum tubes into holes provided in the bars. The wire was then connected to the spring and threaded through the hole of the cap (A). The free end of the wire was passed through the platinum cylinder and into the second cap (B). After the caps were in position, the wire was stretched and spotwelded to a stainless-steel tab inserted in a slot of the cap (B).

The unit was mounted in a gas-tight box, as shown in Figure 13. Connections to the counter wire leads were brought out through screws inserted in the top lucite plate. The counter cylinders were all connected to a common lead which was again brought out through the top lucite plate.

A hot-calcium purifier was provided in order to stabilize the operation of the counters by removing impurities from the argon filling.

The filling procedure was as follows: The unit was first connected to a vacuum system and evacuated to a pressure of about $10^{-3}$ centimeters Hg for several hours. Then the purifier was raised to a temperature of $350^{\circ}$ C until the calcium

Figure 12

Pulsed $\gamma$-ray counter (see Section 10).

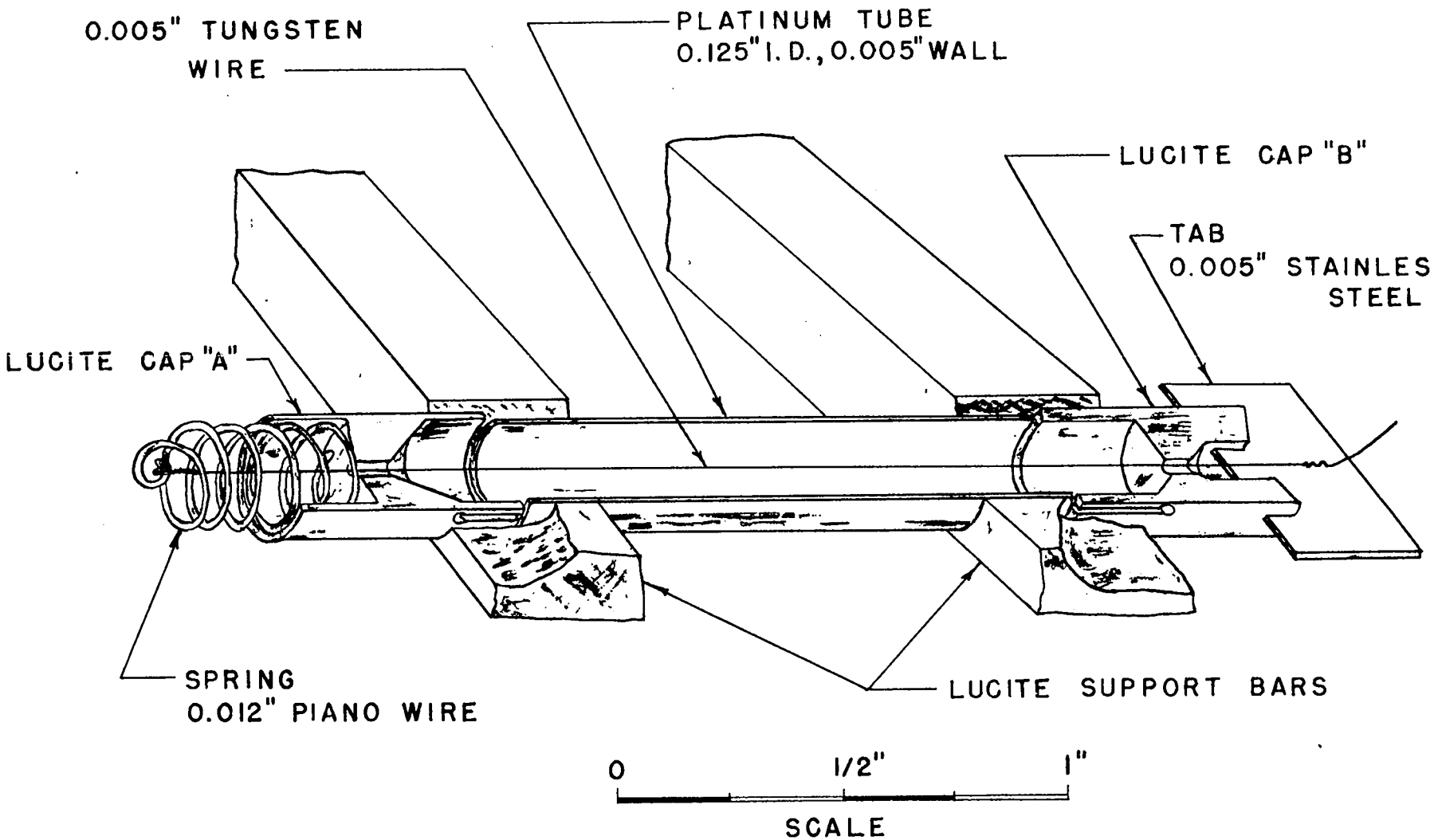


APPROVED FOR PUBLIC RELEASE

Figure 13

Unit of fifty pulsed $\delta$-ray counters.

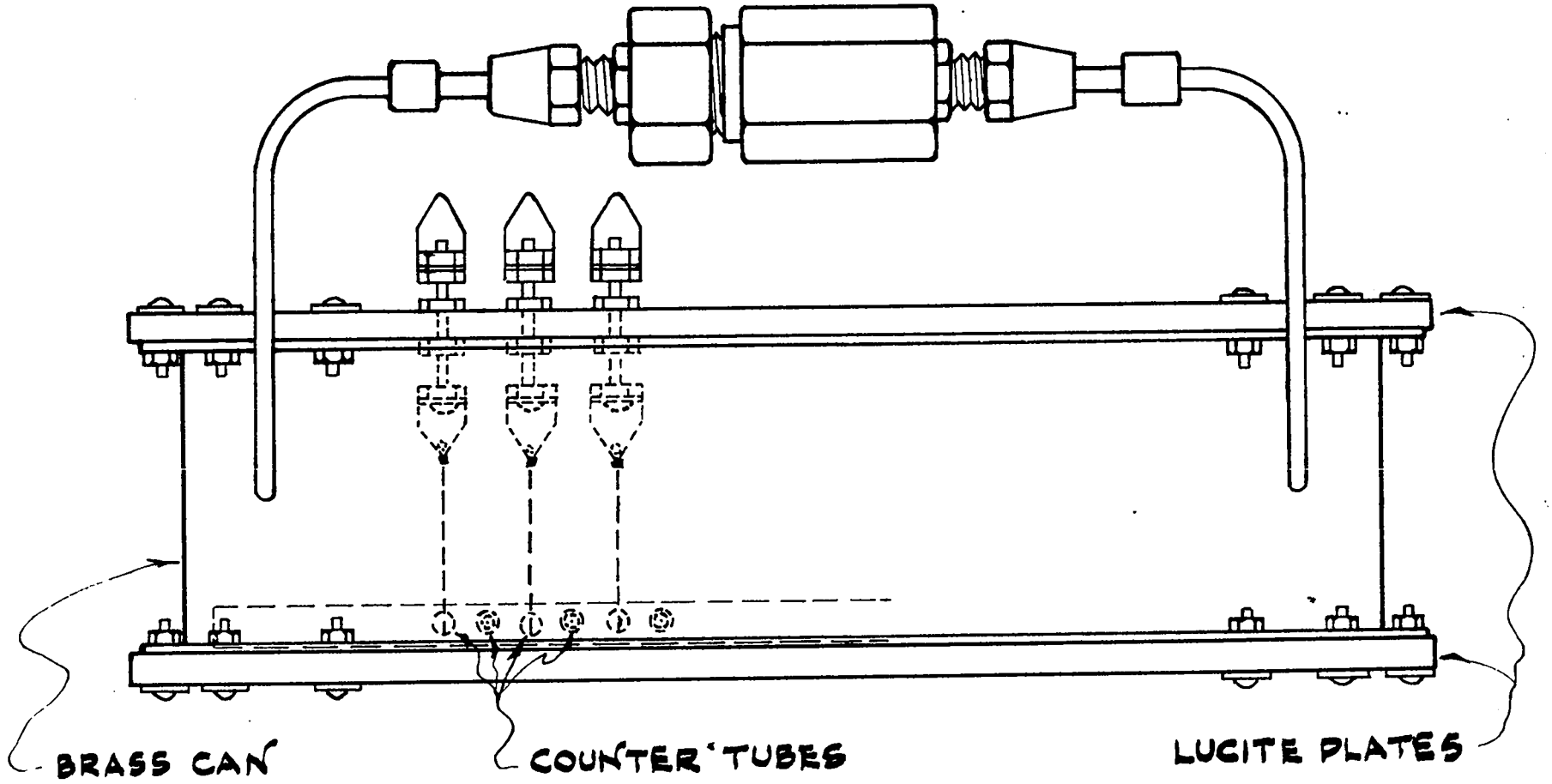


APPROVED FOR PUBLIC RELEASE

was thoroughly outgassed. Argon was then admitted through a $CO_2$ ice trap to a pressure of several centimeters of Hg. A glow discharge was passed through each of the counters for several minutes by means of a spark tester. The unit was evacuated again, and finally filled with argon to a pressure of 59 centimeters of Hg.

The electronic equipment used for testing the counters described above is schematically represented by the block diagram in Figure 14.

The pulser produces a square wave voltage of 450 volts in amplitude with a repetition rate of six per second. The width of the square wave can be varied from 50 to 200 microseconds. This square wave is added by means of an RC coupling network to the base voltage applied to the counter cylinder. The counter wire is connected to ground through a potential divider. When the counter discharges, a pulse of the order of 1000 volts appears at the wire, and a pulse of the order of 50 volts appears at the point A of the potential divider.

The pulse at point A is sufficient to trigger a univibrator driving a message register. In order to observe the pulse shape, one of the vertical deflecting plates of a cathode ray tube may be connected to point A. A stationary pattern on the scope is obtained by using a sweep triggered by the pulser.

A number of tests were made on a unit containing 50 individual counters. In these tests, the square wave had a width of 150 microseconds.

Figure 15 shows the counting rate in an individual counter as a function of the direct current voltage applied to the tube, with a $\gamma$-ray source of the order of one millicurie placed near the counter. This curve resembles the corresponding curve for an ordinary Geiger-Mueller counter. The counting rate increases from zero to the normal value for an increase of voltage of about 60 volts. The counting rate then remains fairly constant over a plateau of 200 to 250 volts width, then starts rising rapidly. We shall define as threshold voltage the voltage at which the counting rate is one-half normal. We shall define as breakdown voltage the voltage at which the counting rate is appreciably above normal.

Figure 14

Schematic diagram of the arrangement used for testing the pulsed counters.

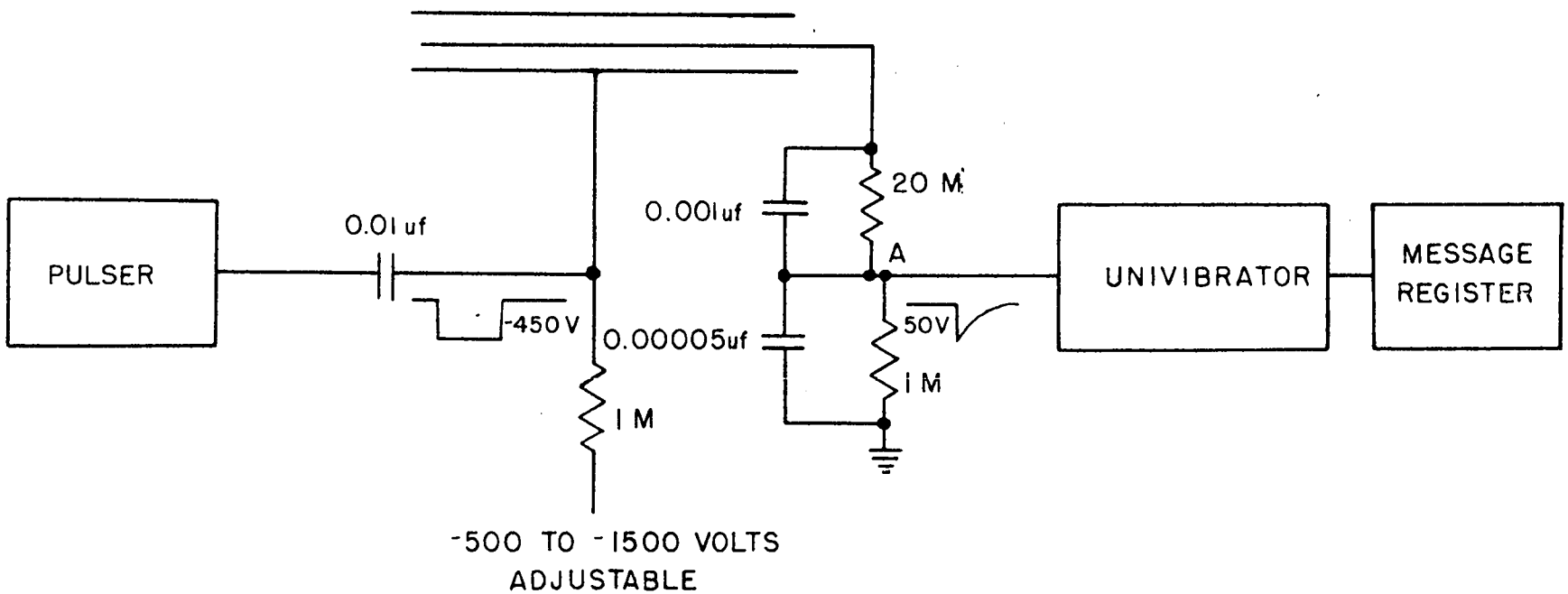


APPROVED FOR PUBLIC RELEASE

Figure 15

Counting rate as a function of the D.C. voltage for a pulsed counter. The square pulses which determine the sensitive period had a duration of 150 microseconds and an amplitude of 450 volts.

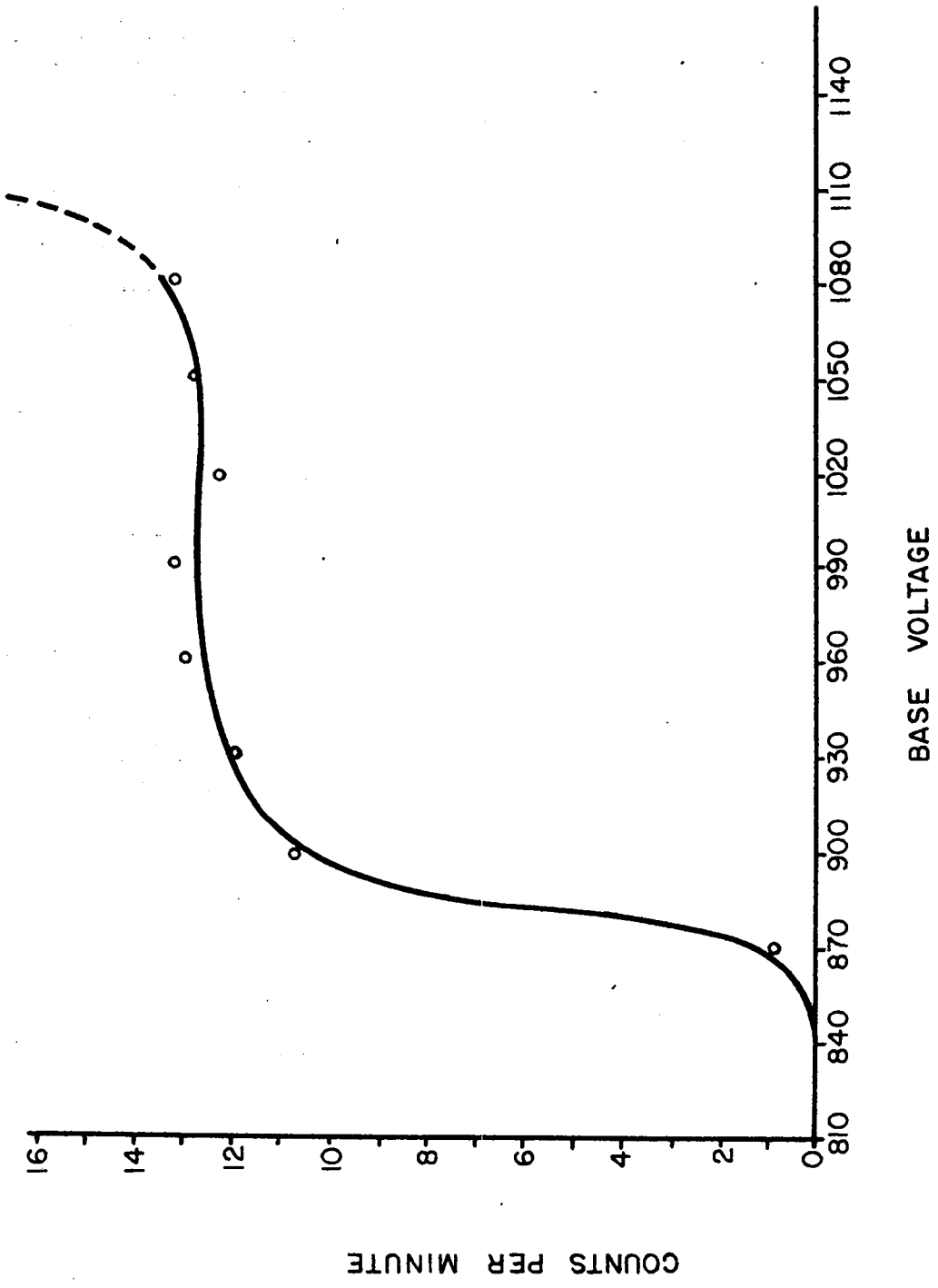

It is obviously desirable that all the counters of a unit have closely the same characteristics so that they can be operated from the same direct current supply. Figure 16 shows threshold voltage and breakdown voltage for the fifty individual counters of the unit used. It appears that the plateaus of the various counters overlap over a comfortably wide range of voltages. It may be pointed out that this result was achieved only after thorough cleaning of the counters and careful centering of the wires.

When the $\gamma$-ray source is removed, the counting rate on the plateau, for a 150 microseconds gate width, drops from a value of about 13 a minute to a value of about 6 per hour. Since the counters are pulsed 6 times a second, this means that the probability for a spontaneous count to be recorded when the counter is pulsed amounts to 1/3600. This background is sufficiently small for all practical purposes, although it seems to be somewhat higher than that expected from cosmic rays and local radioactivity.

The counting yield of the counter tubes was estimated by determining the counting rate with a known $\gamma$-ray source at a known distance and found to be of the order of 2 per cent. This is close to the value which can be expected if all of the secondary electrons penetrating the tube give rise to a discharge.

It may be mentioned that pulsed counters can be made with metals other than platinum for the counter wall (for instance brass or steel) and with air instead of argon as a gas filling. However, in these counters the background was found to be abnormally large and moreover dependent on the past history of the counter. High counting rates were recorded immediately after the removal of a strong $\gamma$-ray source; this spurious counting rate decreased gradually to the normal background in a period of the order of a half-hour. Also the operating voltage was a function of th counter history. An explanation for the high counting rate after strong irradiation may be found in the formation of metastable molecules, an effect which is apparently minimized by the use of argon in a platinum counter.

Figure 16

Threshold voltage ( • ) and breakdown voltage ( ⊙ ) for a unit of fifty pulsed counters.